



THE HONG KONG
POLYTECHNIC UNIVERSITY

香港理工大學

Pao Yue-kong Library

包玉剛圖書館

Copyright Undertaking

This thesis is protected by copyright, with all rights reserved.

By reading and using the thesis, the reader understands and agrees to the following terms:

1. The reader will abide by the rules and legal ordinances governing copyright regarding the use of the thesis.
2. The reader will use the thesis for the purpose of research or private study only and not for distribution or further reproduction or any other purpose.
3. The reader agrees to indemnify and hold the University harmless from and against any loss, damage, cost, liability or expenses arising from copyright infringement or unauthorized usage.

IMPORTANT

If you have reasons to believe that any materials in this thesis are deemed not suitable to be distributed in this form, or a copyright owner having difficulty with the material being included in our database, please contact lbsys@polyu.edu.hk providing details. The Library will look into your claim and consider taking remedial action upon receipt of the written requests.

REVERSAL OF P-GLYCOPROTEIN-
MEDIATED MULTIDRUG
RESISTANCE USING SYNTHETIC,
POTENT AND NON-TOXIC
GALLOYLATED CATECHINS
DERIVATIVES

SUN WENQIN

PhD

The Hong Kong Polytechnic University

2022

The Hong Kong Polytechnic University

Department of Applied Biology and Chemical
Technology

Reversal of P-glycoprotein-mediated
Multidrug Resistance Using Synthetic, Potent
and Non-toxic Galloylated Catechins
Derivatives

Sun Wenqin

A thesis submitted in partial fulfilment of the
requirements for the degree of Doctor of
Philosophy

September 2021

CERTIFICATE OF ORIGINALITY

I hereby declare that this thesis is my own work and that, to the best of my knowledge and belief, it reproduces no material previously published or written, nor material that has been accepted for the award of any other degree or diploma, except where due acknowledgement has been made in the text.

Signed:

Student Name: SUN WENQIN

Abstract

P-glycoprotein (P-gp) was one of well-known drug-resistance transporters. It was a highly efficient efflux pump with broad substrate specificity, including approximately a third of all anticancer drugs. P-gp expression in cancers can therefore confer cross-resistance to anthracyclines, vinca alkaloids, taxanes, epipodophyllotoxins, mitoxantrone and dactinomycin. Three generations of P-gp modulators were developed to overcome the resistance induced by P-gp, but they all failed to get into clinical application. Natural products were promising to be developed to the next generation of P-gp modulators.

Epigallocatechin gallate (EGCG) was one of the well-known galloylated catechins in green tea with various biological activities. It also showed moderate P-gp modulation activity. To improve the P-gp modulation activity of EGCG, a series of compounds were synthesized with modifications including methoxy substitutions in the benzene rings and a long and rigid linker between benzene rings. Compounds, 23, 51, FX3 and WBC5 were the four most potent compounds among all the derivatives. Compared to EGCG ($EC_{50} > 1000$ nM), these four derivatives were significantly more potent ($EC_{50} = 37.0$ to 385.0 nM) in three different cell lines (LCC6MDR, P388ADR and K562/P-gp). Mechanistically, they can enhance intracellular accumulation of both paclitaxel (PTX) and doxorubicin (DOX) in these cell lines by inhibiting the P-gp-mediated DOX efflux.

Pharmacokinetics studies of the four derivatives indicated their bioavailability was high, ranging from 62.88 to 81.81% when they were administrated by i.p. injection.

The plasma level of 51, FX3 and WBC5, when administrated by i.p. injection (30 mg/kg), dropped below their corresponding *in vitro* EC₅₀ value until 1080 minutes post administration. In addition, co-administration of FX3 and PTX suggesting no significant drug-drug interaction in plasma level. Therefore, FX3 was selected for further characterization for its *in vivo* efficacy.

FX3 was co-administered with either PTX or DOX in three *in vivo* efficacy models of drug resistance including LCC6MDR xenografted solid tumor, and two leukemia models including the mouse P388ADR (i.p. inoculated) and human K562/Pgp (i.v. inoculated). In LCC6MDR xenografted model, combination treatment of FX3 and PTX significantly reduced tumor volume by 27.4% ($p < 0.001$) and decreased tumor weight by 34% ($p < 0.01$), when compared to PTX. Intratumor level of PTX was also increased by co-administration of FX3 after 60 to 300 minutes post PTX administration. In P388ADR and K562/P-gp leukemia model, combination treatment of FX3 and DOX could significantly prolong the median survival time by 30.3 ($p < 0.001$) and 15.6% ($p < 0.01$), respectively, compared to DOX alone treatment. In P388ADR leukemia model, co-treatment of DOX with FX3 resulted in a lower toxicity and longer median survival time than DOX with GF120918, which was a well-known P-gp modulator. These results suggested that FX3 can reverse P-gp induced MDR in different animal models.

In summary, P-gp modulating activity of galloylated catechins derivatives was significantly improved compared with that of EGCG. FX3 can reverse MDR by modulating P-gp both *in vitro* and *in vivo* without significant toxicity issue.

List of Publication, Conference Presentation

Iris L.K.Wong, Xing-kai Wang, Zhen Liu, Wenqin Sun, Fu-xing Li, Bao-chao Wang, Peng Li, Sheng-biaoWan, Larry M.C.Chow. Synthesis and evaluation of stereoisomers of methylated catechin and epigallocatechin derivatives on modulating P-glycoprotein-mediated multidrug resistance in cancers. *European Journal of Medicinal Chemistry* In Press; September 1, 2021.

Peng Li, Yunjiao He, Teng Chen, Kit-Ying Choy, Tsun Sing Chow, Iris L.K. Wong, Xinqing Yang, Wenqin Sun, Xiaochun Su, Tak-Hang Chan and Larry M.C. Chow. Disruption of SND1–MTDH Interaction by a High Affinity Peptide Results in SND1 Degradation and Cytotoxicity to Breast Cancer Cells *In Vitro* and *In Vivo*. *Mol Cancer Ther* 2021;20:76–84; December 2, 2020.

Wenqin Sun, Iris K.L. Wong, Xiao-Chun Su, Liu Zhen, Sheng-Biao Wan, Tak-Hang Chan and Larry M. C. Chow. Reversal of P-glycoprotein-mediated cancer multidrug resistance by synthetic, potent and non-toxic green tea polyphenol derivatives. *FEBS Special Meeting 2020. ATP-Binding Cassette (ABC) Proteins: From Multidrug Resistance to Genetic Disease*, Austria, 2020.

Acknowledgements

I would like to express my sincere gratitude to my supervisor Prof. Larry M. C. Chow, for his consistent and illuminating guidance throughout my study. He also always patiently and generously teaches me biological knowledge and solves my puzzles. I am deeply impressed by his professional guidance and constant pursuit for science, which will perform great impact on my future work. My appreciation also goes to Prof. Bill T.H. Chan, whose valuable suggestions always helps me to overcome the problems in this project. Then I would also like to give my special thanks to Prof. Wan Shengbiao, who kindly provides sufficient compounds for this project.

Many thanks to my seniors and lab mates, Dr. Ms. Iris I.K. Wong, Dr. Ms. Clare S.W Yan, Dr. Chen teng, Dr. Liu zhen, Sun Ge Ge, Su Xiaochun and Yang Xinqing for their practical assistance and guidance. It has been an enjoyable experience to work with them, which benefits me a lot.

Special thanks to Dr. Ms LAW, Helen K. W. and Bobby, Shu-po SHIU from the Department of Health Technology and Informatics (HTI), Hong Kong Polytechnic University who kindly provide me the irradiator of Multirad 225 for mice irradiation.

My gratitude goes to Dr. Zhang Huan for training me since I was a FYP student, and the unconditionally technical support and motivation during my study. My warmest gratitude also goes to the peer support from Wu Man Hui, Yu Wenxuan and Zhang Xiaozhe, for their listening and accompany. I also thank all the technical support and comprehensive training from the technical support team in department of Applied Biology and Chemical Technology, and the staff in the University Research Facility in

Life Sciences and Centralized Animal Facilities.

Finally, I would like to express my deepest gratitude to my beloved family unconditional understanding and support throughout my years of study.

Table of Contents

| | |
|--|----|
| Abstract..... | II |
| List of Publication, Conference Presentation..... | IV |
| Acknowledgements..... | V |
| Chapter 1: Introduction | |
| 1.1 Cancer chemotherapy and multidrug resistance | 1 |
| 1.1.1 Drug inactivation..... | 3 |
| 1.1.2 Alteration of drug targets | 3 |
| 1.1.3 DNA damage repair..... | 3 |
| 1.1.4 Drug efflux | 4 |
| 1.2 Overview of ABC transporters | 5 |
| 1.2.1 P-gp | 9 |
| 1.2.2 Breast cancer resistant protein (BCRP)..... | 13 |
| 1.2.3 Multidrug Resistance-associated Protein-1 (MRP-1)..... | 13 |
| 1.3 Reversing MDR1/P-gp resistance..... | 14 |
| 1.3.1 P-gp modulators | 14 |
| 1.3.2 Nanoparticle drug delivery systems | 16 |
| 1.3.3 microRNA (miRNA) modulating P-gp | 17 |
| 1.4 Green tea polyphenols | 17 |
| 1.4.1 Green tea polyphenols and cancer-related biological effect | 17 |
| 1.4.2 Modification of green tea catechins | 22 |
| 1.4.3 Previous work in our group on green tea catechins modification | 24 |
| 1.5 Summary..... | 28 |
| 1.6 Objectives of study | 29 |

Chapter 2: Methodology

| | |
|---|----|
| 2.1 Chemicals and materials for the studies..... | 31 |
| 2.2 <i>In vitro</i> studies..... | 32 |
| 2.2.1 Cell culture | 32 |
| 2.2.2 Cell survival assay | 32 |
| 2.2.3 DOX accumulation assay | 33 |
| 2.2.4 DOX efflux assay | 34 |
| 2.2.5 Determination of P-gp expression using Western blot..... | 34 |
| 2.2.6 Determination of P-gp cellular localization using confocal microscope | 35 |
| 2.2.7 PTX metabolism on human liver microsome..... | 36 |
| 2.2.8 P-gp ATPase activity | 37 |
| 2.2.9 FX3 accumulation and efflux in K562 and K562/P-gp cells | 38 |
| 2.3 UPLC-MS/MS detection method..... | 38 |
| 2.3.1 MRM detection method of modulators | 38 |
| 2.4 <i>In vivo</i> studies | 40 |
| 2.4.1 Animals | 40 |
| 2.4.2 Drug preparation and injection..... | 40 |
| 2.4.3 Pharmacokinetics studies | 41 |
| 2.4.4 <i>In vivo</i> toxicity studies..... | 42 |
| 2.4.5 Establishment of LCC6MDR xenograft model in BALB/c nude mice..... | 43 |
| 2.4.6 <i>In vivo</i> efficacy study of FX3 in LCC6MDR xenograft..... | 44 |
| 2.4.7 Intratumor PTX and FX3 accumulation | 44 |
| 2.4.8 Establishment of P388ADR lymphoma model in B6D2F1 mice..... | 45 |
| 2.4.9 <i>In vivo</i> efficacy study of FX3 in P388ADR lymphoma model | 45 |

| | |
|--|----|
| 2.4.10 Establishment of K562/P-gp leukemia model in NOD/SCID mice | 45 |
| 2.4.11 <i>In vivo</i> efficacy study of FX3 in K562/P-gp leukemia model..... | 47 |
| Chapter 3: Galloylated catechin derivatives reversed MDR by modulating P-gp <i>in vitro</i> | |
| 3.1 Introduction..... | 48 |
| 3.1.1 MDR induced by P-gp and galloylated catechins derivatives..... | 48 |
| 3.1.2 Cell models..... | 49 |
| 3.1.3 Mechanism of P-gp modulation | 50 |
| 3.2 Results..... | 51 |
| 3.2.1 Efficacy of galloylated catechins derivatives to reverse MDR induced by P-gp in different cell lines..... | 51 |
| 3.2.2 Efficacy of galloylated catechins derivatives in reversing drug resistance induced by BCRP and MRP-1 in different cell lines | 55 |
| 3.2.3 Effects of galloylated catechins derivatives on P-gp expression and location.... | 57 |
| 3.2.4 Effect of galloylated catechins derivatives on DOX accumulation and efflux in P-gp overexpressing cell lines..... | 62 |
| 3.2.5 Effect of galloylated catechins derivatives on P-gp ATPase activity..... | 68 |
| 3.2.6 Accumulation of FX3 in sensitive and resistant cells | 70 |
| 3.2.7 Reversibility of FX3 on modulating P-gp | 72 |
| 3.3 Summary | 74 |
| Chapter 4: Pharmacokinetics study of galloylated catechin derivatives by UPLC-Triple Quadrupole Tandem Mass Spectrometry | |
| 4.1 Introduction..... | 75 |
| 4.2 Results..... | 77 |
| 4.2.1 Detection of galloylated catechin derivatives in MRM..... | 77 |

| | |
|---|-----|
| 4.2.2 Formulation selection of galloylated catechins derivatives for animal study | 87 |
| 4.2.3 Plasma level of galloylated catechins derivatives | 90 |
| 4.2.4 Effect of galloylated catechin derivatives on PTX metabolism of human liver microsomes | 93 |
| 4.2.5 Pharmacokinetics study of PTX with or without 51, FX3 or WBC5..... | 95 |
| 4.3 Summary..... | 97 |
| Chapter 5: The efficacy study of galloylated catechin modulators on reversing MDR xenograft models <i>in vivo</i> | |
| 5.1 Introduction..... | 99 |
| 5.1.1 Nude mice and LCC6MDR xenograft model..... | 99 |
| 5.1.2 Application of P-gp modulator in solid tumor | 99 |
| 5.1.3 Leukemia | 100 |
| 5.1.4 B6D2F1 mice and murine leukemia animal model of P388ADR..... | 100 |
| 5.1.5 CML model <i>in vivo</i> | 101 |
| 5.1.6 Application of P-gp modulator in leukemia treatment..... | 101 |
| 5.2 Results..... | 104 |
| 5.2.1 <i>In vivo</i> toxicity studies in BALB/c mice | 104 |
| 5.2.2 <i>In vivo</i> efficacy studies of reversing PTX resistance of LCC6MDR xenograft in BALB/c nude mice using derivatives and EGCG..... | 106 |
| 5.2.3 <i>In vivo</i> efficacy studies of reversing PTX resistance of LCC6MDR xenograft using FX3..... | 106 |
| 5.2.4 FX3 accumulation in LCC6MDR tumor..... | 111 |
| 5.2.5 PTX accumulation in LCC6MDR tumor with or without FX3..... | 111 |
| 5.2.6 <i>In vivo</i> efficacy studies using FX3 to reverse DOX resistance in P388ADR xenograft..... | 113 |

| | |
|---|-----|
| 5.2.7 Establishment of leukemia model (K562/P-gp) | 115 |
| 5.2.8 <i>In vivo</i> efficacy studies of reversing DOX resistance on K562/P-gp in NOD/SCID mice with or without FX3..... | 116 |
| 5.3 Summary | 122 |
| 5.4 Discussion | 122 |
| Chapter 6 Conclusions and perspectives | |
| 6.1 Conclusions..... | 125 |
| 6.2 Perspectives and further study | 129 |
| References..... | 131 |

List of Figures and Tables

| | |
|--|----|
| Figure 1. 1 Structure of NBD of ABC transporters binding with ATP. | 6 |
| Figure 1. 2 Predicted structures of MDR associated members of ABC transporters. | 8 |
| Figure 1. 3 Reciprocating twin-channel model of P-gp drug efflux | 11 |
| Figure 1. 4 Structures of P-gp | 12 |
| Figure 1. 5 Flavonoid family. | 18 |
| Figure 1. 6 Chemical structures of green tea flavonoids..... | 20 |
| Figure 1. 7 The structure of EGCG and its derivatives with chemical modification | 23 |
| Figure 1. 8 The effect of P-gp inhibition with EGCG and its derivatives..... | 23 |
| Figure 1. 9 Scheme of a series of green tea polyphenol derivatives. | 26 |
| | |
| Figure 2. 1 The passages of K562/P-gp cells for <i>in vivo</i> efficacy | 46 |
| | |
| Figure 3. 1 Location and Expression of P-gp in different cell lines. | 61 |
| Figure 3. 2 Effect of galloylated catechin derivatives on DOX and PTX accumulation. | 65 |
| Figure 3. 3 Effect of galloylated catechins derivatives on DOX efflux..... | 67 |
| Figure 3. 4 Effect of galloylated catechins derivatives on vanadate-inhibitable P-gp ATPase activity | 69 |
| Figure 3. 5 Accumulation and efflux of FX3 in K562 and K562/P-gp cells | 71 |
| Figure 3. 6 Experiment design about the interval treatment of FX3 and PTX | 72 |
| | |
| Figure 4. 1 MRM detection of galloylated catechins derivatives | 81 |
| Figure 4. 2 Blank plasma and derivatives in plasma chromatography | 86 |
| Figure 4. 3 Plasma level of FX3 in different formulations | 88 |
| Figure 4. 4 Pharmacokinetics profiles of galloylated catechins derivatives in BALB/c mice..... | 92 |
| Figure 4. 5 Effect of galloylated catechin derivatives on the metabolism of PTX with the human liver microsomes | 94 |

| | |
|--|-----|
| Figure 4. 6 Effect of galloylated catechin derivatives on the pharmacokinetics profile of PTX in BALB/c mice | 96 |
| Figure 5. 1 Toxicity assessment of galloylated derivatives with or without PTX | 105 |
| Figure 5. 2 <i>In vivo</i> efficacy of derivatives on modulating P-gp mediated PTX resistance on LCC6MDR | 110 |
| Figure 5. 3 Intra-tumor level of FX3 and PTX in LCC6MDR | 112 |
| Figure 5. 4 <i>In vivo</i> efficacy study of FX3 reversing resistance of DOX in P388ADR | 114 |
| Figure 5. 5 Establishment of K562/P-gp model <i>in vivo</i> | 120 |
| Figure 5. 6 <i>In vivo</i> efficacy study of FX3 reversing resistance of DOX on K562/P-gp | 121 |

| | |
|---|-----|
| Table 1. 1 List of anti-cancer drugs for chemotherapy in various cancer treatments | 2 |
| Table 1. 2 Distribution and expression of ABC transporter members | 7 |
| Table 1. 3 Green tea compound or EGCG reversing drug resistance in different cancer types via various mechanisms..... | 21 |
| Table 1. 4 Structures of green tea gallate derivatives with high potency of reversing resistance induced by P-gp..... | 27 |
| | |
| Table 2. 1. Ion pairs of all compounds for MRM detection..... | 39 |
| Table 2. 2 Candidate formulations for dissolving FX3..... | 41 |
| | |
| Table 3. 1 Structures and potency of galloylated catechins derivatives in modulating P-gp <i>in vitro</i> | 49 |
| Table 3. 2 IC ₅₀ of DOX and PTX and EC ₅₀ of derivatives in LCC6 and LCC6MDR cell lines | 53 |
| Table 3. 3 IC ₅₀ of DOX and PTX and EC ₅₀ of derivatives in P388 and P388ADR cell lines..... | 54 |
| Table 3. 4 IC ₅₀ of DOX and VCR and EC ₅₀ of derivatives in K562 and K562/P-gp cell lines..... | 54 |
| Table 3. 5 EC ₅₀ s of galloylated catechins derivatives in modulating BCRP and MRP-1 <i>in vitro</i> | 56 |
| Table 3. 6 Reversibility of FX3 in P-gp modulating..... | 73 |
| | |
| Table 4. 1 MS/MS condition optimization..... | 77 |
| Table 4. 2 Standard curve of 23, 51, FX3 and WBC5 | 86 |
| Table 4. 3 Plasma level of FX3 in different formulations..... | 89 |
| Table 4. 4 Pharmacokinetics parameters of galloylated catechins derivatives in BALB/c mice | 93 |
| Table 4. 5 Effect of galloylated catechin derivatives on AUC of PTX in plasma | 96 |
| | |
| Table 5. 1 Phase III trials investigating P-gp modulator in AML..... | 103 |
| Table 5. 2 Median survival day and ILS% in P388ADR efficacy study <i>in vivo</i> | 115 |
| Table 5. 3 Median survival day and ILS% in K562/P-gp efficacy study <i>in vivo</i> | 121 |

List of Abbreviations

| | |
|------------------|--|
| ABC | ATP-binding cassette |
| ABCA | ATP-binding cassette transporter subfamily A |
| ABCB | ATP-binding cassette transporter subfamily B |
| ABCC | ATP-binding cassette transporter subfamily C |
| ABCD | ATP-binding cassette transporter subfamily D |
| ABCE | ATP-binding cassette transporter subfamily E |
| ABCF | ATP-binding cassette transporter subfamily F |
| ABCG | ATP-binding cassette transporter subfamily G |
| ADESC | Animal Subjects Ethics Sub-committee |
| ATP | Adenosine-triphosphate |
| BCRP | Breast Cancer Resistance Protein |
| CML | Chronic Myeloid Leukemia |
| CDDP | Cisplatin |
| DOX | Doxorubicin |
| DMEM | Dulbecco's Modified Eagle Medium |
| EGCG | Epigallocatechin Gallate |
| EC ₅₀ | Half maximal effective concentration |
| FBS | Fetal bovine serum |
| GF120918 | Elacridar |
| HPLC | High performance liquid chromatography |
| IC ₅₀ | Half maximal inhibitory concentration |
| i.p. | Intraperitoneal |
| i.v. | Intravenous |

| | |
|----------|---|
| LC-MS/MS | Liquid chromatography-tandem mass spectrometry |
| MDR | Multiple drug resistance |
| MDR-1 | Multidrug resistance protein 1 |
| MGMT | O-6-methyguanine methyltransferase |
| MRP-1 | Multidrug resistance-associated protein 1 |
| NBD | Nucleotide binding domain |
| NADPH | Nicotinamide Adenine Dinucleotide Phosphate |
| NOD-SCID | Non-dose diabetic-severe combined immunodeficient |
| PBS | Phosphate buffered saline |
| P-gp | P-glycoprotein |
| PK | Pharmacokinetics |
| PMSF | Phenylmethanesulfonyl fluorid |
| PTX | Paclitaxel |
| q.2.d | Every two days |
| QSAR | Quantitative structure-activity relationship |
| Rho123 | Rhodamine 123 |
| RPMI | Roswell Park Memorial Institute |
| s.c. | Subcutaneous |
| TBST | Tris-buffered saline (TBS) and Polysorbate 20 |
| TMD | Transmembrane domain |
| UPLC | Ultra-performance liquid chromatography |

Chapter 1: Introduction

1.1 Cancer chemotherapy and multidrug resistance

There were more than 100 types of cancer, including the most common type of cancer, carcinoma which was derived from epithelial cells. Other types of cancers included sarcoma, leukemia, lymphoma, multiple myeloma, melanoma and brain and spinal cord tumors. The most common treatments included surgery, chemotherapy, radiotherapy and targeted therapy. Chemotherapy can be used before or after surgery. Pre-operative chemotherapy can shrink the tumor whereas postoperative chemotherapy can reduce cancer recurrence. Common anticancer drugs for chemotherapy were listed in **Table 1. 1**. These included DOX, fluorouracil, PTX, docetaxel, cyclophosphamide and gemcitabine. They can be administered alone or in combination. Examples included AC (DOX and cyclophosphamide), followed by T (PTX or docetaxel). TC (docetaxel and cyclophosphamide) and ACT (DOX, cyclophosphamide and docetaxel). Combination therapy increased the success rate of chemotherapy, but the overall success rate of chemotherapy varied widely. Chemoresistance was a huge obstacle in effective chemotherapy. It can be resulted from drug inactivation, drug target alteration, efflux, DNA damage repair, cell death inhibition and the epithelial-mesenchymal transition (EMT).

Table 1. 1 List of anti-cancer drugs for chemotherapy in various cancer treatments

| Class | Chemical reagent | Mechanism | Target disease |
|-------------------|-------------------------|--------------------------------|---|
| Anthracyclines | DOX | Topoisomerase II inhibitor | Leukemias, breast, stomach, lung, ovaries, bladder cancers, Hodgkin's lymphoma |
| | Daunorubicin | | Acute myeloid leukemia and acute lymphocytic leukemia |
| | Epirubicin | | Ovarian cancer, gastric cancer, lung cancer and lymphoma |
| Alkylating agents | Cisplatin | DNA alkylation | Sarcomas, ladder cancer, cervical cancer and germ cell tumors |
| | Cyclophosphamide | | Autoimmune disorders, and AL amyloidosis |
| Vinca alkaloids | Vinblastine | Inhibit mitosis | Hodgkin's lymphoma, non-small cell lung cancer, bladder cancer, brain cancer, melanoma, and testicular cancer |
| | VCR | | Leukemias, lymphomas, neuroblastoma, and sarcomas |
| Taxanes | PTX | Microtubule assembly inhibitor | Ovarian cancer, breast cancer, lung cancer and pancreatic cancer |

1.1.1 Drug inactivation

Drug activation and inactivation were usually mediated by cytochrome P450 (CYP) and glutathione-S-transferase (GST) systems. Many anticancer drugs must undergo metabolic activation to acquire the clinical efficacy (Sampath et al. 2006). Variation in CYP might affect the treatment effectiveness in patients by changing the drug metabolism (Hayes and Pulford 1995). GST superfamily was a group of detoxifying enzymes which catalyzed the conjugation between glutathione and xenobiotics to protect cellular macromolecules (carbohydrates, lipids, proteins, and nucleic acids) from nucleophilic attack (Michael and Doherty 2005). Elevated GST can enhance the detoxification in cancer cells and result in the reduced efficacy of anti-cancer drugs (Hayes and Pulford 1995).

1.1.2 Alteration of drug targets

Alteration of drug target decreased the treatment efficacy. One example was imatinib-resistance in CML. Imatinib was a tyrosine kinase inhibitor targeting the BCR-ABL protein in chronic myeloid leukemia (CML) patients (Maekawa et al. 2007). Primary or acquired resistance to imatinib in CML patients might be caused by the mutation in imatinib-binding kinase domain of BCR-ABL or by gene amplification. Overexpression of efflux drug transporter and activation of ERK1/2 might also cause imatinib resistance (Meenakshi Sundaram et al. 2019).

1.1.3 DNA damage repair

Chemotherapy drugs could be cytotoxic by causing DNA damage directly or indirectly. For example, cisplatin (CDDP) caused harmful DNA crosslinks, resulting in apoptosis (Dasari and Tchounwou 2014). O-(6)-methylguanine-DNA methyltransferase (MGMT) can repair the damaged DNA, thereby causing CDDP

resistance. Therefore MGMT-proficient cells were highly resistant to CDDP (Chen et al. 2015). Drugs targeting MGMT were developed to reverse resistance but had limited success clinically due to non-specific toxicity.

1.1.4 Drug efflux

A common cause of chemo-resistance was the reduced drug accumulation resulting from the overexpression of ATP-binding cassette (ABC) transporter family proteins (Juliano and Ling 1976). Elevated expression of ABC transporter in tumor cells was associated with poor clinical outcomes (Tamaki et al. 2011). Through the conformational change, ABC transporters can pump the drug substrates out of cells. ABC transporters had broad substrate specificity, thereby resulting in the resistance to a wide range of unrelated chemotherapy drugs. These substrates included vinca alkaloid (vinblastine and vincristine (VCR)), anthracyclines (DOX and daunorubicin), RNA transcription inhibitor (actinomycin-D) and microtubule-stabilizing drug (PTX) (Ambudkar et al. 2003).

1.2 Overview of ABC transporters

ABC transporters could be found in many different organisms and they carried out many different functions, either exporters and importers. Structurally, they had two distinct domains, namely nucleotide binding domain (NBD) and transmembrane domain (TMD). The NBDs of these transporters were highly conserved among all ABC transporters. The TMDs were responsible for substrate binding and unique in different ABC transporters.

As shown in **Figure 1. 1**, the highly conserved NBD contained the following domains (1) Walker A motif (also known as P-loop responsible for phosphate binding) (2) Walker B motif (3) H loop (a highly conserved histidine responsible for binding to ATP) (4) Q loop (a highly conserved Q involved in coupling of the nucleotide hydrolysis to conformational change of TMD). In those ABC transporters with two NBDs, they could form a dimer upon binding to ATP (Hung et al. 1998, Wilkens 2015). On the other hand, the TMDs displayed no significant sequence conservation. This probably explained why ABC transporters had a wide range of substrate specificity. Each TMD had 6 to 10 transmembrane α -helices. In general, NBD bound and hydrolyzed ATP, resulting in a conformational change in TMD and drove the substrate removal from TMD.

In human, there were 49 ABC transporters grouped into seven subfamilies (ABCA–ABCG). They had a very wide range of tissue distribution, substrate specificity and functions (**Table 1. 2**). Four subfamilies (A, B, C and G) were related to drug resistance in cancer (Wilkens 2015). The most important ones included ABCB1/MDR1/P-gp, ABCC1/MRP-1, ABCG2/BCRP. Their general structures were shown in **Figure 1. 2**.

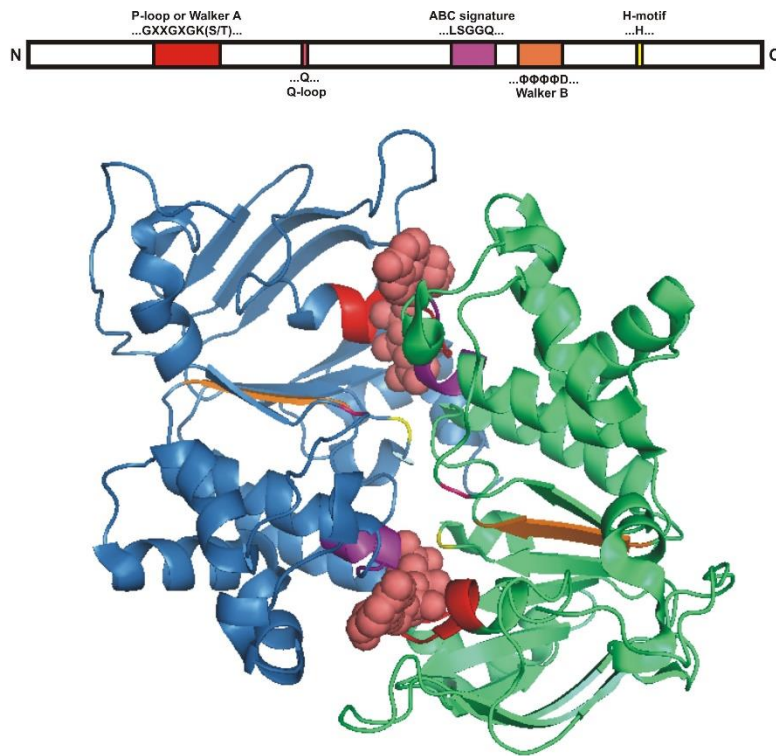


Figure 1. 1 Structure of NBD of ABC transporters binding with ATP.

Blue and green parts were NBD1 and NBD2, respectively. Red regions were Walker A motifs. Orange regions were Walker B motifs. Purple regions were ABC signature motifs. Yellow lines were H loops and red lines were Q loops (Rees et al. 2009).

Table 1. 2 Distribution and expression of ABC transporter members

| Family | Members | Tissue expression | Function |
|---------------|------------------------------------|--|--|
| ABCA | ABCA1(ABC1, TGD, HDLDT1, CERP) | Plasma membrane | Removal of phospholipids and cholesterol on to high-density lipoprotein particles |
| | ABCA2 (ABC2) | Brain, kidney, lung, heart, lysosomal membrane | Steroid transport |
| ABCB | ABCB1 (MDR1, P-gp, P-glycoprotein) | Epithelial cells of kidney, liver, choroid plexus, intestine; endothelial cells of brain capillaries | Multidrug resistance |
| | ABCCB2; ABCB3 | Ubiquitous (ER) | Peptide transport |
| | ABCB4 | Liver | Phosphatidylcholine transport |
| | ABCB6; ABCB7 | Ubiquitous in mitochondria | Iron transport |
| | ABCB11 | Liver | Bile salt transport |
| ABCC | ABCC1(MRP-1) | Ubiquitous in normal tissues (mainly lung and choroid plexus epithelial cells and brain capillary endothelial cells) | Drug resistance |
| | ABCC2 | Liver, intestine, kidney, brain endothelial cells | Organic anion efflux, hepatobiliary extrusion of amphiphatic ions |
| | ABCC3 | Liver, bile ducts, gut, adrenal cortex of kidney, intestine, placenta | Drug resistance |
| | ABCC6 | Kidney, liver (plasma membrane) | Elastic tissue |
| | ABCC12 | Brain and testis lower in all other tissues | |
| ABCD | ABCD1-4 | Many tissue (peroxisomes) | Very long chain saturated fatty-acyl-CoA (VLCFA) transport regulation |
| ABCE | ABCE1 | Ovary, testes, spleen | Oligoadenylate binding protein |
| ABCG | ABCG2 (ABCP, BCRP) | Liver, placenta, small intestine; also in heart, lung, skeletal muscle, kidney, spleen, thymus, brain capillaries | Drug resistance, stem-cell differentiation, survival of stem cells (under hypoxic condition) |
| | ABCG4, 5, 8 | Liver, intestine | Sterol transport, biliary cholesterol secretion / absorption |

(Liu and Pan 2019)

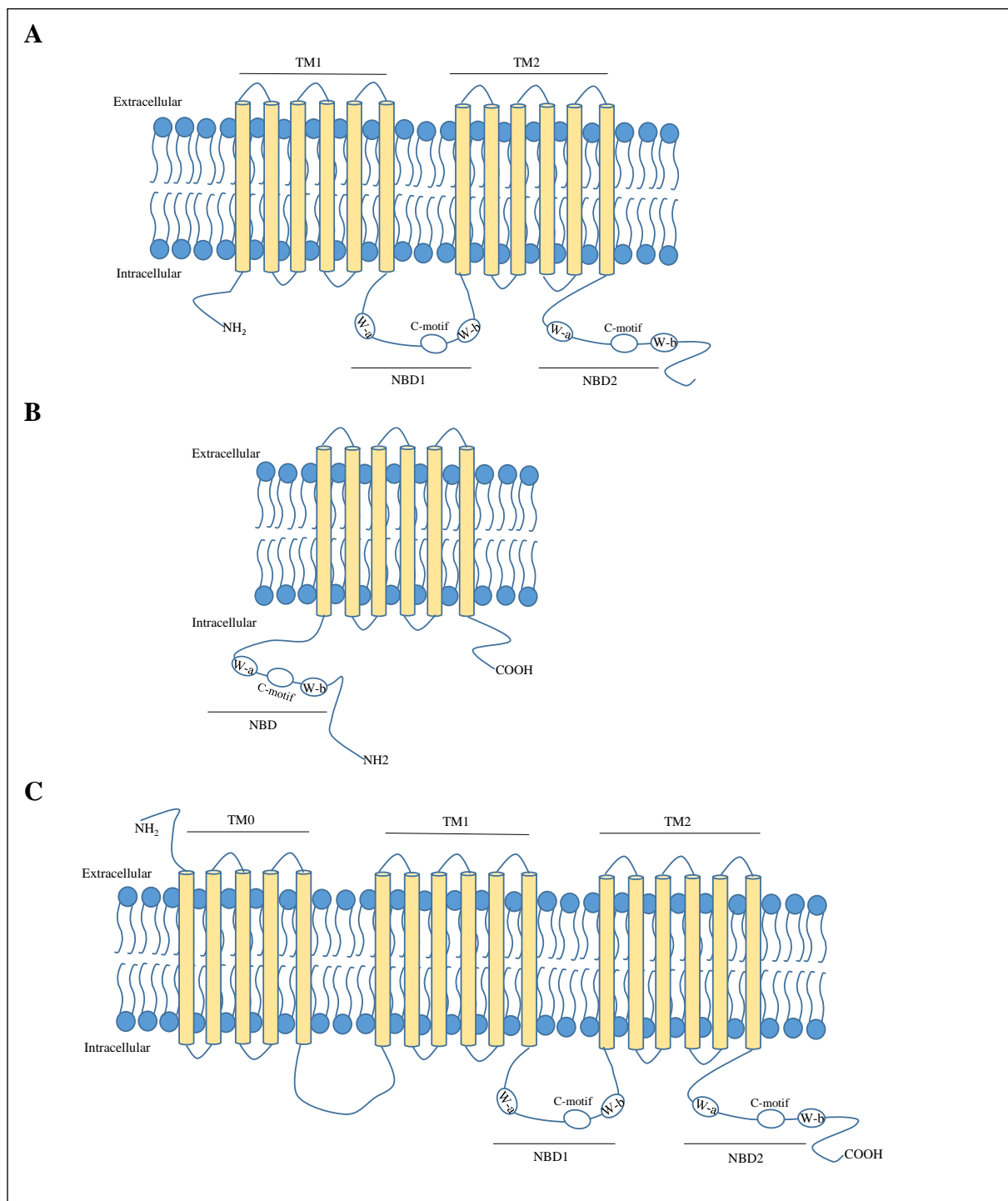


Figure 1. 2 Predicted structures of MDR associated members of ABC transporters.

W-a was Walker A motif. W-b was Walker B motif. C-motif was C loop. NBD was nucleotide binding domain. TM was transmembrane domain shown as yellow rectangles. (A) Predicted structure of ABCB1; (B) predicted structure of ABCG2; (C) predicted structure of ABCC1.

1.2.1 P-gp

Active efflux of multiple drugs in drug-resistant cells resulted in cross-resistance in chemotherapy agents. This phenomenon was called multi-drug resistance (MDR). MDR phenotype was first identified as an overexpression of a membrane protein termed P-gp. P-gp was encoded by the ABCB1 (MDR-1) gene and it was a transmembrane protein of 170kDa with 1280 amino acids (Riordan et al. 1985). The crystal structures of P-gp have been determined for mouse, *C.elegans*, and *Cyanidioschyzon merolae* orthologs. All of these structures had similar conformation with 4 domains including 2 transmembrane domains (TMD) and 2 nucleotide-binding domains (NBDs) (**Figure 1. 2. A**). Two TMDs contained 12 transmembrane (TM) α -helices segments and each TMD was consisted of 6 TM helices. Two TMDs formed a large and flexible internal cavity opened to cytoplasm, which were highly hydrophobic and responsible for substrate binding and efflux. Each TMD was linked to one NBD. NBDs were highly hydrophilic and responsible for ATP-binding and hydrolysis. The whole pumping process of P-gp included the substrate binding to TMDs, two MgATPs binding to NBDs and dimerization of NBDs. ATP hydrolysis at NBDs drove the conformational change of TMD. Substrate was released. NBD was dissociated with P-gp turning to the ground state for the next cycle.

The “reciprocating twin-channel” model explained the transport mechanism (**Figure 1. 3**). The model indicated that one ATP hydrolysis cycle at each NBD was coupled to a complete event of one substrate translocation (Jones and George 2014). ATP binding on NBD1 opened the binding site on TMD2 for the substrate. ATP hydrolysis and the release of ADP was coupled with the translocation and release of substrate. Subsequently, another ATP bound to NBD2 causing the efflux of substrate on TMD1. The affinity of two binding sites on TMD 1 and 2 was drug-specific (Jones and

George 2014). These binding sites were highly flexible and accommodated multiple chemicals simultaneously. For example, LDS-751 and rhodamine123 could interact with P-gp in a non-competitive manner (Loo et al. 2003).

In a recent study, the structure of human P-gp in an ATP-bound, outward-facing conformation was determined by electron cryo-microscopy at 3.4-Å resolution as shown in **Figure 1. 4. A**. The structure was stabilized by mutations that prevented P-gp from ATP hydrolysis. Such structure probably reflected a state that occurred after NBD dimerization but before ATP hydrolysis. In this outward-facing model, the TM helices packed closely in the membrane inner leaflet. The two “crossing” helices in each TMD (TM 4-5 in TMD1 and TM 10-11 in TMD2) pivot inward, bringing the NBDs closer to each other during the transition of P-gp from the inward- to the outward-facing conformation (**Figure 1. 4. A**). In addition, the extracellular regions of TM 7 and 8 pulled away from TM 9-12, resulting in an outward-facing configuration (**Figure.1. 4. A**). The two cytosolic NBDs made extensive contact with each other and two ATP molecules were bound at the dimer interface, interacting with the Walker A motif of one NBD and the ABC signature motif of the other NBD (**Figure 1. 4. B**). In this outward facing conformation of human P-gp, the drug-binding site was collapsed and the substrate was absent in this conformation suggesting that substrate release occurred prior to ATP hydrolysis (Kim and Chen 2018).

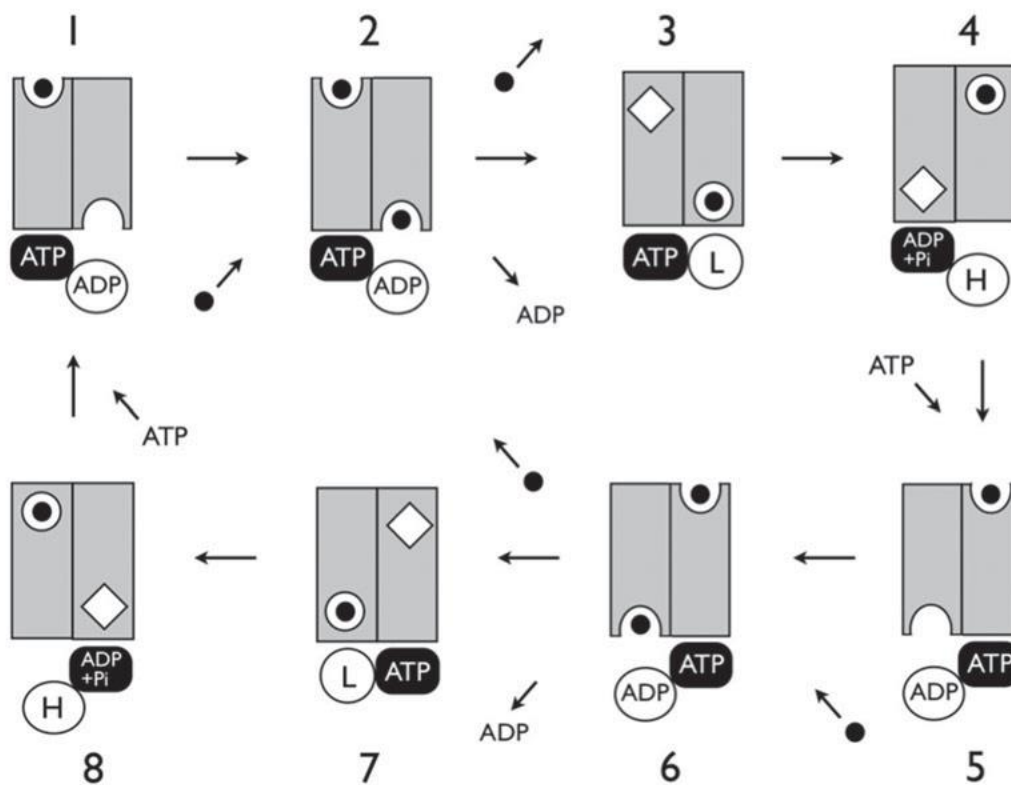


Figure 1. 3 Reciprocating twin-channel model of P-gp drug efflux

Black circle was the substrate. White semi-circle was the opening of substrate binding site. Grey rectangle was the TMD.

(1-2) One ATP binding on NBD1 induced substrate binding on TMD2.

(3-4) One ATP hydrolysis and the substrate on TMD2 was translocated.

(5-6) Another ATP bound on NBD2 induced the substrate binding on TMD1 and the translocated substrates on TMD2 was ready to release.

(6-8) The substrate on TMD2 was efflux. With the hydrolysis of ATP on NBD2, resulting in the translocation of substrate on TMD1.

(Jones and George 2014)

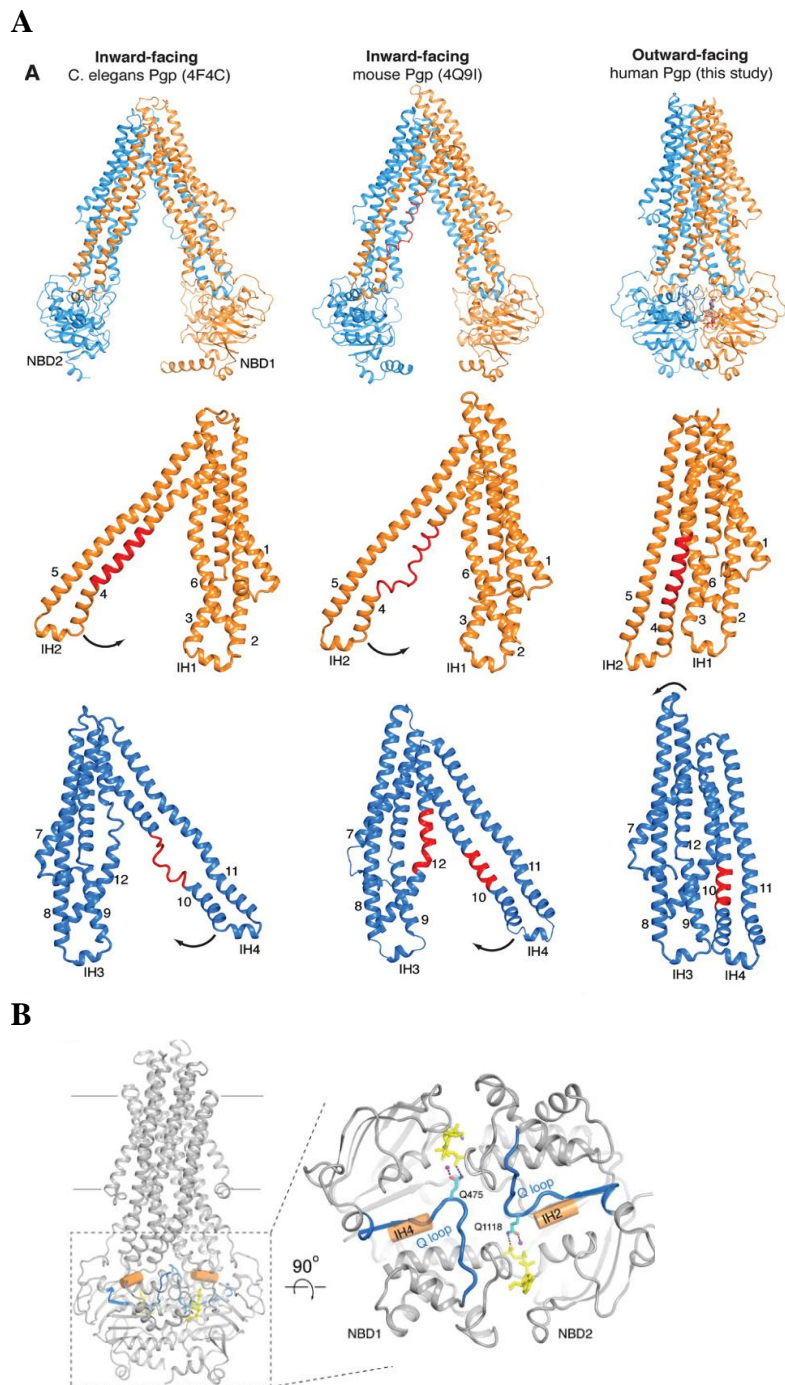


Figure 1. 4 Structures of P-gp

(A) Structures of two representative inward-facing P-gp and the outward-facing human P-gp. TM1-6 of TMD1 were labelled in orange and TM 7-12 of TMD2 were labelled in blue. The flexible regions in TM4 and TM1 were colored in red. Rotations of TM4-5 (yellow) and TM10-11 (blue) necessary for the transitions were indicated by black arrows. (B) Two symmetrical ATPase sites. The Q loops (shown in blue) in the NBD dimer were positioned to interact with Mg^{2+} /ATP (magenta and yellow) and the TMDs through the two intracellular helices IH2 and IH4 (orange). Q475 and Q1118 were the highly conserved glutamine residues in the Q loops (Kim and Chen 2018).

1.2.2 Breast cancer resistant protein (BCRP)

BCRP, also known as ABCG2, belonged to the ABCG subfamily in ABC transporter. BCRP was widely expressed in the placenta, blood-brain barrier, gastrointestinal tract, liver, kidney, testis, and lactating breast (Han et al. 2018). Overexpression of BCRP conferred resistance to a wide range of chemotherapeutics such as mitoxantrone, topoisomerase I inhibitor and several TKIs (imatinib, gefitinib and nilotinib)(Noguchi et al. 2014). BCRP expression was correlated with the poor clinical outcomes in non-small cell lung cancer, acute myelogenous leukemia or acute lymphocytic leukemia patient with MDR (Sargent et al. 2001, Ota et al. 2009, Noguchi et al. 2014). BCRP only had one TMD and one NBD. This meant that BCRP was a half transporter with six transmembrane α -helices in one TMD as shown in **Figure 1. 2. B**. Dimerization of BCRP was required to activate its transport function (Krishnamurthy and Schuetz 2005, Noguchi et al. 2014).

1.2.3 Multidrug Resistance-associated Protein-1 (MRP-1)

The human multidrug resistance-associated protein (MRP) family currently had seven members. They also transported a wide range of anti-cancer drugs out of cells resulting in drug resistance. Among the MRPs family, MRP-1 (ABCC1) was firstly discovered from a human lung carcinoma cell line (Cole et al. 1992) and it was a well-studied transporter causing MDR (Lu et al. 2015). MRP-1 was a 190 kDa polypeptide and was composed of three TMDs and two NBDs as shown in **Figure 1. 2. C**. It contained an additional TMD with five transmembrane α -helices segments, which was transmembrane domain zero (TMD₀), at the amino terminus compared to P-gp. The similarity of the structure between P-gp and MRP-1 resulted in the overlap in their drug resistance spectra (Brangi et al. 1999, Litman et al. 2000). However,

taxanes were substrates of P-gp but not MRP-1 (Brooks et al. 2003).

The function of each transporter in the MRP family was clarified in recent studies. MRP transporters were organic anion transporters and had a role in resistance to nucleoside analogues for cancer chemotherapy. MRP-1, MRP-2 and MRP-3 can also cause resistance to neutral organic drugs. MRP-1 conferred resistance to arsenite and MRP-2 to cisplatin (Borst et al. 2000).

1.3 Reversing MDR1/P-gp resistance

The P-gp knock-out mice showed increased drug absorption and decreased drug elimination indicating that P-gp played a role in drug absorption, distribution, metabolism, and excretion profile (Lund et al. 2017). Clinical studies indicated that P-gp was expressed in 41% breast tumor (Trock et al. 1997). Overexpression of P-gp in breast cancer can increase the likelihood of chemotherapy failure and relapse by 3-folds (Choi and Yu 2014). Adult patients with P-gp positive acute myeloid leukemia also had a higher chance of treatment failure and shorter survival (Shaffer et al. 2012). Many strategies were proposed to overcome MDR by inhibiting P-gp, including small molecules for P-gp modulating, nanoparticle drug delivery systems of anticancer drug and modulation of P-gp by microRNA.

1.3.1 P-gp modulators

Inhibition of P-gp by small molecule inhibitors appeared to be a logical approach to circumvent MDR. P-gp inhibitors were mainly divided into competitive and non-competitive inhibitors depending on the modulation mechanism (Mora Lagares et al. 2019). Competitive inhibitors exerted their function by tight binding and blocking the substrate binding pockets. Non-competitive inhibitors inhibited the ATPase activity or

modulated transporters' function allosterically.

The development of P-gp inhibitor could be categorized into three generations. First-generation P-gp inhibitors (verapamil, cyclosporin A) were found to be competitive inhibitors. The low potency and toxicity of the first-generation P-gp inhibitors precluded them from further development for clinical use (Palmeira et al. 2012).

Second generation P-gp modulators (PSC833) were generated by optimizing the first-generation P-gp modulators. Although they were less toxic and more potent, they were limited by their unpredictable pharmacokinetic interactions with the anti-cancer drugs by inhibiting CYP3A (Fischer et al. 1998). It was also reported that PSC833 and cyclosporin A affected the detoxification of chemotherapeutic agents by inhibiting bile salt export pump and reducing bile salts secretion (Akashi et al. 2006). The second-generation modulators ultimately failed to improve the outcome in clinical trial because of the compromised dosage of anticancer agents to prevent toxicity.

Third generation P-gp modulators were developed by quantitative structure-activity relationship (QSAR) studies and high throughput screening. They included XR-9576 (tariquidar) (Fox and Bates 2007), LY335979 (zosuquidar) (Tang et al. 2008) and R101933 (laniquidar). They were highly selective for P-gp, potent and safe in *in vitro* studies. In Phase I study of tariquidar and zosuquidar, there was no noteworthy side effect and pharmacokinetic interaction, and they could be safe to patient with AML or solid tumor. However, zosuquidar failed to improve the clinical outcome in a randomized placebo-controlled double-blind trial in patients with AML in Phase III (Cripe et al. 2010). The failure can be partly due to poor patient selection criteria, but the main reason was the benefit of P-gp modulation could be overwhelmed by other resistance mechanisms.

Some P-gp inhibitors also displayed dual inhibitory effect on ABCG2 including

tariquidar and elacridar (Hyafil et al. 1993, Gardner et al. 2009). The activity of dual inhibitor was a double-side sword. It could effectively overcome the MDR induced by both two transporters and increase the potency of anticancer drug as the substrate of both transporters. However, the dual inhibitors might inhibit physiological regulation of endogenous and xenobiotic compounds in the body. The narrow therapeutic dosage of the anticancer agent should be considered.

From a safety point of view, it was ideal to develop the P-gp specific inhibitor with no pharmacokinetics interaction with anticancer drugs. P-gp modulators from natural products have been referred to as the fourth-generation inhibitor. Some of these compounds originally displayed effect on cancer prevention or treatment, but their sensitizing effects to chemotherapeutics by modulating P-gp can also be improved. Different flavonoids had potential to be potent modulators of ABC transporter including quercetin, apigenin and galloylated catechins (Bin et al. 2013, Wong et al. 2015, Wong et al. 2021).

1.3.2 Nanoparticle drug delivery systems

Nanoparticle drug delivery systems meant encapsulating drugs in liposomal nanoparticles for the targeted delivery and controlled release. The nanoparticle can solve the low solubility problem of the drug, increase the bioavailability and effectively deliver drugs to target site. Tumors had abnormal blood vessel structure that favored accumulation of nanoparticles. Some encapsulated drugs in nanoparticles were approved for clinical application with promising outcome such as Doxil and Abraxane. They were approved for cancer treatment after intolerance or failure of prior systemic chemotherapy (Tejada-Berges et al. 2002, Kundranda and Niu 2015). Additionally, encapsulation of DOX in hydrophobic polymeric micelles can inhibit P-gp-mediated drug efflux and enhance intracellular drug concentration without

affecting P-gp expression (Jin et al. 2015). Nanoparticle delivering the combination of P-gp modulator and anticancer drug was also a promising approach to overcome MDR (Patil et al. 2009).

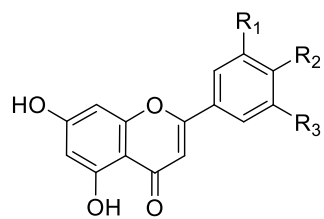
1.3.3 microRNA (miRNA) modulating P-gp

MicroRNAs (miRNAs) were small non-protein-coding RNAs with 18–25 nucleotides in length that can regulate multiple target genes at the post-transcriptional level. miRNAs bound to the 3' Untranslated Region (3' UTR) of targets mRNA and induce mRNA degradation or repression of protein translation. Several studies reported that miRNA could modulate the expression of P-gp. Up-regulation of miR-27a and miR-451 and down-regulation of miR331-5p were involved in activating the expression of P-glycoprotein in ovarian cancer, leukemia, and hepatocellular carcinoma (Zhu et al. 2008, Feng et al. 2011). These miRNAs could be potentially used to reverse MDR because miRNAs were naturally occurring endogenous molecules, ensuring their safety. However, miRNA research was a relatively new topic and the understanding of miRNA modulation was still insufficient. Off-target effects and RNA degradation remained unresolved issues.

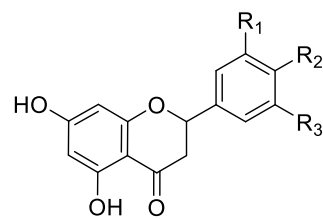
1.4 Green tea polyphenols

1.4.1 Green tea polyphenols and cancer-related biological effect

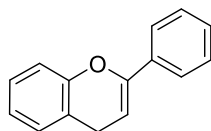
The chemical composition in the green tea was complicated, but one of the most important and well-known chemicals was polyphenols. Flavonoids was a sub-family of polyphenols. It was constituted by a large family of compounds including flavones, flavanones, flavonols and flavanols (**Figure 1. 5**).



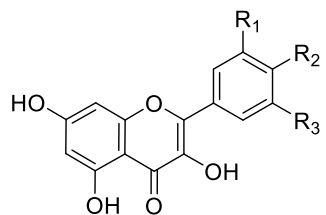
Flavones



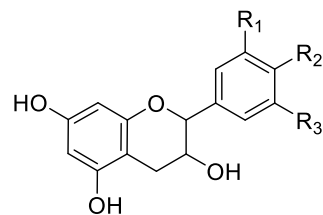
Flavanones



Basic Flavonoid Structures



Flavonols



Flavanols

Figure 1. 5 Flavonoid family.

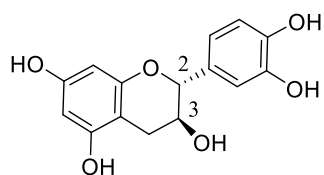
The chemical structures of flavonoid family including flavones, flavanones, flavonols and flavanols, were listed.

Catechin compounds were the main flavonols in green tea. The main structure of catechins contained a benzopyran skeleton with a phenyl group substituted at the 2-position and a hydroxyl or ester group at the 3-position (**Figure 1. 6**). Catechin compounds could be mainly divided into two categories including catechins and galloylated catechins (**Figure 1. 6**). Catechins contained catechin (C), epicatechin (EC), gallocatechin (GC) and epigallocatechin (EGC). When an extra gallate was attached to the 3 position of above 4 catechins, they were named (-)-catechin gallate (CG), (-)-epicatechin gallate (ECG), gallocatechin gallate (GCG) and epigallocatechin-3-gallate (EGCG) respectively (McKay and Blumberg 2002). The hydroxy or ester groups at the 3-position of the C and EC was in a cis and trans configuration respectively. Same was true for the pairs of GC and EGC, CG and ECG, GCG and EGCG (Ai et al. 2019).

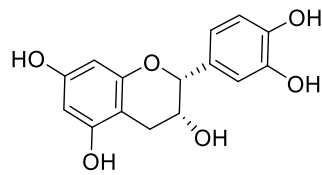
EGCG was the most abundant flavonols (up to 59%) in green tea (Cabrera et al. 2006). It can prevent cancer, cardiovascular and neurodegenerative disease, probably through its excellent antioxidant effect and other activities. The antioxidant activity of EGCG was 25-100 times more potent than Vitamin C (Rice-Evans et al. 1996, Chowdhury et al. 2016). EGCG induced cancer cell apoptosis and cell cycle arrest through several signaling pathway. Interestingly, EGCG displayed the above effects without interfering normal cells (Khan and Mukhtar 2008). Epidemiological studies revealed that the increasing consumption of green tea reduced the frequency of cancer occurrence, particularly in ovarian and prostate cancer (Steevens et al. 2007, Syed et al. 2007, Chen et al. 2008, Kurahashi et al. 2008).

EGCG can also reverse chemo-resistance by enhancing the DNA damaging effect of anticancer drugs or by modulating P-gp to inhibit drug efflux. The reversal activities of EGCG in different cancer types were summarized (**Table 1. 3**).

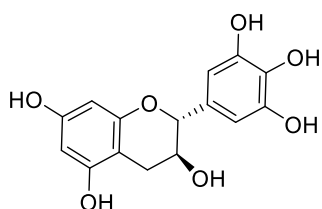
Catechins



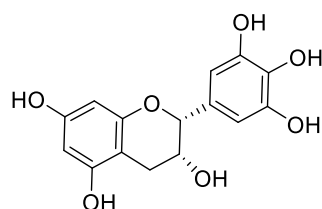
Catechin (C)



Epicatechin (EC)

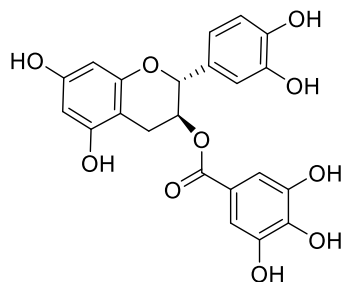


Gallocatechin (GC)

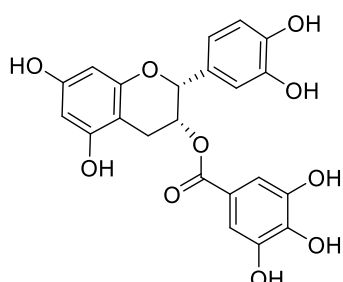


Epigallocatechin (EGC)

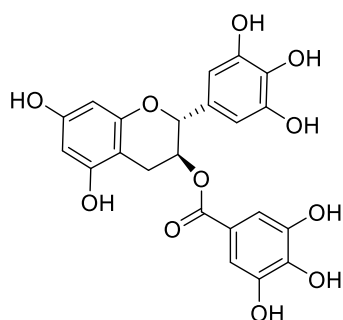
Galloylated catechins



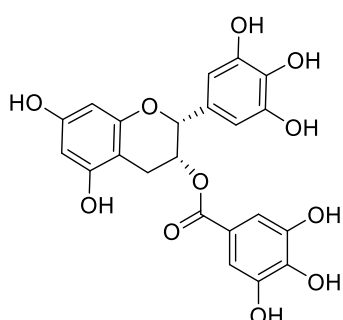
Catechin gallate (CG)



Epicatechin gallate (ECG)



Gallocatechin gallate (GCG)



Epigallocatechin gallate (EGCG)

Figure 1. 6 Chemical structures of green tea flavonoids

Catechins and galloylated catechins were main flavonols in green tea. The difference of the two groups compounds was the gallic acid group at 3-position.

Table 1. 3 Green tea compound or EGCG reversing drug resistance in different cancer types via various mechanisms

| Compound | Anti-cancer drug | Resistant cell line | Sensitization mechanism | Reference |
|-------------------------------------|--|---|---|---|
| EGCG | Cisplatin | A549/DDP (NSCLG) | Decreased methylation of GAS1, TIMP4, ICAM1 and WISP2 Inhibition of DNA methyltransferase (DNMT) activity and histone deacetylase (HDAC) activity | (Zhang et al. 2015) |
| Green tea polyphenol (GTP) and EGCG | Doxorubicin | KB-A-1 BEL740/DOX (Human HCC cell line) | Down-regulation of P-gp and HF1- α gene expression Increase anticancer drug accumulation through inhibition of ATPase activity of P-gp | (Mei et al. 2004, Zhang et al. 2004, Zhang et al. 2015) |
| GTP and EGCG | Vinblastine | CHRC5 Caco-2 | Inhibition of photolabeling of P-gp by 75% GTPs, particularly EGCG, inhibit the binding and efflux of drugs by P-gp. | (Jodoin et al. 2002) |
| EGCG | Tamoxifen | MCF-7/TAM (Human breast cancer cell line) | Down-regulation of Nrf-2 | (Esmaeili 2016) |
| EGCG | Adriamycin | MCF-7/ADR | Inhibition of the activity of P-glycoprotein | (Zhu et al. 2001) |
| EGCG | Paclitaxel | SKOV-3-ip2 (Ovarian cancer cell) | Promoting DNA damage response | (Chen et al. 2013) |
| GTP+quercetin | Docetaxel | PC-3 (Prostate cancer) | Potentiating the downregulation of most growth factors including VEGF, EGF, NGF- β , SCF, TNF- α , FGF- β , and TGF- β and increase the tumor cell apoptosis | (Wang et al. 2015) |
| EGCG | Overexpression of stem cell marker CD133 and ALDH1 | U87 glioma stem-like cells (GSLGs) | Downregulation of p-AKT, Bcl-2, P-gp and PARP | (Zhang et al. 2015) |

1.4.2 Modification of green tea catechins

Some studies tried to chemically modify the green tea catechins to improve their modulating activities. Sugihara studied the P-gp modulation activity of EGC, EGCG and their derivatives. Their structures were listed in **Figure 1. 7**. The results demonstrated that EGCG and ECG were more potent P-gp modulator than EGC and EC (**Figure 1. 8. A**), suggesting that the gallate moiety and the ester group were important for inhibiting P-gp. Furthermore, the mono-substitution of a methoxyl group at the 3' position (EGCG-3'O-ME) further improved the P-gp modulating activity of EGCG (**Figure 1. 8. B**) (Sugihara et al. 2011).

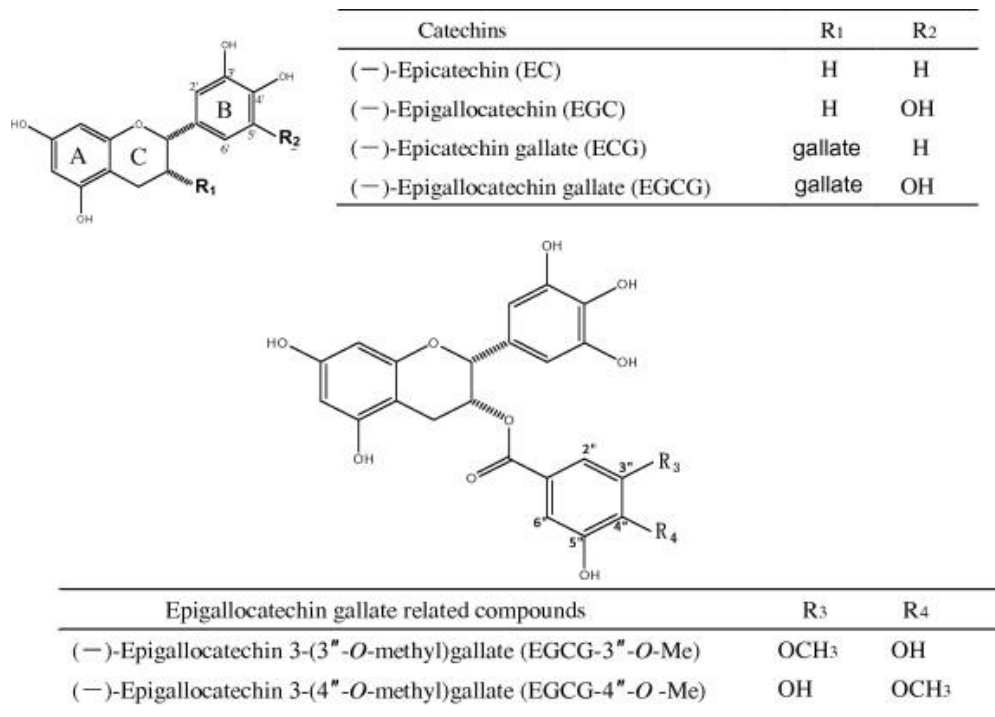


Figure 1. 7 The structure of EGCG and its derivatives with chemical modification

Chemical structures of EC, EGC, ECG, EGCG, EGCG-3''-O-Me and EGCG-4''-O-Me (Sugihara et al. 2011).

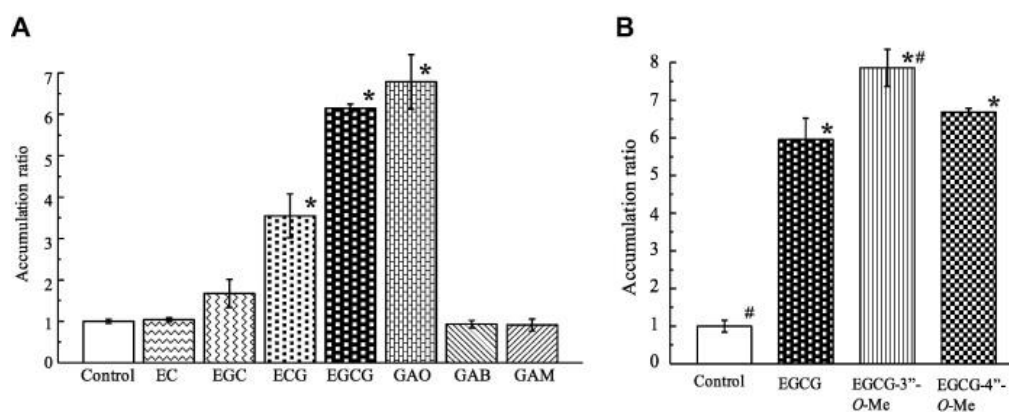


Figure 1. 8 The effect of P-gp inhibition with EGCG and its derivatives

Accumulation ratio of Rho123 fluorescence in LLG-GA5-CoL150 cells with different treatments. Chemical compounds were added to the medium at a concentration of 50µM. Rho 123 was added to the medium at a final concentration of 5µM. *, significant difference from the control value; $p < 0.05$. #, significant difference from the value of EGCG, respectively; $p < 0.05$ (Sugihara et al. 2011).

1.4.3 Previous work in our group on green tea catechins modification

Others and our group previously demonstrated side-chain methylation in quercetin and permethyl ningalin B could increase the P-gp modulating activity compared to their parent compounds (Ferte et al. 1999, Zhang et al. 2010, Bin et al. 2013). These results indicated that methylation could improve P-gp modulating activity.

Catechins (EGC, GC, EC and C; row 1 in **Figure 1. 9**) were modified by permethylation and addition of gallate to position 3 at ring C, resulting in the catechin derivatives in Row 2 (**Figure 1. 9**) (Wong et al. 2015, Wong et al. 2021).

Subsequently, the linker length and rigidity between rings C and D were further modified (Row 3 in **Figure 1. 9**). The P-gp modulating activity of these derivatives was evaluated by measuring the IC₅₀ (nM) towards PTX in LCC6MDR cells in the presence of 1 μM compounds. Lower IC₅₀ indicated a better P-gp modulating activity.

In the presence of 1 μM EGCG (compound 2 in Row 1, IC₅₀ of PTX=124.1 nM) and permethylated EGCG (compound 4 in Row 2, IC₅₀ of PTX= 25.0 nM), IC₅₀ of PTX was decreased by 5.2- fold (**Figure 1. 9**), suggesting that permethylation could decrease the IC₅₀ of PTX and enhance P-gp modulating activity.

In the presence of 1 μM compound 3 (mono-methoxy substitution on ring D, IC₅₀ of PTX=34.2 nM) or compound 4 (tri-methoxy substitutions on ring D, IC₅₀ of PTX=25.0 nM) (**Figure 1. 9**), the decrease of IC₅₀ suggested that tri-methoxy substitution displayed better P-gp modulating activity than mono-methoxy substitution.

In the presence of 1 μM compound 4 (carbonyl linker, IC₅₀ of PTX=25.0 nM) with compound 6 (oxycarbonylvinyl linker, IC₅₀ of PTX=3.7 nM) or compound 8 (oxycarbonylphenylcarbamoyl linker, IC₅₀ of PTX=3.3 nM) (**Figure 1. 9**), IC₅₀ of PTX was decreased by 6.8- or 7.6- fold, suggesting the linker length and rigidity

between rings C and D could further improve P-gp modulating activity. Same was true for the modification in other series of GC, EC and C compounds.

Compounds 6 and 10 were named as 23 and 51. They also displayed BCRP-modulating activity but no MRP-1 inhibiting activity (Wong et al. 2015). The compounds, WBC5 and FX3, with similar modification of EC and C series compounds, also displayed potent P-gp modulating activity (Wong et al. 2021).

23, 51, FX3 and WBC5 would be further studied in this thesis. Their structures and molecular weights were listed in **Table 1. 4**.

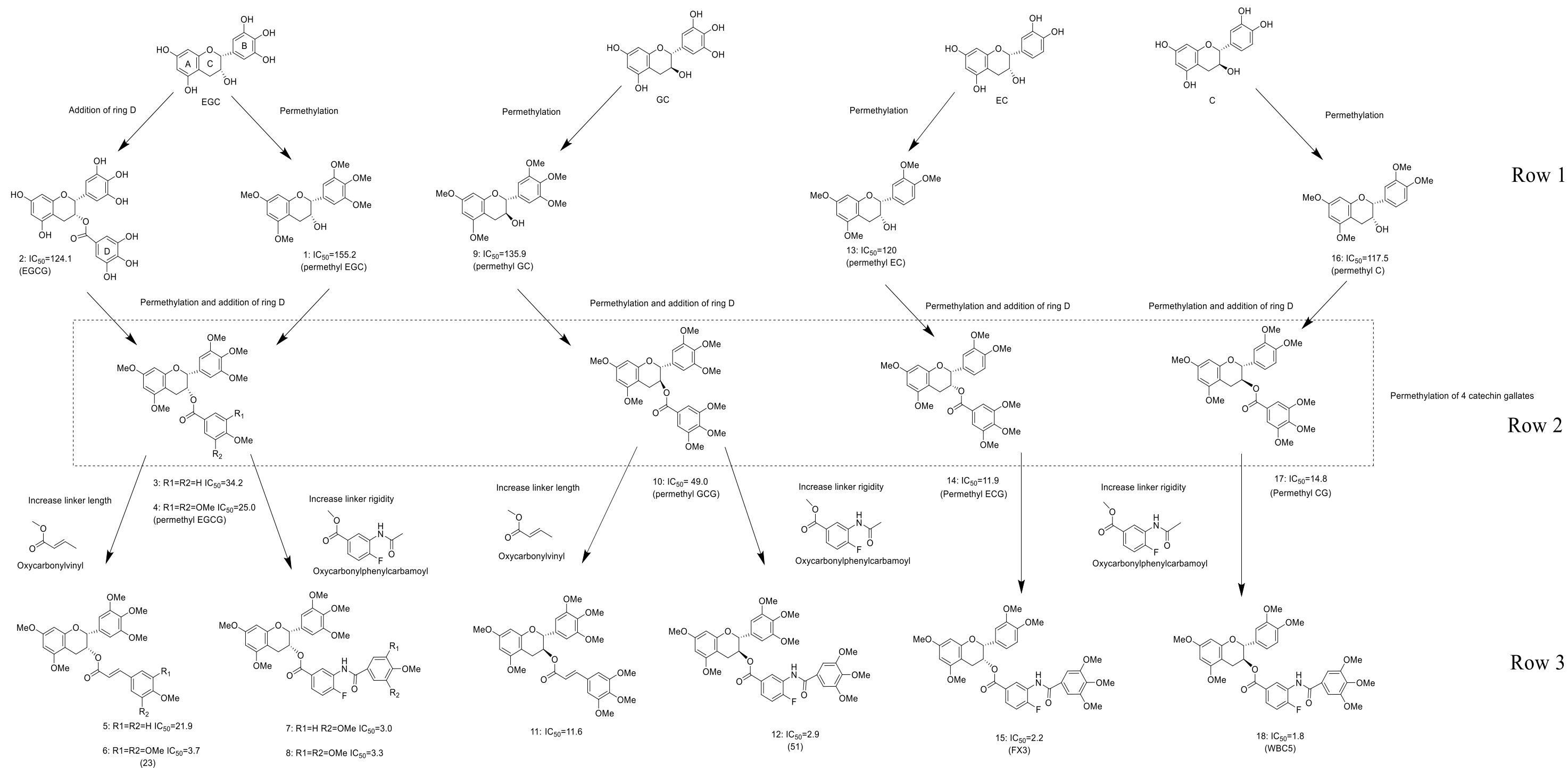
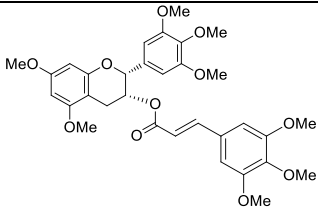
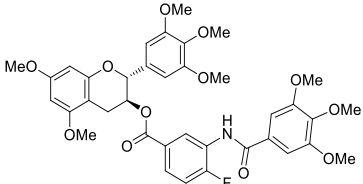
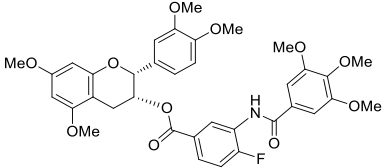
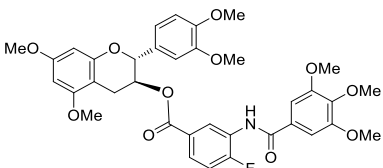


Figure 1. 9 Scheme of a series of green tea polyphenol derivatives.

The structures of a series of green tea polyphenol derivatives were listed. IC₅₀ (nM) was the concentration of PTX with the presence of 1 μM derivatives tested on LCC6MDR cells (Wong et al. 2015).

Table 1. 4 Structure of galloylated catechins derivatives with high potency of reversing resistance induced by P-gp.

| Compound | IUPAC name | Structure | Chemical Formula | Molecular Weight |
|----------|---|---|---|------------------|
| 23 | (2R,3R)-5,7-dimethoxy-2-(3,4,5-trimethoxyphenyl)chroman-3-yl (E)-3-(3,4,5-trimethoxyphenyl)acrylate |  | C ₃₂ H ₃₆ O ₁₁ | 596.226 |
| 51 | (2R,3S)-5,7-dimethoxy-2-(3,4,5-trimethoxyphenyl)chroman-3-yl 4-fluoro-3-(3,4,5-trimethoxybenzamido)benzoate |  | C ₃₇ H ₃₈ FNO ₁₂ | 707.696 |
| FX3 | (2R,3R)-2-(3,4-dimethoxyphenyl)-5,7-dimethoxychroman-3-yl 4-fluoro-3-(3,4,5-trimethoxybenzamido)benzoate |  | C ₃₆ H ₃₆ FNO ₁₁ | 677.67 |
| WBC5 | (2R,3S)-2-(3,4-dimethoxyphenyl)-5,7-dimethoxychroman-3-yl 4-fluoro-3-(3,4,5-trimethoxybenzamido)benzoate |  | C ₃₆ H ₃₆ FNO ₁₁ | 677.67 |

1.5 Summary

The main strategy for cancer therapies included surgery, radiotherapy, chemotherapy, and targeted therapy. Among them, chemotherapy was the most common approach, but drug resistance was a critical problem to therapy success. Drug resistances could be induced by different mechanisms. One of them is the drug efflux by ABC transporters.

ABC transporters were membrane proteins that could actively expel various cytotoxic drugs. P-gp was the first and best characterized transporter in ABC transporter family. Many chemotherapeutic compounds including taxanes (PTX, docetaxel), anthracyclines (DOX, daunorubicin), and vinca alkaloids (vinblastine, VCR) were substrates of P-gp and they could be expelled by P-gp resulting in the intracellular drug concentration below therapeutic level. Efflux of chemotherapeutic drug induced MDR phenomenon and limited the clinical efficacy. One possible approach to tackle the MDR problem was to modulate the function of P-gp and reduce the drug efflux. Three generations of P-gp modulators have been developed but they were not that successful, because of low potency and drug-drug interaction between the modulator and anti-cancer drug. Natural products have been investigated, as the potential fourth generation P-gp modulators. Green tea polyphenols have been shown to be potent P-gp modulators *in vitro* and *in vivo*. They were food-derived and therefore low toxicity was expected. Green tea polyphenols were comprised of catechins and galloylated catechins. A series of chemical modification on galloylated catechins were done in our

group (Wong et al. 2015, Wong et al. 2021). Structural modification could improve the potency of P-gp modulating activity.

1.6 Objectives of study

Based on the hypothesis that modulating P-gp could increase the anticancer drug accumulation and reverse MDR, the potent and non-toxic P-gp modulators were synthesized to reverse the MDR caused by P-gp. The objectives of this study were as following.

1. To demonstrate the modulating effect of novel galloylated catechin derivatives on P-gp and to reverse drug resistance *in vitro*.

The candidate derivatives would be used on P-gp overexpressing, BCRP overexpressing and MRP1-overexpressing cells to investigate the reversal efficacy *in vitro*. The activity of derivatives would be investigated in increasing the intracellular accumulation of anti-cancer drug and their general mechanism in P-gp modulating.

2. To study the pharmacokinetics of the galloylated catechins derivatives *in vivo*.

The four derivatives would be administrated by i.p. or i.v *in vivo*. Their plasma level would be measured by LC-MS/MS and be used to decide the optimal administration route and dosages in the subsequent efficacy assays. In addition, their pharmacokinetics study of co-administration with anticancer drugs would be conducted to check for potential drug-drug interaction.

3. To investigate the modulating efficacy of galloylated catechin derivatives on chemo-resistant tumor model *in vivo*.

LCC6MDR xenograft, P388ADR and K562/P-gp leukemia animal models would be established *in vivo*. The combination treatment of a derivative and anti-cancer drug would be administrated to demonstrate the safety and efficacy of the derivative in reversing MDR by modulating P-gp in laboratory animals.

Chapter 2: Methodology

2.1 Chemicals and materials for the studies

Methylated galloylated catechin derivatives (FX3, WBC5, 23 and 51) were provided by Professor Shengbiao Wan (Ocean University of China, Qingdao, Shandong Province, China). Their synthesis routes were reported previously (Wong et al. 2015, Wong et al. 2021). The purity of these compounds was analyzed by HPLC and all had purity over 98%. (3-(4,5-dimethylthiazol-2-yl)-5-(3-carboxymethoxyphenyl)-2-(4-sulfophenyl)-2H-tetrazolium) (MTS) and phenazine methosulfate (PMS) were purchased from Promega. PSC833 was kindly provided by Novartis. GF120918 was purchased from MedChemExpress (China), Shanghai, China. Doxorubicin (DOX), topotecan and paclitaxel (PTX) were purchased from Wuhan Hezhong Biochemical Manufacture Co, Ltd, Wuhan, China. All other chemicals and reagents in this study were purchased from Sigma-Aldrich. All organic solvents used were high performance liquid chromatography (HPLC) grade. Dulbecco's Modified Eagle Medium (DMEM), Roswell Park Memorial Institute (RPMI) 1640 medium, typsin/EDTA acid and penicillin/streptomycin (P/S) were purchased from Gibco. Fetal bovine serum (FBS) was obtained from Hyclone. 2008/MRP1, S1M180, LCC6, LCC6MDR, P388, P388ADR, K562 and K562/P-gp cell lines were used in the study. Human breast cancer cell lines LCC6 and LCC6MDR were kindly provided by Dr. Robert Clarke (Georgetown University, USA). Human leukemia cell lines K562 and K562/P-gp, and human colon cell line S1M180 were kindly provided by Professor Kenneth To (Chinese University of Hong Kong, Hong Kong SAR). The ovarian

cancer cell line 2008/MRP1 was kindly provided by Prof. Piet Borst (University of Amsterdam, Netherlands). Murine lymphoma cell lines P388 and P388/ADR were obtained from the National Cancer Institute (Bethesda, MD).

2.2 *In vitro* studies

2.2.1 Cell culture

LCC6 and LCC6MDR cells were cultured in DMEM medium with 10% FBS, 100 U/mL penicillin, and 100 µg/mL streptomycin. P388, P388ADR, K562 and K562/P-gp cells were cultured in RPMI1640 medium with 10% FBS, 100 U/mL penicillin, and 100 µg/mL streptomycin. All cell lines were cultured at 37°C in a humidified atmosphere of 5% CO₂.

2.2.2 Cell survival assay

In each well of 96-well plate, 6,500 cells of LCC6MDR and 10,000 cells of P388ADR or K562/P-gp cells were seeded in 180 µL complete medium (DMEM or PRMI1640) and incubated at 37°C incubator overnight. The four derivatives (23, 51, FX3 and WBC5) at different concentrations (0, 62.5, 125, 250, 500, 1000 nM in 10 µL) were added into the well. PTX or DOX was co-treated from 0 to 400 nM and from 0 to 40 µM, respectively. The final volume in each well of 96-well plate was 200 µL. Then, the plate was incubated at 37°C for 72 hr. MTS assay was used for determining the cell survival. MTS (2 mg/mL) and PMS (0.92 mg/mL) were dissolved in PBS. They were freshly mixed at the ratio of 50:1 before the MTS assay. For adherent cell lines (LCC6, LCC6MDR, S1M180 and 2008/MRP1), the medium in

each well was aspirated and then replaced by 50 μL of fresh DMEM media containing 10 μL mixture of MTS and PMS. For suspension cell lines (P388, P388ADR, K562 and K562/P-gp), 10 μL mixture of MTS and PMS was directly added into each well. The 96-well plate was incubated at 37°C in the dark for 1-2 hour and then performed the absorption detection at 490 nm using the microplate reader (Bio-rad). The % of cell survival, IC_{50} of the anticancer drug and EC_{50} of the modulator were analyzed using the nonlinear regression in Prism 5.0. IC_{50} was the concentration of anticancer drug killing 50% of cell population. EC_{50} was the concentration of the derivative at which it can decrease the IC_{50} of anticancer drug by half. All experiments were performed in triplicate, and the results were shown as mean \pm standard error of mean (sem).

2.2.3 DOX accumulation assay

DOX accumulation assay was done in 1000 μL volume. A 500,000 cells of P-gp overexpressing cells and their wild types were freshly put into the Eppendorf tube with complete medium. The cells were incubated with 20 μM DOX with or without modulators (0, 0.1, 0.5 and 1 μM) for 2.5 hr at 37°C in the dark. After incubation, cells were washed by cold PBS twice. Cell pellet was resuspended in 100 μL lysis buffer (0.2% triton and 0.75M HCl in isopropanol). Each sample was vortexed for 1 min and incubated at room temperature for 10 min. Then, the cells were centrifuged at 14,000 rpm for 5 min. The supernatant was collected and the DOX level was measured using Clariostar microplate reader (BMG LabTech) with an excitation wavelength of 460 nm and emission wavelength of 610 nm. All experiments were

performed in triplicate, and the results were shown as mean \pm sem.

2.2.4 DOX efflux assay

In the efflux assay, 500,000 cells were pre-loaded with 20 μ M DOX for 45 min at 37°C. Then, the cells were washed with cold PBS twice and replaced with drug-free complete medium with or without derivatives (0, 0.1, 0.5 and 1 μ M). The cells were further incubated at 37°C and collected at 1, 2 and 3 hr, respectively. Then, the cells were washed by cold PBS and finally resuspended in 100 μ L FACS buffer (1% bovine serum albumin and 1 mM EDTA in PBS). The intracellular DOX level at different time points was detected using BD Accuri™ C6 flow cytometer. All experiments were repeated at least three times. The values were presented as mean \pm standard error of mean.

2.2.5 Determination of P-gp expression using western blot

Cells (200,000/ well) were seeded in a 6-well plate one day before treatment. Then, the cells were treated with derivatives (23, 51, FX3 and WBC5) at 2 μ M for 72 hours. After treatment, medium was aspirated and cells were washed by cold PBS twice. The cells in each well were lysed with 100 μ L lysis buffer (50 mM Tris-HCl pH8.0, 150 mM NaCl, 1.0% NP-40, 0.5% sodium deoxycholate, 0.1% SDS, and 0.2 mM PMSF) at 4 °C for 15minutes. The lysed cells were centrifuged at 14,000 rpm at 4 °C for 10 min, the supernatant was collected. The protein concentration of the cell lysate was determined using Bradford assay. In the assay, the supernatant of cell lysate was 200-fold diluted using water. Diluted cell lysate (100 μ L) was mixed with 100 μ L of

Braford reagent. Then, the mixture was read at 595 nm using microplate reader. A standard curve of protein concentration was constructed using a serial dilution of BSA from 2 to 15 $\mu\text{g}/\text{mL}$. The correlation coefficient R^2 of the standard curve should be over 0.99. Y-axis was absorbance at 595 nm and X-axis was the protein BSA concentration. The protein amount of the cell lysate can be determined according to the BSA standard curve.

A 30 μg cell lysate of each sample was loaded on a 7.5% SDS-PAGE and then transferred to PVDF membrane. The membrane was blocked for with 5% non-fat dry milk in TBST buffer (0.1% Tween-20, 10 mM Tris-buffer pH 7.5 and 150 mM NaCl) 1 hour at room temperature, then it was incubated with 1:1000 primary antibody of mouse anti-P-gp (D-11, SC-55510, Santa Cruz) or 1:1000 mouse anti- β -actin (C4, SC-47778, Santa Cruz) at 4°C overnight. After gentle washing by TBST buffer, the membrane was incubated with 1:3000 secondary antibody (Goat anti mouse, IgG conjugated HRP, Santa Cruz) for 1 hour at room temperature. A chemiluminescent substrate was added to the membrane and its signal was detected using ChemiDoc Touch from Bio-Rad.

2.2.6 Determination of P-gp cellular localization using confocal microscope

Cells (100,000/ well) were seeded on a sterile glass coverslip in a 24-well plate overnight. The coverslip was pre-treated with poly-L-lysine for suspension cell adhesion. Coverslip with cells were fixed with 4% paraformaldehyde for 15 min at room temperature and then washed with PBS for three times. For cell permeabilization, the cells were incubated with 3% bovine serum albumin (BSA) and

0.1% triton-X100 in PBS for 30 mins at room temperature. After PBS washing, the cells were incubated with 1:100 primary antibody of MDR1 (clone D-11, SC-55510, Santa Cruz) at 4°C overnight. After PBS washing, the cells were incubated with 1:100 secondary antibody conjugated with Alexa Fluor 594 nm for 1 hour at room temperature. Then, the cells were then incubated with 1 µg/mL of DAPI (4',6-diamidino-2-phenylindole) for 10 min at room temperature. Coverslip was dried and sealed on a glass slide. The Leica TCS SPE inverted microscope was used for determining the localization of P-gp in P388, P388ADR, LCC6 and LCC6MDR cells. Laser of 405 nm was used for DAPI excitation and 561 nm was used for Alexa Fluor 594 excitation.

2.2.7 PTX metabolism on human liver microsome

Human liver microsome (1 mg/mL) was stored in -80 °C. Before the experiment, human liver microsome was freshly thawed on ice. A 100 µL human liver microsome was incubated with 10 µM PTX with or without derivatives (0, 0.1, 1, 5 and 10 µM). PTX and derivatives were dissolved in ACN. In the whole reaction, ACN content was lower than 0.25% to avoid the interference of metabolism. After 3-min pre-incubation at 37°C, 20 mM of nicotinamide adenine dinucleotide phosphate (NADPH) was added to initiate the metabolism reaction. For the negative control, same volume of distilled water was added. The reaction was kept at 37°C for 1 hour. The reaction was terminated by adding 300 µL ACN on ice. After ACN extraction, the samples were centrifuged at 14,000 rpm for 10 min and the supernatant was collected for determining PTX metabolites by LC-MS/MS.

2.2.8 P-gp ATPase activity

It was reported that trapping nucleotide by vanadate sufficiently inhibited the ATPase activity of P-gp (Urbatsch et al. 1995). P-gp ATPase activity in the microsome could be completely inhibited by Na₃VO₄ (sodium orthovanadate). ATP consumption was attributed to minor non-P-gp ATPase activity in membrane microsome. The basal level ($\Delta Luminescence Basal$) was the difference in luminescence between the remaining ATP level of Na₃VO₄ treated sample and remaining ATP level of non-treated sample. The results of the test compounds ($\Delta Luminescence Tested Compound$) were the difference in luminescence between the remaining ATP level of Na₃VO₄ treated sample and the remaining ATP level of verapamil, FX3 or WBC5-treated samples at different concentrations, respectively.

$$\Delta Luminescence Basal = Luminescence (Na_3VO_4 - No\ treatment)$$

$$\Delta Luminescence Tested Compound = Luminescence (Na_3VO_4 - Tested\ Compound)$$

P-gp ATPase activity was measured by P-gp-Glo assay system (Promega) with human P-gp membrane. Human P-gp membrane was stored at -80 °C and freshly thawed on ice before the experiment. A 20 μ L of P-gp-Glo™ Assay Buffer or 0.25 mM of Na₃VO₄ was incubated with verapamil and EGCG (in 20 μ L volume) from 0.01 to 200 μ M, FX3 and WBC5 from 0.01 to 70 μ M. A 20 μ L of P-gp membrane was pre-incubated in each well for 3 min at 37 °C. The reaction was initiated by adding 10 μ L of 25 mM MgATP and incubated at 37°C for 1 hour. After incubation, 50 μ L of ATP detection reagent was added to terminate the reaction. After 20-min incubation at room temperature, the remaining level of ATP was measured by a Clariostar

microplate reader (BMG LabTech). Vanadate-inhibitable P-gp ATPase activity was determined by calculating the difference in luminescence signal in the samples with and without sodium vanadate.

2.2.9 FX3 accumulation and efflux in K562 and K562/P-gp cells

For accumulation assay, 1,000,000 cells of K562 or K562/P-gp were incubated with FX3 at different concentrations (0.1, 1 and 10 μM) at 37°C for 2.5 hr. For efflux assay, the cells were pre-loaded with FX3 at 1 μM at 37 °C for 2.5 hr. Then, the cells were washed with PBS and resuspended in drug free medium. The cells were further incubated for 0, 30, 60 and 150 min. After the FX3 accumulation and efflux assays, medium was removed and cells were washed by PBS twice at different time points. The cell pellet was extracted by 300 μL ACN with 10-min sonication and then centrifuged at 14,000 rpm for 10 min. The supernatant was filtered by polymer membrane before ultra-performance liquid chromatography tandem mass spectrometry (UPLC-MS/MS) analysis.

2.3 UPLC-MS/MS detection method

2.3.1 MRM detection method of modulators

Agilent UPLC-triplequadrupole Mass Spectrometry was used for quantification. Multiple reaction monitor (MRM) was used to monitor the target compounds. The ion pairs of all compounds were shown in **Table 2. 1**.

Table 2. 1. Ion pairs of all compounds for MRM detection

| Compound | | MRM | | | Internal Standard |
|---------------------|----------------------|-------|---|-----------|---------------------|
| 23 | [M +Na] ⁺ | 579.2 | > | 181.1 m/z | 51 |
| 51 | [M +Na] ⁺ | 708.3 | > | 181.1 m/z | FX3 |
| FX3 | [M +Na] ⁺ | 678.3 | > | 151.0 m/z | 51 |
| WBC5 | [M +H] ⁺ | 678.2 | > | 151.0 m/z | 51 |
| PTX | [M +H] ⁺ | 854.5 | > | 286.0 m/z | ¹³ C PTX |
| C3'-OH PTX | [M +H] ⁺ | 870.0 | > | 302.0 m/z | PTX |
| 6 α -OH PTX | [M +H] ⁺ | 870.0 | > | 286.0 m/z | PTX |
| ¹³ C PTX | [M +H] ⁺ | 860.5 | > | 286.0 m/z | - |

2.3.2 Chromatography condition of modulators and PTX detection

Sample was injected into Acquity UPLC BEH C18 Column (1.7 μ m, 2.1*50 mm, Waters) at 0.3 mL/min. The elution solution was consisted of H₂O with 0.1% formic acid (Solvent A) and ACN with 0.1% formic acid (Solvent B). The gradient elution for the derivatives detection started from 80% solvent A and 20% solvent B. A linear gradient was performed from 20% to 45% of solvent B in 2 min and solvent B was continuously increased from 45% to 60% of solvent B from 2 to 13 min. For 14-15 min, solvent B reached 90% and then decreased to 20% in 1 min. The mobile phase was restored to start the condition at the 16th min for equilibration. The gradient elution for PTX and its metabolites detection started from 90% solvent A and 10% solvent B for 1 min and then linearly increased from 10% to 85% solvent B in 4 min. For 4-5 min, solvent B was kept at 85% and then mobile phase restored to start condition in 1 min. 90% solvent A and 10% solvent B were running from 6-8 min for equilibration.

2.4 *In vivo* studies

2.4.1 Animals

Female BALB/c mice (6-8 weeks old) were used in pharmacokinetics study and toxicity study. Female BALB/c nude mice (6-8 weeks old), male B2DF1 mice (6-8 weeks old) and female NOD/SCID mice (4-5 weeks old) were used in LCC6MDR xenograft, P388ADR and K562/P-gp efficacy experiments, respectively. Before the experiment, mice were allowed to adapt for 12-hr light/dark cycle for at least 7 days. Nude mice and B2DF1 mice were purchased from Beijing Vital River Laboratory Animal Technology Co. Ltd. NOD/SCID mice were purchased from The Laboratory Animal Services Centre of Chinese University of Hong Kong. These studies were approved by the Animal Subjects Ethics Sub-committee (ASESC) of The Hong Kong Polytechnic University and ASESC of Shenzhen Research Institute of The Hong Kong Polytechnic University.

2.4.2 Drug preparation and injection

PTX at 40 mg/mL was prepared in 50% ethanol and 50% Cremophor EL. Firstly, PTX was dissolved in ethanol and heated to 80 °C with agitation until PTX was totally dissolved. Equal volume of Cremophor EL was then added into the drug solution and vortexed until it became clear. This stock solution was stable for over one month at room temperature. Prior to injection, stock solution would be freshly diluted to 4 mg/mL by PBS. Diluted drug solution should be consumed within 15 min to avoid precipitation.

Galloylated catechin derivatives were dissolved in different combinations of solvent and co-solvent to determine the optimal formulation for the pharmacokinetics (PK) study. FX3 in different formulations, listed in **Table 2. 2**, was i.v. injected to BALB/c mice and the blood was collected at 30 and 60 min post administration. To screen the optimal formulation, concentration of FX3 in plasma was detected by LC-MS/MS.

Table 2. 2 Candidate formulations for dissolving FX3

| Solvent | Co-solvent | Solvent: Co-solvent: PBS (V/V/V) |
|----------------|-------------------|---|
| Ethanol | Cremophor EL | 1:1:8 |
| | Tween-80 | |
| | Tween-20 | |
| NMP | Cremophor EL | 1:1:8 |
| | Tween-80 | |
| | Tween-20 | |

FX3 was dissolved in different formulations at 1 mg/mL.

2.4.3 Pharmacokinetics studies

2.4.3.1 Administration strategy

6-8-week-old BALB/c mice were fasted overnight before drug administration. Galloylated catechins derivative (1 mg/mL) was i.v. injected at a dosage of 10 mg/kg or derivative (3 mg/mL) was i.p. injected at a dosage of 30 mg/kg. The blood was collected by cardiac puncture at 10, 30, 60, 120, 240, 480 min post administration after the mice were anesthetized. The whole blood was collected in heparin anticoagulant tube. After 3,000 rpm centrifugation for 10 min, plasma was collected and stored at -20°C until quantification analysis.

2.4.3.2 Plasma sample preparation

The standard of the derivatives or PTX tested were ranged from 2.75- 5500 ng/mL in

ACN. A 10 μ L of standard solution and 10 μ L of internal standard were mixed with 90 μ L blank plasma. For sample preparation, 10 μ L internal standard was directly mixed with 100 μ L plasma sample. The mixture was precipitated by 3-fold volume of ACN and then centrifuged at 14,000 rpm for 10 min. The supernatant was filtered by polymer membrane before UPLC-MS/MS analysis. A linear standard curve was established for sample quantification. The coefficient of determination (R^2) of the standard curve should be over 0.99.

2.4.4 *In vivo* toxicity studies

6-8-week-old BALB/c mice were divided into 10 groups (n=3 mice in each group) including (1) solvent control, (2) PTX 12 mg/kg, (3-5) co-treatment of 51/FX3/WBC5 30 mg/kg and PTX 12 mg/kg, (6-7) co-treatment of FX3/WBC5 60 mg/kg and PTX 12 mg/kg and (8-10) 51/FX3/WBC5 30 mg/kg, respectively. PTX was i.v. injected and the derivative was i.p. injected. In the co-treatment groups, the derivative was injected 1 hour before PTX administration. The administration was performed every other day for 22 days (q.2.d x 13). During the treatment period, the activity and the bodyweight of mice were recorded. The percentage of bodyweight loss was calculated by the following formula:

$$\% \text{ Bodyweight change} = \frac{\text{Bodyweight Day } n - \text{Bodyweight Day } 0}{\text{Bodyweight Day } 0} \times 100\%$$

After the completion of treatment, the bodyweight was still observed for 7 days for delayed toxicity assessment. Over 15% body weight loss, slowness in activity and treatment-related death were regarded as toxicity symptoms.

2.4.5 Establishment of LCC6MDR xenograft model in BALB/c nude mice

6-8-week-old BALB/c nude mice were kept in a sterile environment with sterile food and water. All studies were formed in accordance with the Cap 340 Animal License of Department of Health in Hong Kong. LCC6MDR cells (1,000,000) in PBS were i.p injected into one nude mouse. After 3-4 weeks, ascites was formed and ascites (100 μ L) was subcutaneously (s.c.) inoculated into the nude mouse until the solid tumor grew to 200 mm^3 . The nude mouse was euthanized, and the tumor was removed and sliced into 1 mm^3 cube. The tumor cubes were s.c. inoculated into nude mice immediately under sterile environment. The tumor size was monitored by electronic caliper and tumor volume was calculated by the formula:

$$\text{Estimated tumor volume (mm}^3\text{)} = \frac{l \times w^2}{2}$$

l stands for the longest diameter of the tumor and w was the diameter perpendicular to the longest diameter.

The tumor volume (%) was calculated by the formula:

$$\text{Tumor volume}(\%) = \frac{\text{Tumor volume} - \text{Tumor volume 0}}{\text{Tumor volume 0}} \times 100\%$$

Tumor volume was the tumor volume at day of measurement. Tumor volume 0 was the tumor volume of initial day of treatment. Tumor doubling time was calculated by the formula:

$$\begin{aligned} &\text{Tumor doubling time (d)} \\ &= (t_2 - t_1) \frac{\log 2}{\log(\text{tumor volume } t_2) - \log(\text{tumor volume } t_1)} \end{aligned}$$

t_2 was final day and t_1 was initial day of treatment.

2.4.6 *In vivo* efficacy study of FX3 in LCC6MDR xenograft

When the tumor volume reached 100 mm³, the tumor bearing mice were randomized into four groups and given treatment (n=8 mice in each group). Four treatment groups included (1) solvent control, (2) PTX 12 mg/kg, (3) co-treatment of FX3 60 mg/kg and PTX 12 mg/kg and (4) co-treatment of FX3 30 mg/kg twice a day and PTX 12 mg/kg. In treatment group 3, FX3 was i.p. injected 1 hour before PTX injection. In the treatment group 4, FX3 was injected twice a day and the second injection was given 5 hours after the PTX injection. All treatments were given every two days for 13 times. Activity, bodyweight and tumor volume of the mice were monitored during the whole experiment. Statistical analysis of tumor volume was performed by two-way-ANOVA with Dunnett's multiple comparison at the end of the experiment.

2.4.7 Intratumor PTX and FX3 accumulation

LCC6MDR xenografts were established as described above. Treatments were given when the tumor reached 150-300 mm³. The mice were randomized into two groups: (1) PTX 12 mg/kg and (2) co-treatment of FX3 30mg/kg and PTX 12mg/kg. FX3 was administrated 1 hour before PTX administration. The plasma and tumors were collected at 1, 3, 5, 7 and 9-hour post PTX administration and stored at -80°C. Each excised tumor was homogenized with 3-fold volume of PBS. A total of 95 µL extracted sample was mixed with 5 µL of internal standard. 100 µL of homogenate was extracted with 300 µL of ACN. After 14,000 rpm centrifugation, supernatant was collected for PTX or FX3 quantification using UPLC-MS/MS.

2.4.8 Establishment of P388ADR lymphoma model in B6D2F1 mice

A total of 1×10^6 cells of P388ADR cells were resuspended in 100 μL of PBS and i.p. injected into each male B6D2F1 mice. Ascites was collected and passed (1:500) to another mouse after 9 days growth. The survival time and bodyweight of mice were monitored.

2.4.9 *In vivo* efficacy study of FX3 in P388ADR lymphoma model

5-7-week-old male B6D2F1 mice were i.p. inoculated with 1×10^6 cells of P388ADR from ascites. The mice were randomized into four groups: (1) no treatment-control group, (2) DOX 3 mg/kg, (3) FX3 60 mg/kg + DOX 3 mg/kg and (4) GF120918 20 mg/kg + DOX 5 mg/kg. The cell inoculation day was day 0. In group 2, DOX was i.p. administered on days 2, 6, 10, 14 and 18. In group 3, FX3 was i.p. administered on days 1, 2, 5, 6, 9, 10, 13, 14, 17 and 18 and DOX was i.p. administered on days 2, 6, 10, 14 and 18. In group 4, the treatment was only given on day 1. GF120918 was i.v. injected 1 hour before i.p. injection of DOX. Survival and changes in bodyweight were monitored during the treatment. Statistical analysis on the survival time was done by Log-rank (Mantel-Cox) Test in Prism 5.0.

2.4.10 Establishment of K562/P-gp leukemia model in NOD/SCID mice

NOD/SCID mice were irradiated at 1.2 Gy in MultiRad225 biological irradiator. Within 24 hours after irradiation, 1×10^7 cells of K562/P-gp (resuspended in 200 μL of PBS) were i.v. injected into irradiated NOD/SCID mice. To ensure the adaptability of cells *in vivo*, K562/P-gp cells were passed twice to the NOD/SCID mice before the

animal efficacy study (**Figure 2. 1**).

First, K562/P-gp cells were i.v. injected into mice #1-3. Ascites was collected from mice #1-3 and cultured in the laboratory. After the first round of cell proliferation *in vitro*, ascites cells were i.v. injected into mice #4-5 and the cells from peripheral blood were isolated and cultured in the laboratory again. The second-round *in vitro* cells were used for animal efficacy study. The mice survival was monitored after K562/P-gp cell inoculation. The heavy paralysis of mice was defined as animal death.

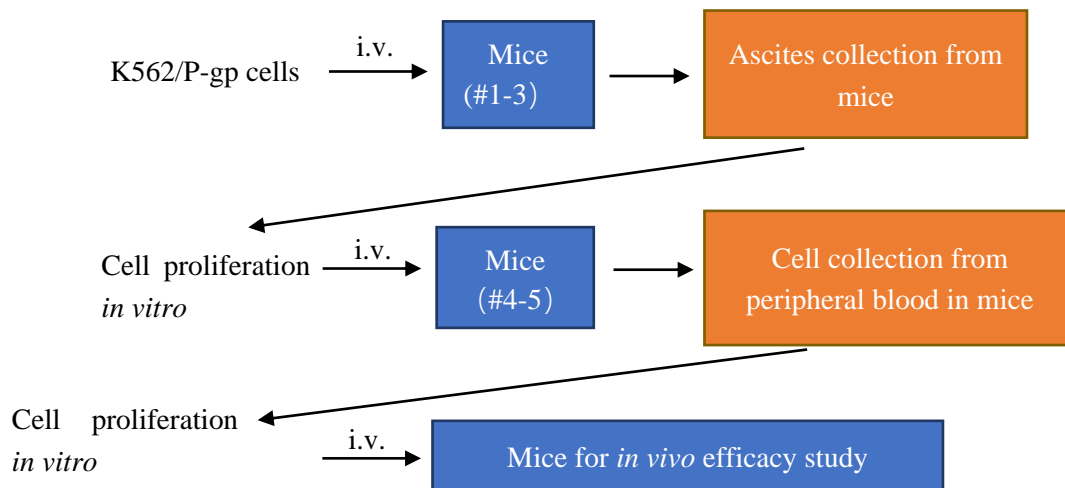


Figure 2. 1 The passages of K562/P-gp cells for *in vivo* efficacy

K562/P-gp cells were passed twice in mice before animal efficacy study.

2.4.11 *In vivo* efficacy study of FX3 in K562/P-gp leukemia model

Four-week-old female NOD/SCID mice were i.v. inoculated with 1×10^7 cells of K562/P-gp. The mice were randomized into three groups: (1) no treatment-control group, (2) DOX 0.9 mg/kg and (3) FX3 30 mg/kg + DOX 0.9 mg/kg. The irradiation was on day 0 and cell inoculation day was on day 1. FX3 was i.p. injected and DOX was i.v. injected on days 7, 11, 15, 19, 23 and 27. FX3 was given 1 hour before DOX injection. Survival and bodyweight of mice were monitored during the treatment. Statistical analysis on the survival time was done by Log-rank (Mantel-Cox) Test in Prism 5.0.

Chapter 3: Galloylated catechin derivatives reversed MDR by modulating P-gp *in vitro*

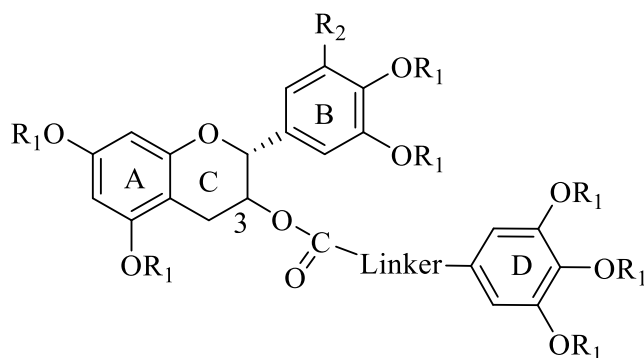
3.1 Introduction

3.1.1 MDR induced by P-gp and galloylated catechins derivatives

MDR was one of the reasons for chemo-therapy failure. Overexpression of ABC transporters on the cell membrane was one possible reason to induce MDR. The transporters efflux the anticancer drug and decreased intracellular level of anticancer drug. MDR-1/ABCB1/ P-gp was one of most classic transporters in ABC transporters family (Chen et al. 1986). Knockdown of P-gp in different cancer cells restored the sensitivity to chemotherapy drugs (Rumpold et al. 2005, Zhu et al. 2013). One of the promising ways to reverse chemotherapy resistance was downregulating P-gp expression or inhibiting the efflux of P-gp.

Galloylated catechins were chemically modified to improve their P-gp modulating activity. After screening a large library of derivatives synthesized in our research group, four novel galloylated catechins derivatives (23, 51, FX3 and WBC5) were found to have a high potency in P-gp modulation (Wong et al. 2015, Wong et al. 2021). Their structures were listed in **Table 3. 1**. Modifications included the followings. Permethylation with tri-methoxy substitution was made at ring D. Bi-methoxy and tri-methoxy substitution was made at ring B. By using oxycarbonylvinyl linker or oxycarbonylphenylcarbamoyl linker, linker length and rigidity between C3 and ring D were increased. These modifications enhanced the P-gp modulating activity compared to EGCG, which was one of the parent compounds. The potency of P-gp modulation activity and the mechanism of reversing MDR by the four derivatives would be studied in this Chapter.

Table 3. 1 Structures and potency of galloylated catechins derivatives in modulating P-gp *in vitro*.



| | R ₁ | R ₂ | Linker | Position 3 | IC ₅₀ of PTX (nM) |
|-------------|----------------|----------------|--------|------------|------------------------------|
| EGCG | H | OH | - | R | 124.1 |
| 23 | Me | OMe | | R | 3.7 |
| 51 | Me | OMe | | S | 2.9 |
| FX3 | Me | H | ditto | R | 2.2 |
| WBC5 | Me | H | ditto | S | 1.8 |

3.1.2 Cell models

The drug-resistant cell lines used in the present study were LCC6MDR, P388ADR and K562/P-gp.

MDA435/LCC6 cells were derived from human melanocyte at M.D. Anderson Hospital and Tumor Institute. This cell line was obtained from pleural effusion. No systemic therapy had been given prior to establishing the cell line (Brinkley et al. 1980). To generate a model for the screening of MDR1-reversing agents, MDA435/LCC6 was transduced with a retroviral vector directing the constitutive expression of the MDR1 cDNA, producing a cell line with a classical MDR1 resistance pattern (MDA435/LCC6MDR1) (Leonessa et al. 1996).

P388 leukemia was lymphoid neoplasm which was chemically induced in a DBA/2 mouse by painting the skin with methylcholanthrene. To study drug resistance and cross-resistance, 16-drug-resistant P388 leukemia cell lines were established (Teicher

2011). These resistant cell lines were resistant to different anticancer drugs including alkylating agents, antimetabolites, DNA binders and tubulin binders. The P388ADR cell line with P-gp overexpression used in this study was resistant to actinomycin D, DOX, etoposide, amsacrine, mitoxantrone, vinblastine, VCR and marginally resistant to PTX.

The cell line K562 was established from pleural effusion during the blast crisis of a chronic myeloid leukemia (CML) patient (Lozzio and Lozzio 1975). Blast crisis of CML was hard to tackle for cancer chemotherapy. One possible reason was MDR caused by P-gp overexpression. K562 was transduced with human MDR1 cDNA from the pHaMDR1/A expression vector to generate resistant K562 cells. Resistant K562 clones were 20- to 30-fold resistant to vinblastine and were cross-resistant to DOX (Hait et al. 1993). The resistant K562 clones, K562/P-gp cells, would be used in the following study.

3.1.3 Mechanism of P-gp modulation

The mechanism of P-gp modulation included competitive and non-competitive mechanism. Competitive modulators could compete with the substrate drugs for the substrate-binding on P-gp, thereby increasing the intracellular accumulation of the substrate drugs. Most of the first and second generations of P-gp modulators, such as verapamil and PSC833, were P-gp substrates and acted as competitive inhibitors. Non-competitive inhibitors neither occupied transport site of P-gp nor were translocated by the protein efflux. They non-competitively inhibited the P-gp efflux by binding to an allosteric modulatory site or inhibiting ATPase activity. The third generation of P-gp modulators, such as tariquidar, elacridar and zosuquidar, were non-transported P-gp inhibitors (Srivalli and Lakshmi 2012).

The mechanism of P-gp modulating by the four derivatives would be studied in this

Chapter in whether they competitively or non-competitively modulated P-gp.

3.2 Results

3.2.1 Efficacy of galloylated catechins derivatives to reverse MDR induced by P-gp in different cell lines

To verify the potency of galloylated catechins derivatives modulating P-gp, different cell models were used. LCC6, P388 and K562 were the sensitive human breast cancer, mouse lymphoma and human CML cell lines, respectively. LCC6MDR, P388ADR, K562/P-gp were their resistant cell lines with P-gp overexpressing. PTX, DOX and VCR were commonly used for chemotherapy and were substrates of P-gp. These chemotherapy drugs were applied on the cell models to test the resistance of the three cell lines. LCC6MDR was 12.7- and 80.3- fold resistant to DOX and PTX compared with LCC6 as shown in **Table 3. 2**. P388ADR was 35.7- and 62.7-fold resistant to DOX and PTX than P388 as shown in **Table 3. 3**. K562/P-gp was 6.3- and 164.9-fold resistant to DOX and VCR compared with K562 as shown in **Table 3. 4**.

Compounds, 23, 51, FX3 and WBC5, were chemically modified from galloylated catechins (Wong et al. 2015, Wong et al. 2021) and they were the most representative ones among a library of derivatives. The presence of 1 μ M of 23, 51, FX3 or WBC5 could decrease IC₅₀ of DOX by 10.8- to 12.3- fold and decrease IC₅₀ of PTX by 41.2- to 84.7-fold on LCC6MDR cells. FX3 and WBC5 at 1 μ M could reverse the resistance of LCC6MDR to sensitive level as LCC6 (**Table 3. 2**). The presence of 1 μ M of the four derivatives could decrease IC₅₀ of DOX by 3.3- to 31.2- fold and IC₅₀ of PTX by 10.8- to 91.1- fold on P388ADR cells. (**Table 3. 3**). The presence of 1 μ M of the four derivatives could decrease IC₅₀ of DOX by 6.5- to 9.0- fold and IC₅₀ of VCR by 127.4- to 336.4- fold on K562/P-gp cells (**Table 3. 4**).

One parameter to assess P-gp modulating activity was EC₅₀. Compounds with a low EC₅₀ meant potent modulating activity. EC₅₀ of 23, 51, FX3 or WBC5 ranged from 158.8 to 244.2 nM in reversing DOX resistance and from 90.8 to 127.0 nM in reversing PTX resistance towards LCC6MDR cells (**Table 3. 2**). EC₅₀ of the four derivatives ranged from 186.3 to 385.0 nM in reversing DOX resistance and from 168.4 to 496.3 nM in reversing PTX resistance towards P388ADR cells (**Table 3. 3**). EC₅₀ of the four derivatives ranged from 93.3 to 165.0 nM in reversing DOX resistance and ranged from 37.0 to 106.7 nM in reversing VCR resistance towards K562/P-gp cells (**Table 3. 4**). EC₅₀s of EGCG in reversing MDR in the three resistant cell lines were over 1000 nM, which was significantly higher than EC₅₀s of the four derivatives (**Table 3. 2 to 3. 4**).

In summary, FX3 at 1 µM could significantly decrease the IC₅₀ of the anti-cancer drugs to the level of sensitive cells, while EGCG at 1 µM could not decrease the IC₅₀ of anti-cancer drugs. FX3 and WBC5 were more potent than 23 and 51 because the EC₅₀s of FX3 and WBC5 were lower than that of 23 and 51 in different cell lines towards different anti-cancer drugs.

Table 3. 2 IC₅₀s of DOX and PTX and EC₅₀s of derivatives in LCC6 and LCC6MDR cell lines

| | IC ₅₀ of DOX with or without 1μM derivative (nM) | Fold Change | EC ₅₀ in reversing DOX (nM) | IC ₅₀ of PTX with or without 1μM derivative (nM) | Fold Change | EC ₅₀ in reversing PTX (nM) |
|----------------|---|-------------|--|---|-------------|--|
| LCC6MDR | 10310.2 ± 240.2 | 1.0 | / | 152.5 ± 9.7 | 1.0 | / |
| 23 | 836.1 ± 34.2 | 12.3 | 244.2 ± 23.4 | 3.7 ± 0.9 | 41.2 | 127.0 ± 30.2 |
| 51 | 950.7 ± 42.7 | 10.8 | 232.9 ± 35.8 | 2.9 ± 0.8 | 52.6 | 82.3 ± 14.3 |
| FX3 | 844.3 ± 39.1 | 12.2 | 158.8 ± 21.3 | 2.2 ± 0.1 | 69.3 | 93.8 ± 21.4 |
| WBC5 | 868.3 ± 20.3 | 11.9 | 179.9 ± 18.4 | 1.8 ± 0.3 | 84.7 | 90.8 ± 5.4 |
| EGCG | 9768.3 ± 48.3 | 1.1 | >1000 | 140.5 ± 8.7 | 1.1 | >1000 |
| LCC6 | 814.9 ± 20.1 | 12.7 | / | 1.9 ± 0.2 | 80.3 | / |

C₅₀s of PTX and DOX towards LCC6 and LCC6MDR cells were measured by MTS assay. EC₅₀s of derivatives were calculated by Prism 5.0. Data in table was shown as mean ± sem (n=3-6).

Table 3. 3 IC₅₀s of DOX and PTX and EC₅₀s of derivatives in P388 and P388ADR cell lines

| Compounds | | IC ₅₀ of DOX with or without 1 μM derivative (nM) | Fold Change | EC ₅₀ in reversing DOX (nM) | IC ₅₀ of PTX with or without 1 μM derivative (nM) | Fold Change | EC ₅₀ in reversing PTX (nM) |
|----------------|-------------|--|-------------|--|--|-------------|--|
| P388ADR | | 1790.3 ± 139.2 | 1.0 | / | 1447.8 ± 174.9 | 1.0 | / |
| | 23 | 536.3 ± 67.3 | 3.3 | 385.0 ± 15.8 | 184.5 ± 23.2 | 7.8 | 168.4 ± 47.4 |
| | 51 | 176.4 ± 44.0 | 10.1 | 335.1 ± 15.4 | 134.2 ± 60.3 | 10.8 | 496.3 ± 12.0 |
| | FX3 | 57.5 ± 12.4 | 31.2 | 186.3 ± 30.6 | 15.9 ± 4.3 | 91.1 | 248.8 ± 18.4 |
| | WBC5 | 80.0 ± 16.9 | 22.4 | 260.4 ± 60.2 | 113.0 ± 46.6 | 12.8 | 216.3 ± 10.4 |
| | EGCG | 1701.2 ± 13.8 | 1.1 | >1000 | 1400.2 ± 20.5 | 1.0 | >1000 |
| P388 | | 50.2 ± 1.8 | 35.7 | / | 23.1 ± 2.9 | 62.7 | / |

IC₅₀s of DOX towards P388 and P388ADR cells were measured by MTS assay. EC₅₀s of derivatives were calculated by Prism 5.0. Data in table was shown as mean ± sem (n=3-6)

Table 3. 4 IC₅₀s of DOX and VCR and EC₅₀s of derivatives in K562 and K562/P-gp cell lines

| Compounds | | IC ₅₀ of DOX with or without 1 μM derivative (nM) | Fold Change | EC ₅₀ in reversing DOX (nM) | IC ₅₀ of VCR with or without 1 μM derivative (nM) | Fold Change | EC ₅₀ in reversing VCR (nM) |
|------------------|-------------|--|-------------|--|--|-------------|--|
| K562/P-gp | | 1963.1 ± 125.9 | 1.0 | / | 84.1 ± 6.4 | 1.0 | / |
| | 23 | 303.7 ± 40.0 | 6.5 | 165.1 ± 22.1 | 0.31 ± 0.03 | 271.3 | 106.7 ± 6.2 |
| | 51 | 223.7 ± 30.9 | 8.8 | 129.4 ± 35.7 | 0.25 ± 0.02 | 336.4 | 76.6 ± 7.4 |
| | FX3 | 219.3 ± 53.9 | 9.0 | 93.3 ± 32.8 | 0.54 ± 0.11 | 155.7 | 37.0 ± 9.5 |
| | WBC5 | 281.7 ± 89.6 | 7.0 | 93.3 ± 20.5 | 0.66 ± 0.10 | 127.4 | 59.8 ± 11.9 |
| | EGCG | 1373.0 ± 43.3 | 1.4 | >1000 | 76.7 ± 2.3 | 1.1 | >1000 |
| K562 | | 312.5 ± 41.6 | 6.3 | / | 0.51 ± 0.10 | 164.9 | / |

IC₅₀s of DOX towards K562 and K562/P-gp cell lines were measured by MTS assay. IC₅₀s of VCR towards K562 and K562/P-gp cell lines were measured by Celltiter-glo assay. EC₅₀s of derivatives were calculated by Prism 5.0. Data in table was shown as mean ± sem (n=3-6).

3.2.2 Efficacy of galloylated catechins derivatives in reversing drug resistance induced by BCRP and MRP-1 in different cell lines

To investigate the modulating activity on BCRP and MRP-1, compounds (23, 51, FX3 and WBC5) were tested on S1M180 and 2008/MRP1 respectively. BCRP was overexpressing in S1M180 which was resistant to topotecan. MRP-1 was overexpressing in 2008/MRP1 which was resistant to DOX.

The presence of 1 μ M of 23, 51, FX3 and WBC5 cannot reduce the IC₅₀ of DOX in 2008/MRP1 cells and their EC₅₀ was 958 to over 1000 nM (**Table 3. 5**). This indicated that 23, 51, FX3 and WBC5 had no cross-modulation effect on MRP-1.

On the other hand, the presence of 1 μ M of 23, 51, FX3 and WBC5 can reduce the IC₅₀ of topotecan on S1M180 cells (**Table 3. 5**). This indicated that the four derivatives could reverse resistance of topotecan by modulating BCRP. However, the EC₅₀ of the four compounds ranged from 343 to >1000 nM, which was much higher than the EC₅₀ in reversing P-gp-induced MDR. This suggested that the four derivatives had more potent modulating activity on P-gp than on BCRP. Among the four compounds, FX3 had the highest modulating P-gp activity and the lowest BCRP modulating activity (**Table 3. 5**). It indicated that FX3 was specific to P-gp modulating.

Table 3. 5 EC₅₀s of galloylated catechins derivatives in modulating BCRP and MRP-1 *in vitro*

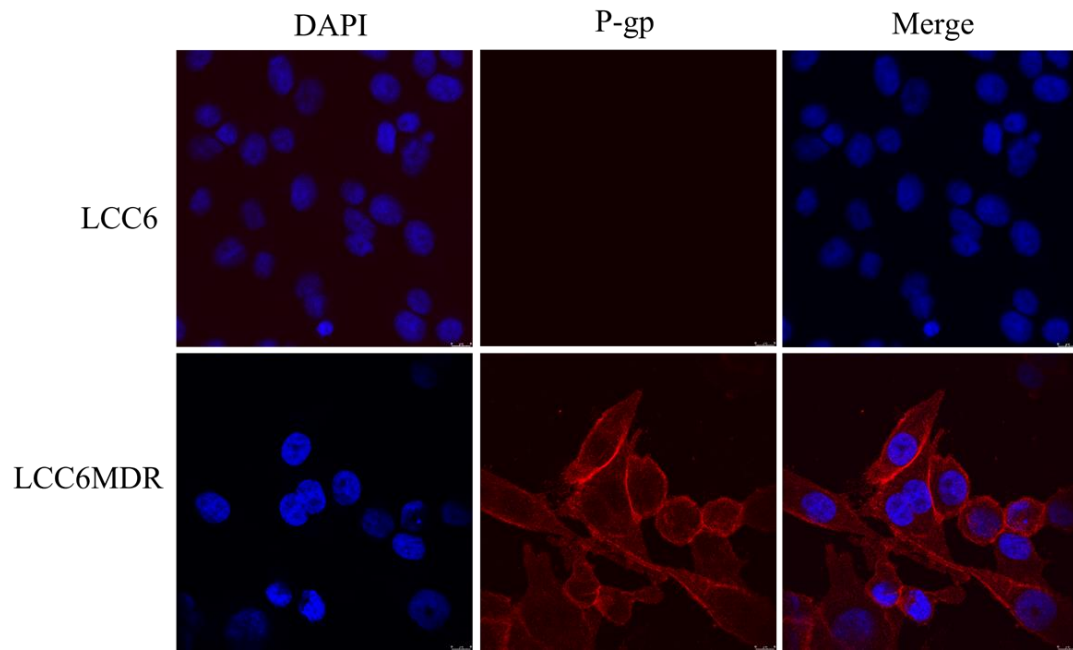
| BCRP | | | | MRP-1 | | | |
|-----------|-------------|--|--|-------------|-------------|--|--|
| Cell line | Compounds | IC ₅₀ of topotecan with or without 1 μM derivative (μM) | EC ₅₀ in reversing topotecan (nM) | Cell line | Compound | IC ₅₀ of DOX with or without 1 μM derivative (nM) | EC ₅₀ in reversing DOX (nM) |
| S1M180 | / | 35.3 ± 14.6 | / | 2008/MRP1 | / | 880.7 ± 105.7 | / |
| | 23 | 3.6 ± 1.0 | 730.0 | | 23 | 705.9 ± 225.3 | >1000 |
| | 51 | 5.5 ± 1.5 | 600.0 | | 51 | 455.2 ± 113.5 | 1000 |
| | FX3 | 17.0 ± 3.1 | >1000 | | FX3 | 388.2 ± 21.0 | 958 |
| | WBC5 | 3.4 ± 2.3 | 343.0 | | WBC5 | 725.4 ± 308.9 | >1000 |
| | EGCG | 49.5 ± 2.0 | >1000 | EGCG | >1000 | >1000 | |
| S1 | / | 0.8 ± 0.3 | / | 2008/P | / | 63.0 ± 5.0 | / |

IC₅₀s of S1M180 towards topotecan and IC₅₀s of 2008/MRP1 towards DOX were measured by MTS assay. EC₅₀s of derivatives were calculated by Prism 5.0.

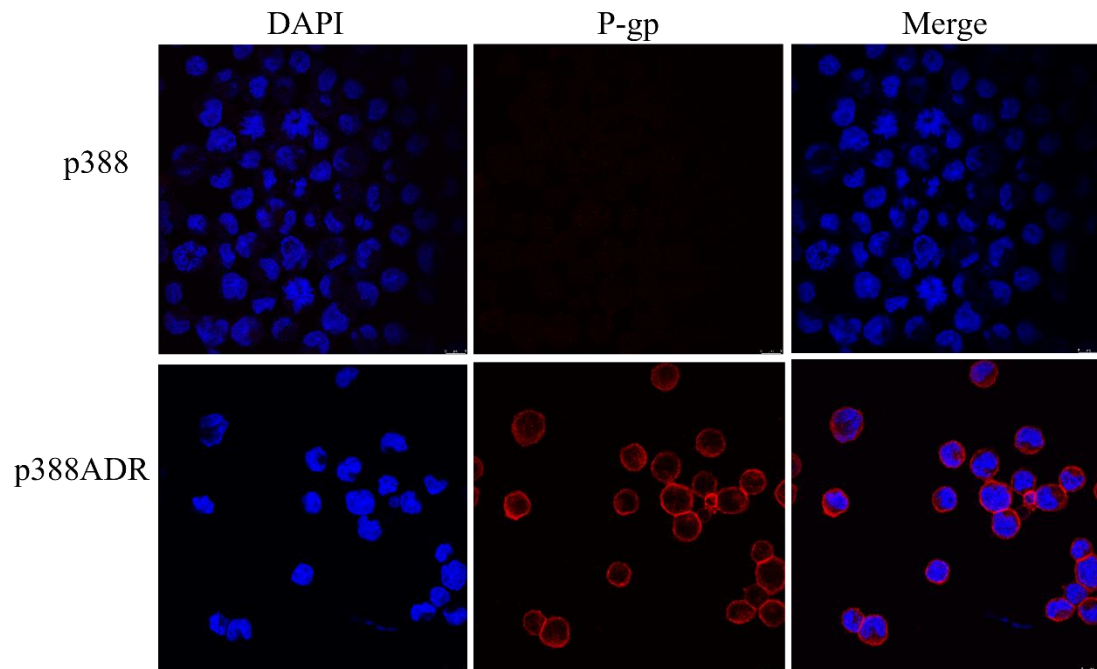
3.2.3 Effects of galloylated catechins derivatives on P-gp expression and location

The effects of 23, 51, FX3 and WBC5 on regulating P-gp expression were studied. In **Figure 3. 1. A-B**, P-gp on the membrane of LCC6MDR and P388ADR cells could be detected but not on LCC6 and P388. In **Figure 3. 1. C**, after treatment of derivatives (51, FX3 and WBC5) at 2 μ M, the P-gp expression on surface of LCC6MDR and K562P-gp cells was significantly enhanced by 1.5- to 1.7- fold. The reason why P388ADR cells was not used here was that the antibody used was a human P-gp specific antibody. In western blot assay, P-gp was detected in LCC6MDR, P388ADR and K562/P-gp cells but not in the sensitive counterparts LCC6, P388 and K562 (**Figures 3. 1. D-F**). Galloylated catechins derivatives had no effect on the total expression of P-gp in LCC6MDR, P388ADR and K562/P-gp cells (**Figure 3. 1. D-F**). The result suggested that the P-gp modulating mechanism by the derivatives was not by downregulating P-gp expression level. The enhancement of P-gp expression on cell membrane could be explained by that there was specific binding between P-gp and the derivatives and the binding induced conformational changes in P-gp with a high level by antibody detection.

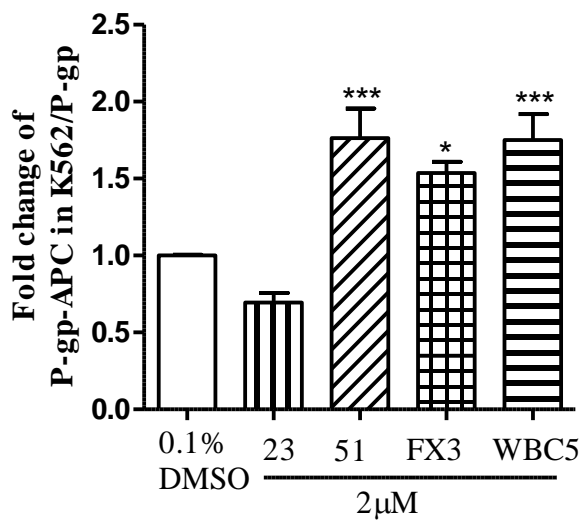
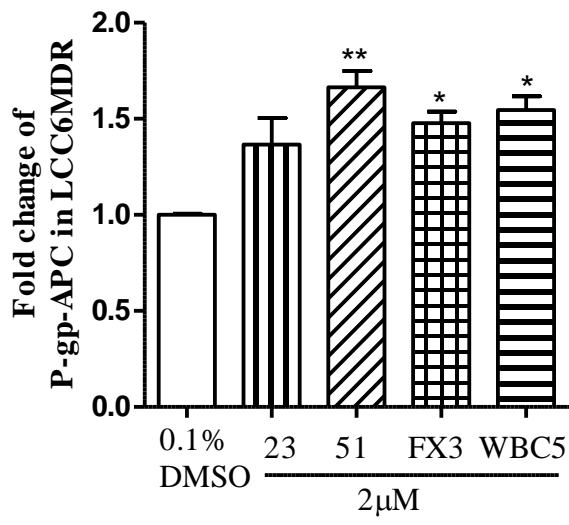
(A)



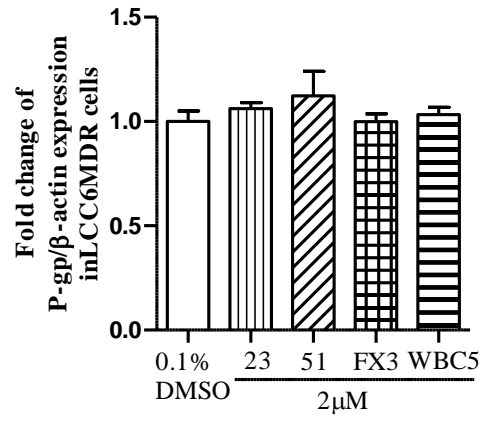
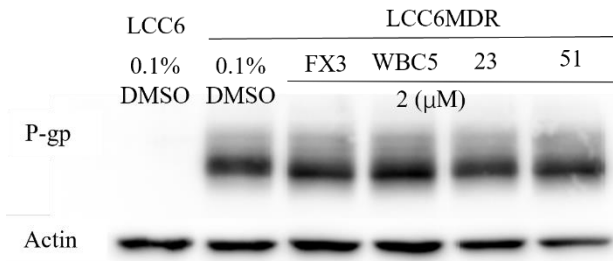
(B)



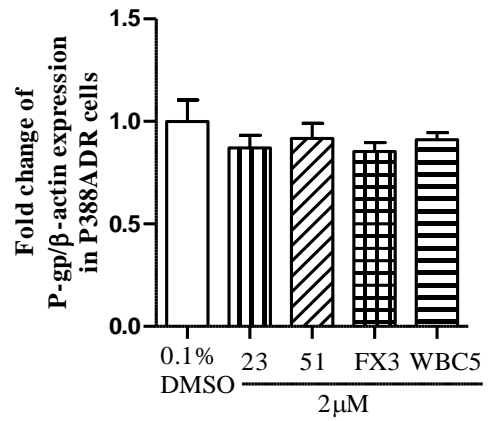
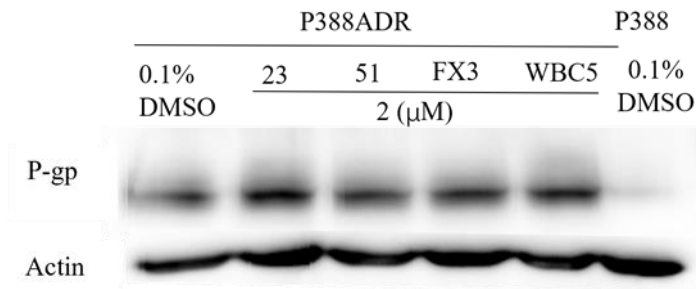
(C)



(D)



(E)



(F)

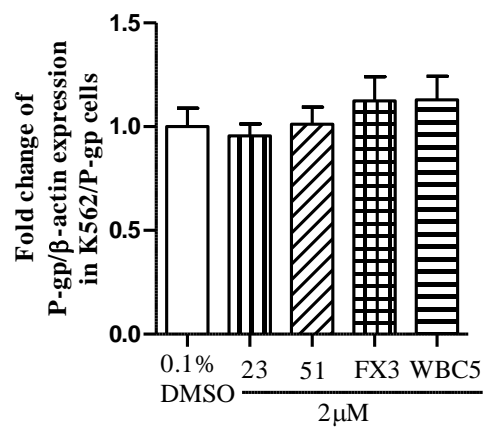
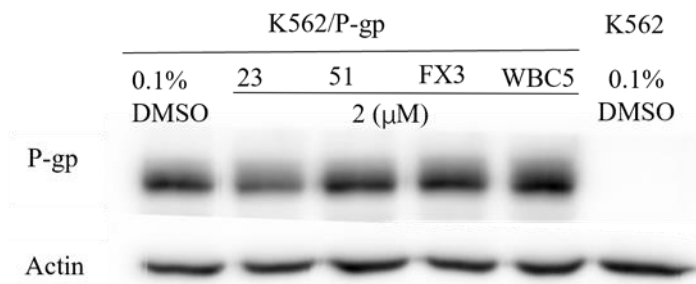


Figure 3. 1 Location and Expression of P-gp in different cell lines.

(A-B) Expression and localization of P-gp in LCC6MDR and P388ADR cells were detected by confocal microscopy. Nucleus was stained with DAPI (Blue), P-gp was detected by MDR1 (D-11) antibody (Red). (C) LCC6MDR, P388ADR and K562/P-gp cells were treated with galloylated catechins derivatives at 2 μ M. Expression of P-gp on LCC6MDR and K562/P-gp cell membrane with or without treatment of galloylated catechins derivatives was investigated by flow cytometry. (D-F) LCC6MDR, P388ADR and K562/P-gp cells were treated with the four derivatives at 2 μ M. Expression level of P-gp in LCC6MDR, P388ADR and K562/P-gp cells was characterized by western-blot. The expression of P-gp was normalized by β -actin. The results were shown in mean \pm sem. All treatment groups were compared with control by unpaired two-tail t-tests in Prism 5.0. *, $p < 0.05$; **, $p < 0.01$.

3.2.4 Effect of galloylated catechins derivatives on DOX accumulation and efflux in P-gp overexpressing cell lines

To investigate the mechanism of reversing P-gp-mediated MDR, DOX accumulation in P-gp-overexpressing cells was measured. A series of concentration of derivatives (23, 51, FX3 and WBC5) was co-incubated with DOX in LCC6MDR, P388ADR or K562/P-gp cells. The four derivatives can increase intracellular DOX and PTX accumulation in resistant cell lines in dose-dependent manner (**Figure 3. 2**).

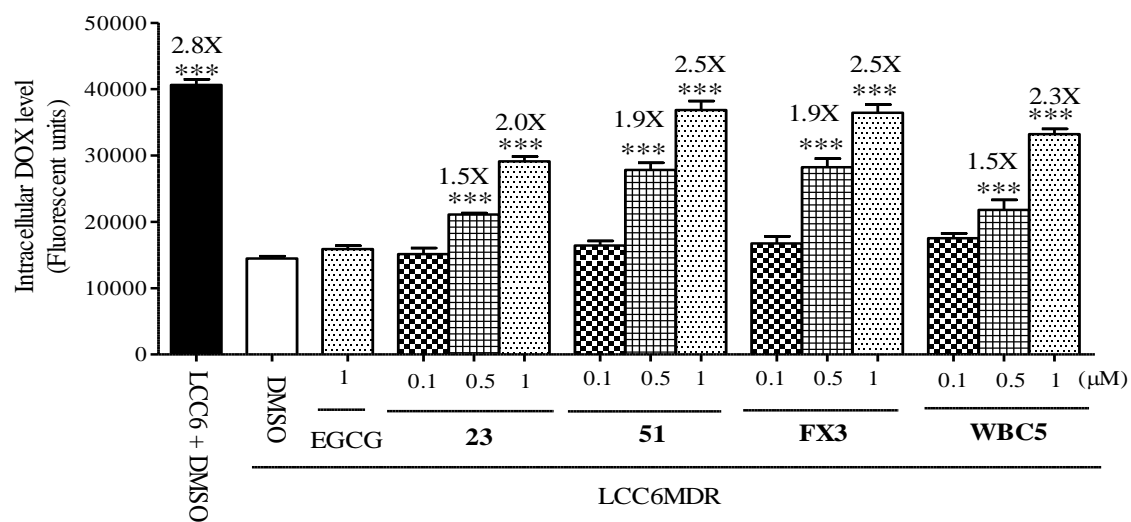
In the presence of 1 μ M of the four galloylated catechin derivatives, the intracellular level of DOX in LCC6MDR cells can be increased to that level in the parental LCC6 cells. In contrast, EGCG at 1 μ M cannot increase DOX accumulation in LCC6MDR cells (**Figure 3. 2. A**). A similar observation was made in P388ADR and K562/P-gp cells co-treated with DOX and a series of concentrations of galloylated catechins derivatives (**Figures 3. 2. B and C**). In addition, the four derivatives can also enhance intracellular PTX level in LCC6MDR cells (**Figure 3. 2. D**).

To measure the effect of the derivatives on P-gp mediated DOX efflux, P388 or P388ADR cells were first loaded with DOX, followed by incubation in a DOX-free medium. P388 cells accumulated 80.3% DOX, whereas P388ADR cells accumulated only 15.7% (**Figure 3. 3**). The results suggested that P-gp-overexpressing resistant cells efflux more DOX than sensitive cells.

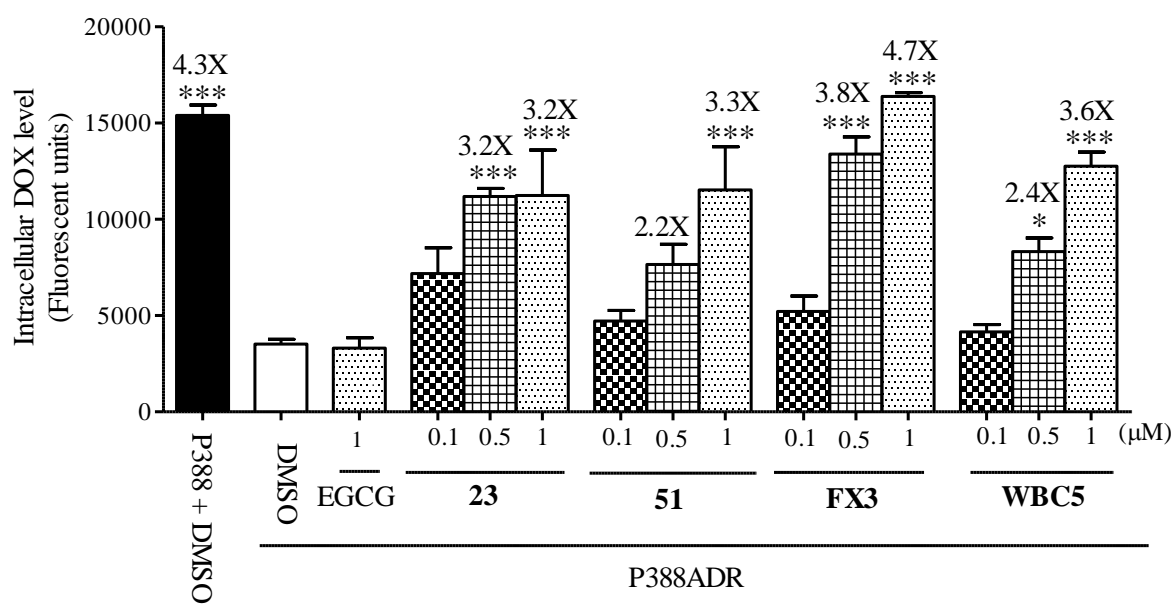
In the presence of 1 μ M of the four derivatives, the DOX in P388ADR cells significantly increased from 15.7% to 37.1-61.5% respectively. In the presence of 0.1 μ M of galloylated catechins derivatives, the remaining intracellular DOX level was 19.8-23.2%. It showed no significant inhibition in DOX efflux compared with the control group (15.7%) (**Figure 3. 3. A-D**). At the time point of 180 minutes, the inhibitory effect of the four derivatives on DOX efflux was better than GF120918

(24.3%), which was a well-known P-gp and BCRP dual-inhibitor (**Figure 3. 3. E**). These results suggested that all four derivatives could inhibit P-gp-mediated DOX efflux in a dose-dependent manner and these derivatives increased intracellular DOX accumulation by inhibiting efflux.

(A)



(B)



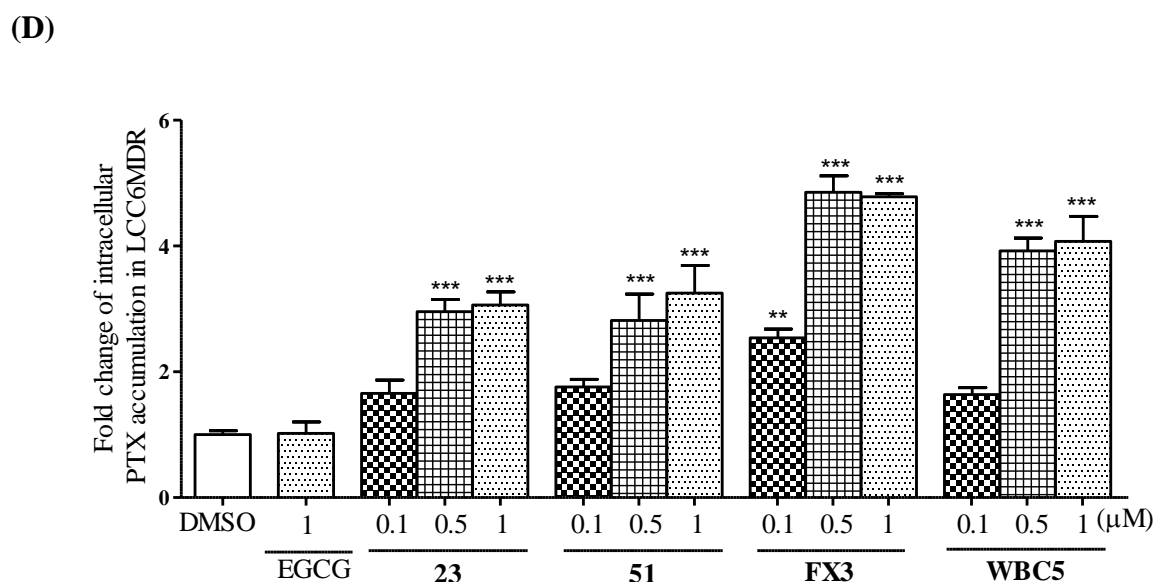
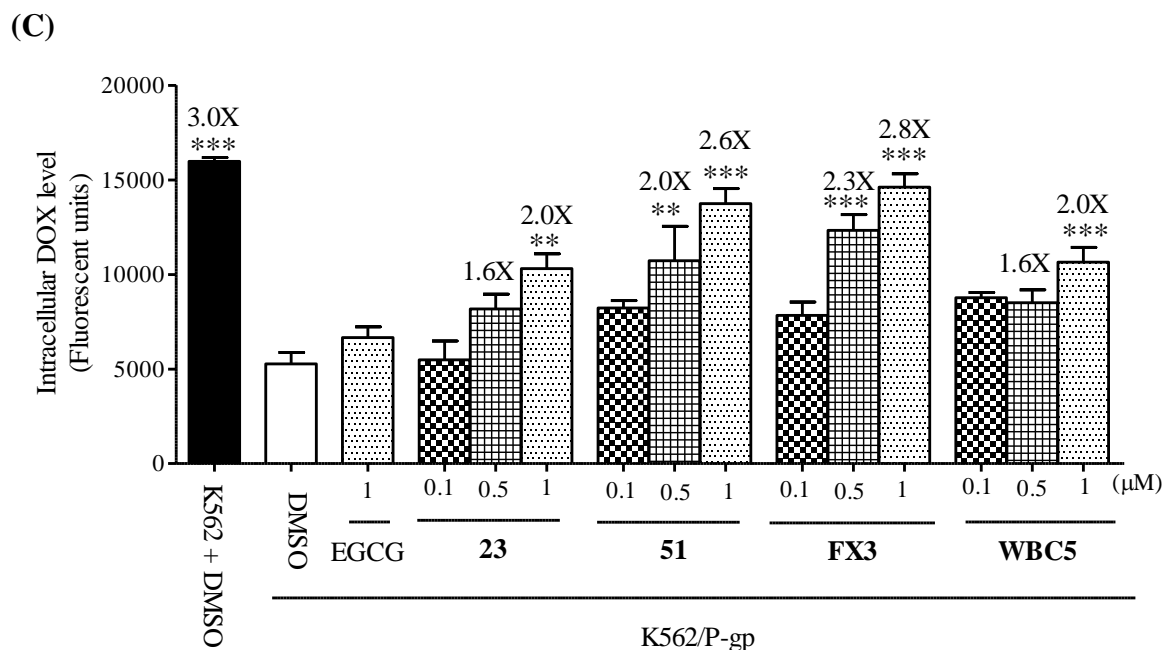
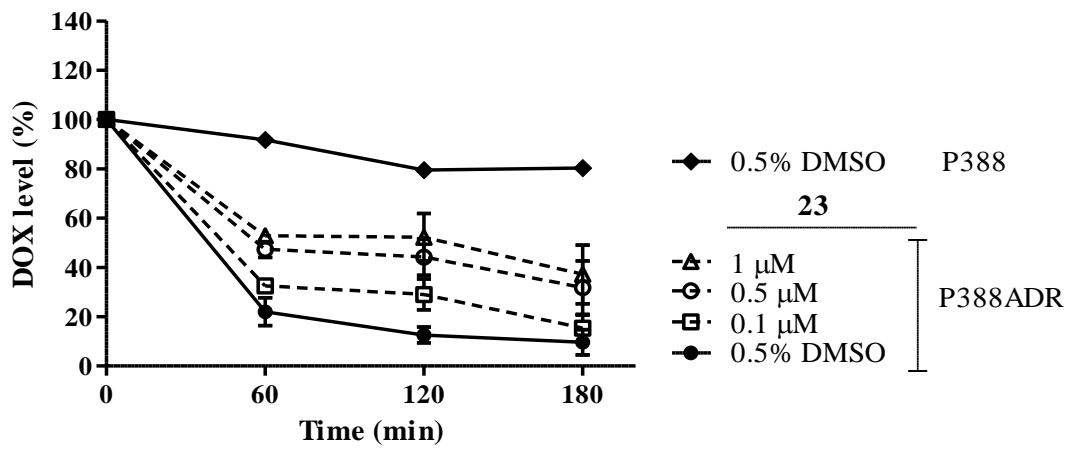


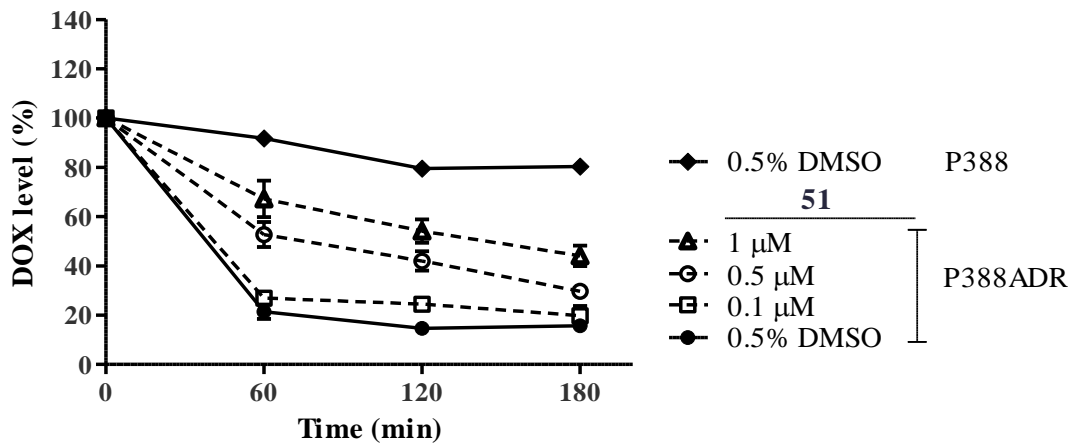
Figure 3. 2 Effect of galloylated catechin derivatives on DOX and PTX accumulation in resistant cell lines.

The intracellular fluorescence level of DOX in LCC6 and LCC6MDR cells (A), P388 and P388ADR cells (B) and K562 and K562/P-gp cells (C) with or without galloylated catechins derivatives. (D) The fold change of intracellular PTX level in LCC6MDR cells with or without galloylated catechins derivatives. Data was shown as mean \pm sem. (n=3). *, $p < 0.05$; **, $p < 0.01$; ***, $p < 0.001$.

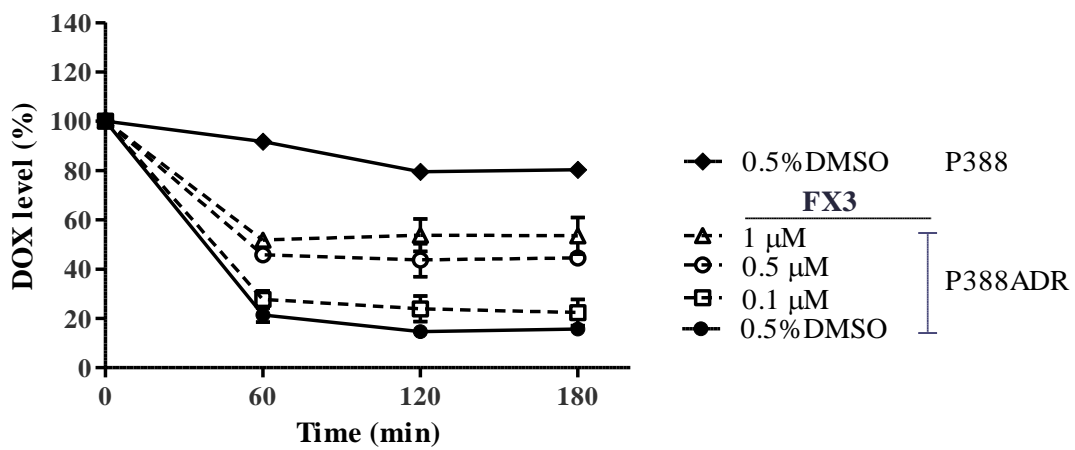
(A)



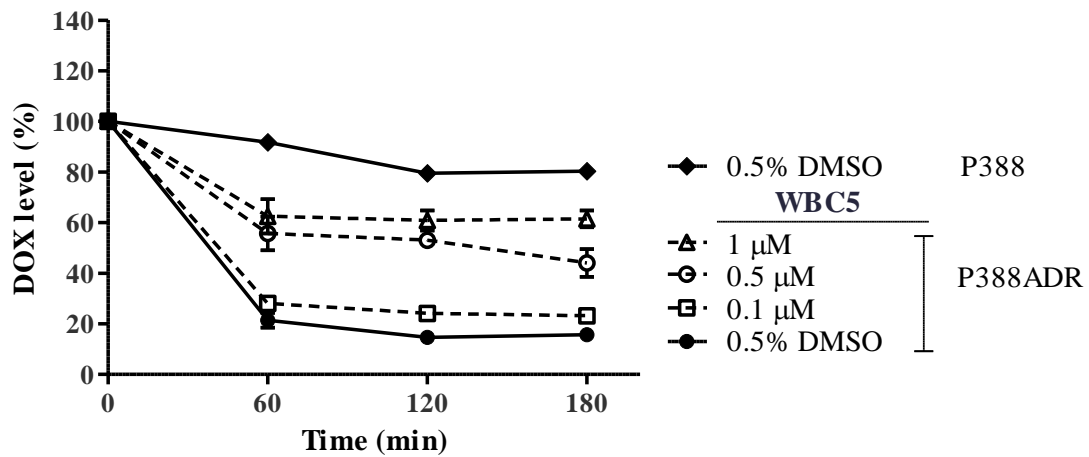
(B)



(C)



(D)



(E)

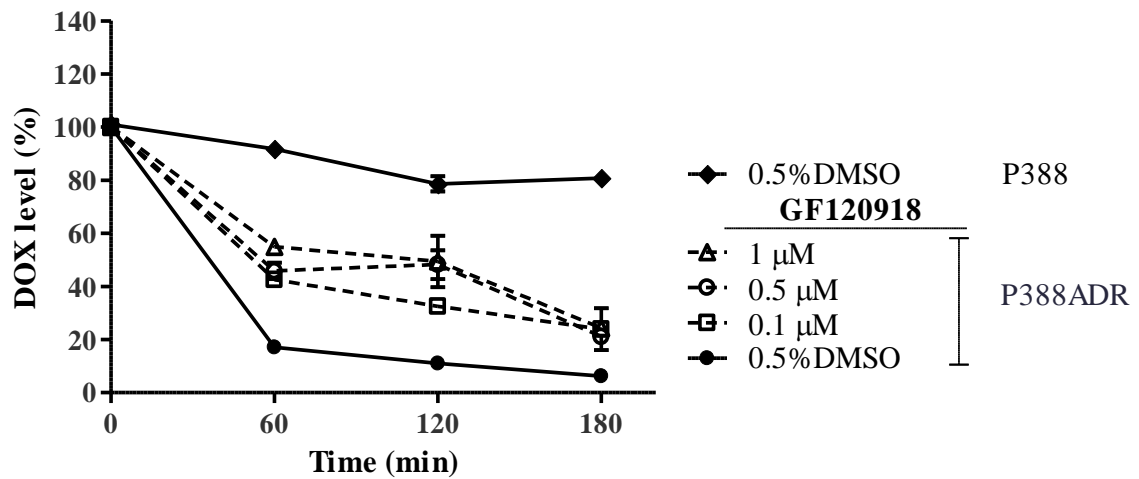


Figure 3. 3 Effect of galloylated catechins derivatives on DOX efflux

The DOX fluorescence meant the remaining intracellular DOX. The DOX fluorescence was measured by flow-cytometry at different time points post replacement of DOX-free medium. GF120918 was used as positive control. Data was shown as mean \pm sem. (n=3)

3.2.5 Effect of galloylated catechins derivatives on P-gp ATPase activity

ATPase activity was required for the function of P-gp. Modulation of P-gp could be mediated by either inhibiting or stimulating P-gp ATPase. Modulator can inhibit P-gp ATPase activity by binding to the NBD. It could slow down the efflux by P-gp. Modulator stimulated P-gp ATPase activity by binding to the substrate-binding site. It prevented the efflux of other substrates.

To investigate whether FX3 and WBC5 stimulated or inhibited P-gp ATPase activity, the effect of ATPase activity of FX3 and WBC5 on vanadate-inhibitable P-gp was measured. Verapamil, a first-generation of P-gp modulator, could stimulate ATPase activity. When Δ luminescence_{tested compound-treated} sample was higher than the Δ luminescence_{basal}, the compound stimulated the ATPase activity. When Δ luminescence_{tested compound-treated} was lower than Δ luminescence_{basal}, the compound inhibited ATPase activity.

In **Figure 3. 4**, verapamil could stimulate the ATPase activity of P-gp in dose-dependent manner. Verapamil at 50 μ M stimulated the ATPase activity by 3.3-fold. FX3 and WBC5 (0.01 to 70 μ M) can also stimulate ATPase by 1.0 to 2.6-fold, and the concentration of FX3 and WBC5 was limited by the solubility. EGCG, at 50 to 200 μ M, which were the effective concentrations for P-gp modulating (Sugihara et al. 2011), displayed inhibitory effect on ATPase activity. This indicated that the mechanism of P-gp modulation of EGCG and FX3 or WBC5 was different. EGCG modulated P-gp by inhibiting ATPase activity of P-gp, but FX3 and WBC5 stimulated ATP consumption. It was proposed that FX3 and WBC5 did not bind at NBD of P-gp.

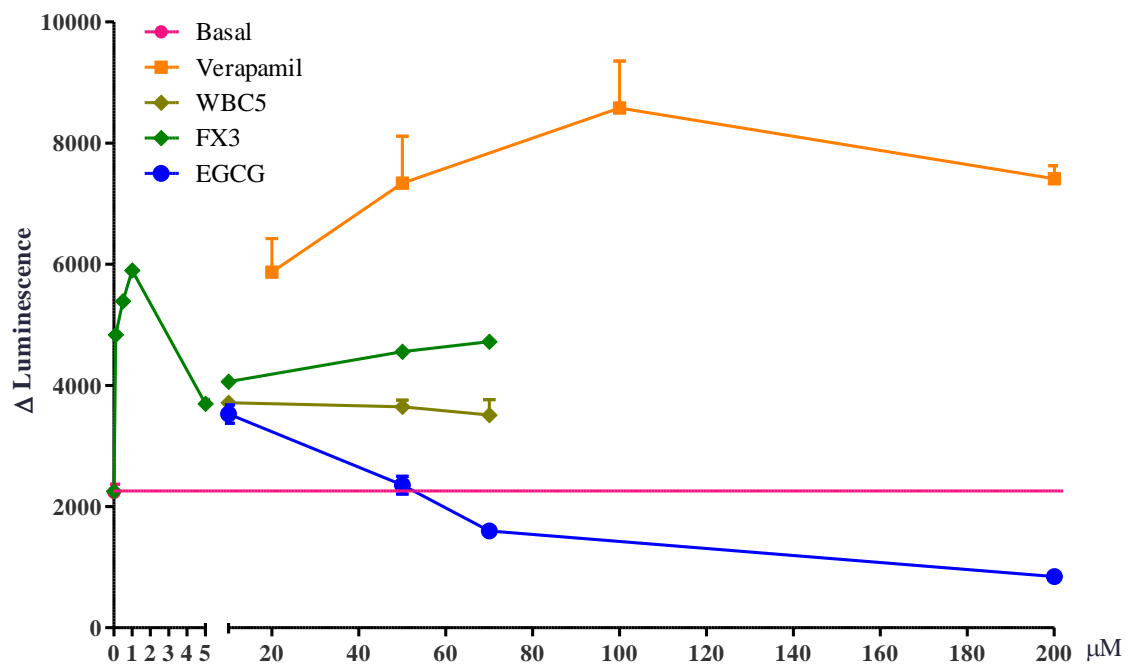


Figure 3. 4 Effect of galloylated catechins derivatives on vanadate-inhibitable P-gp ATPase activity

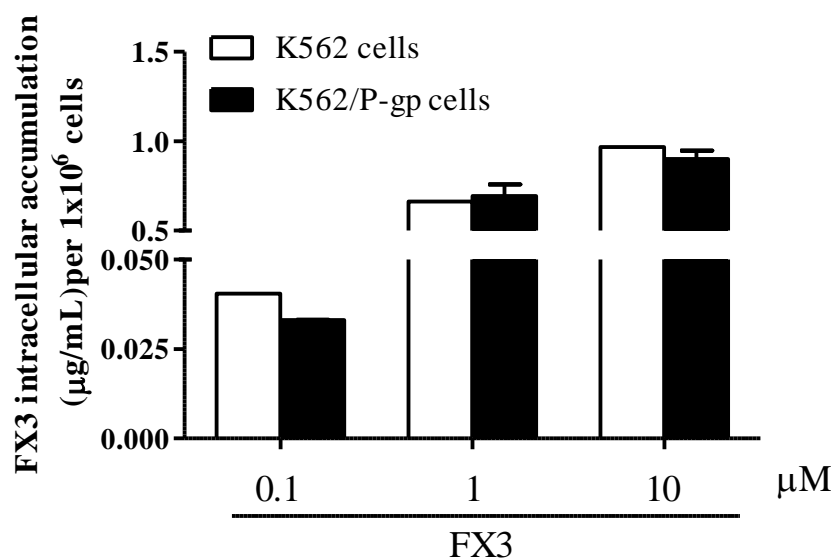
Δ luminescence reflected the difference of remaining ATP between Na_3VO_4 treated sample and non/verapamil/FX3/WBC5/EGCG-treated sample in human P-gp microsome. Verapamil, a known stimulator to P-gp ATPase activity, was used as a control.

3.2.6 Accumulation of FX3 in sensitive and resistant cells

The previous section indicated that FX3 could stimulate the ATPase activity of P-gp. It raised a question of whether FX3 was a competitive P-gp modulator or not. If so, it might also be a substrate of P-gp and it could be transported by P-gp. An ideal modulator would not be transported by P-gp. Therefore, the intracellular accumulation of such modulator can remain at same level in both sensitive and resistant cell lines. To investigate this, the accumulation of FX3 in K562/P-gp and K562 cells was studied.

It was found that the accumulation level of FX3 in both cell lines was similar (**Figure 3. 5. A**). The efflux rate of FX3 in both cell lines was also similar (**Figure 3. 5. B**). These data suggested that FX3 cannot be transported by P-gp. However, FX3 could rapidly leave cells by passive diffusion or other transporters on both cell lines when there was not sufficient FX3 in medium.

(A)



(B)

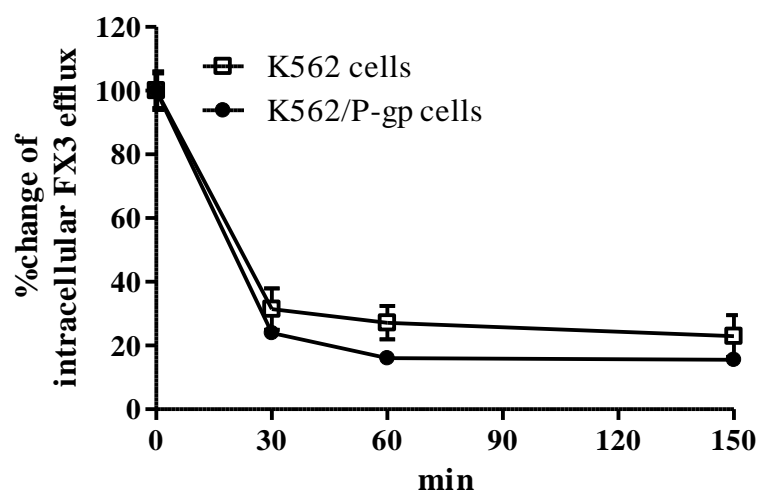


Figure 3. 5 Accumulation and efflux of FX3 in K562 and K562/P-gp cells

(A) K562 and K562/P-gp cells were incubated with FX3 at 0.1, 1 or 10 μM for 2.5 hours. Intracellular accumulation of FX3 was analyzed by UPLC-MS/MS. (B) K562 and K562/P-gp cells were incubated with FX3 at 1 μM for 2.5 hours. After incubation, FX3 was removed and replaced with fresh medium. Cells were collected at different time points and the intracellular level of FX3 was measured by UPLC-MS/MS.

3.2.7 Reversibility of FX3 in modulating P-gp

This section investigated whether FX3 could inhibit P-gp permanently. If so, FX3 could be removed after initial treatment and the inhibitory effect would remain. The experimental design was shown in **Figure 3. 6**. In the co-treatment group, FX3 and PTX were co-incubated together for the whole period. In the interval treatment group, LCC6MDR cells were pre-loaded with FX3 for 24 hours, washed with PBS, and PTX was added 0, 3 or 5 hours afterwards. PTX sensitivity was then measured by MTS test. The IC₅₀ of PTX was 212.9 nM in LCC6MDR without any modulator. Co-incubation of FX3 and PTX could significantly reduce IC₅₀ of PTX to 5.1 nM and EC₅₀ of FX3 was 111.2 nM (**Table 3. 6**). However, in the interval treatment group, IC₅₀ of PTX was ranging from 36.7 to 114.2 nM and EC₅₀ of FX3 was increased from 427.5 to 999.8 nM when the interval time was increased from 0 to 5 hours (**Table 3. 6**). The results of IC₅₀ and EC₅₀ in co-treatment group was significantly lower than those in interval treatment group. It suggested that the P-gp modulating potency of FX3 decreased in a time-dependent manner and the modulating activity was reversible. Co-incubation of FX3 and PTX performed the best in reversing MDR.

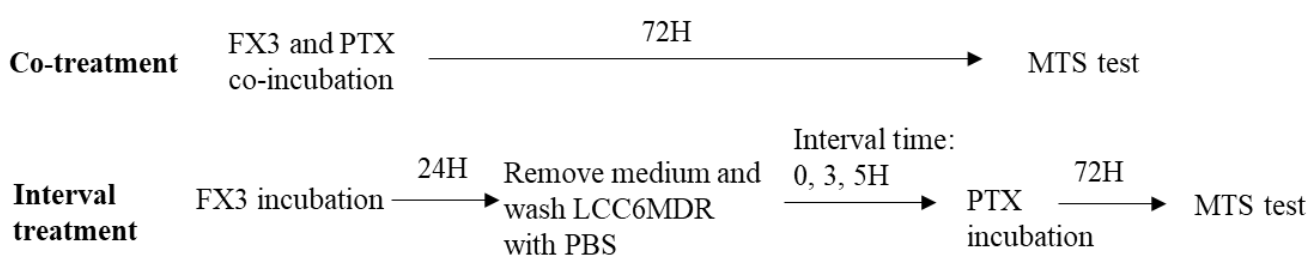


Figure 3. 6 Experiment design about the interval treatment of FX3 and PTX

FX3 and PTX were co-incubated or separately incubated with different interval time on LCC6MDR cells. The design of the treatments was shown.

Table 3. 6 Reversibility of FX3 in P-gp modulating

| Interval time between PTX and FX3 | | IC₅₀ of PTX (nM) | EC₅₀ of FX3 (nM) | |
|--|-----------|------------------------------------|------------------------------------|-------|
| | | Without FX3 | 1μM FX3 | |
| Co-treatment | | | 5.1 | 111.2 |
| Interval treatment | 0h | 212.9 | 36.7 | 427.5 |
| | 3h | | 61.2 | 691.6 |
| | 5h | | 114.2 | 999.8 |

Cell survival was measured by MTS and the result was analyzed by Prism 5.0 to calculate the IC₅₀ of PTX and EC₅₀ of FX3.

3.3 Summary

LCC6MDR was 12.7- and 80.3- fold more resistant to PTX and DOX than LCC6, respectively. P388ADR was 35.7- and 62.7- fold more resistant to DOX and PTX than P388. K562/P-gp was 6.3- and 164.9- fold more resistant to DOX and VCR than K562, respectively. The resistance resulted from P-gp overexpressing on the cell membrane.

The four derivatives, 23, 51, FX3 and WBC5, could reverse MDR by modulating P-gp in LCC6MDR, P388ADR and K562/P-gp. Compared with the EC₅₀ of EGCG (over 1000 nM), the four derivatives were potent in modulating P-gp with EC₅₀ ranging from 37.0 to 385.0 nM. The four derivatives had lower modulating activity on BCRP compared with P-gp, with higher EC₅₀ ranging from 343.0 to over 1000 nM, but they had no modulating activity on MRP-1. Among the four derivatives, FX3 was the most potent and specific in P-gp modulating.

The four derivatives had no effect on P-gp expression. They increased intracellular DOX accumulation by inhibiting DOX efflux in a dose-dependent manner. These results indicated that the four derivatives reversed MDR by inhibiting the efflux function of P-gp but not down-regulating P-gp expression.

The interaction between FX3 and P-gp were studied. First, it was found that FX3 could bind at TMD or an allosteric site of P-gp. Because it can stimulate instead of inhibiting P-gp ATPase activity. Second, FX3 cannot be transported by P-gp. But it left cells rapidly by passive diffusion or other transporters. Third, the P-gp modulating activity of FX3 was reversible and the potency of FX3 decreased in a time-dependent manner. To reach the best activity of reversing MDR, simultaneous presence of FX3 and anti-cancer drug displayed best effect of reversing MDR.

Chapter 4: Pharmacokinetics study of galloylated catechin derivatives by UPLC-Triple Quadrupole Tandem Mass Spectrometry

4.1 Introduction

Pharmacokinetics was the study of time course of absorption, distribution, metabolism and excretion of a drug in the body. Pharmacokinetics of a drug depended on both patient-related factors (e.g renal function, genetic makeup, sex and age) and chemical properties of the drug. Undesirable pharmacokinetics of a drug such as low bioavailability, short elimination half-life or drug-drug interaction were reasons in drug development failure (Prentis et al. 1988). Pharmacokinetics study was increasingly emphasized in the drug discovery process. EGCG was widely studied for its antioxidation, anti-inflammatory, anti-cancer and anti-cardiovascular effect, but its erratic bioavailability was also well known. The elimination half-life of EGCG was 62 ± 11 and 48 ± 13 min for i.v. (10 mg/kg) and oral (100 mg/kg) administration, respectively. The pharmacokinetic data indicated that the oral bioavailability of EGCG in a conscious and freely moving rat was about 4.95% (Lee et al. 2002, Lin et al. 2007, Eng et al. 2018, Fujiki et al. 2018).

The four derivatives (23, 51, FX3 and WBC5) were chemically modified from galloylated catechins including C, GC, EC and EGC. Their P-gp modulating activity *in vitro* were better than EGCG, one of their parent compounds, as demonstrated in the previous Chapter. In this Chapter, the pharmacokinetics study of the four derivatives was conducted.

Drug-drug interaction with anti-cancer drug was the major obstacle in development of P-gp modulator for clinical use. PSC833 (Valsporda), a well-known P-gp modulator,

1 reduced the clearance of etoposide by 50-57% and caused hematological toxicity in
2 Phase I clinical trial. The dose of PSC833 should be adjusted based on the PK
3 interactions between PSC833 and the chemotherapy agents in use (Visani et al. 2001).
4 These reasons resulted in the failure of PSC833 in clinical trials. In this Chapter,
5 pharmacokinetics of PTX with or without the derivatives (23, 51, FX3 and WBC5)
6 was also studied *in vitro* and *in vivo* in order to test whether drug-drug interaction
7 might occur between PTX and the derivatives.

4.2 Results

4.2.1 Detection of galloylated catechin derivatives in MRM

The detection methodology for the four derivatives (23, 51, FX3 and WBC5) by LC-MS/MS was established. The structurally-similar compound of 51 was used as the internal standard for the detection of 23, FX3 and WBC5, whereas FX3 was used as the internal standard for detection of 51.

$[M+H]^+$ and $[M+Na]^+$ parent ions were detected in MS2 scan (**Figure 4. 1**).

Optimization of fragmentor was performed to maximize the responses of the parent ions. Different collision energies were tried and the one yielding the highest response was chosen to be used to generate the daughter ion (**Table 4. 1**). After MS/MS condition optimization, the quantification of 23, 51, FX3 and WBC5 was performed by MRM at $597.2 > 181.1$ m/z, $708.2 > 181.2$ m/z, $678.3 > 151.1$ m/z and $678.3 > 151.2$ m/z, respectively (**Figure 4. 1**). Comparing the standard sample of galloylated catechins derivatives with blank plasma sample, there was no endogenous interference with the current detection method (**Figure 4. 2**).

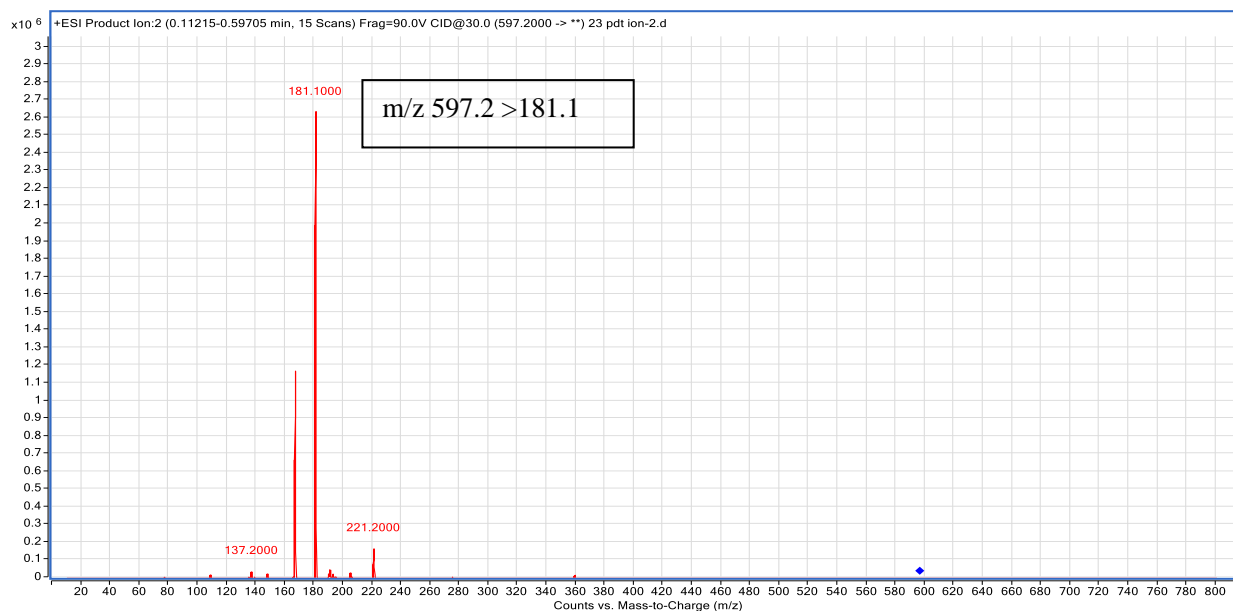
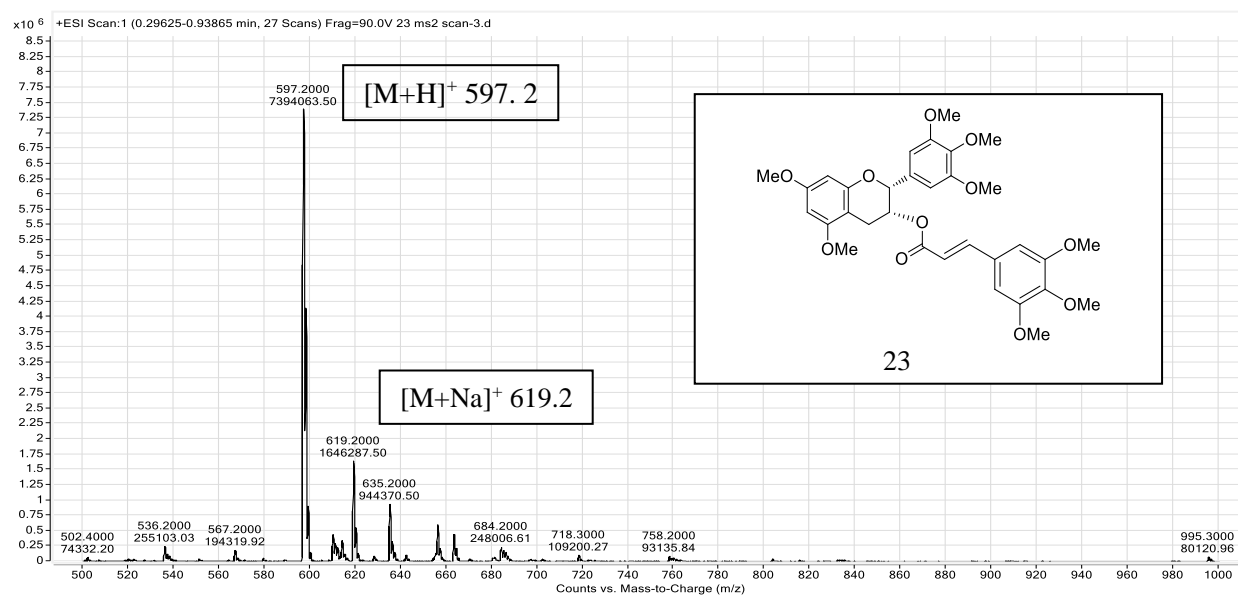
For pharmacokinetics profile of 23, 51, FX3 and WBC5 detection, the elution time, standard curves and detection concentration range were established and listed in **Table 4. 2**.

Table 4. 1 MS/MS condition optimization

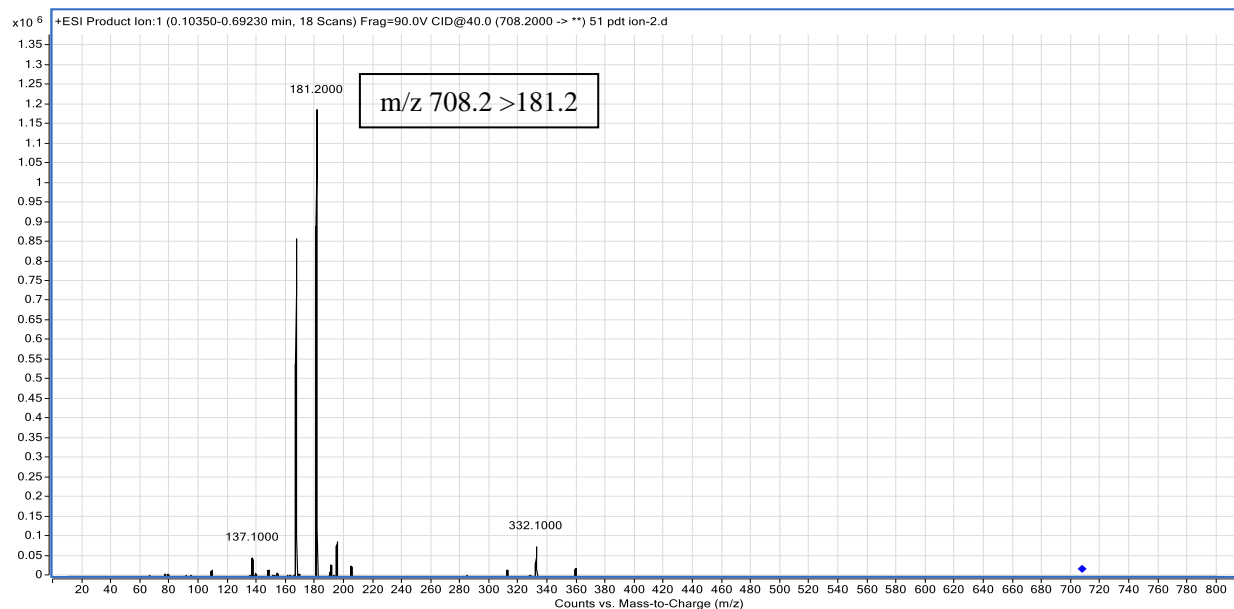
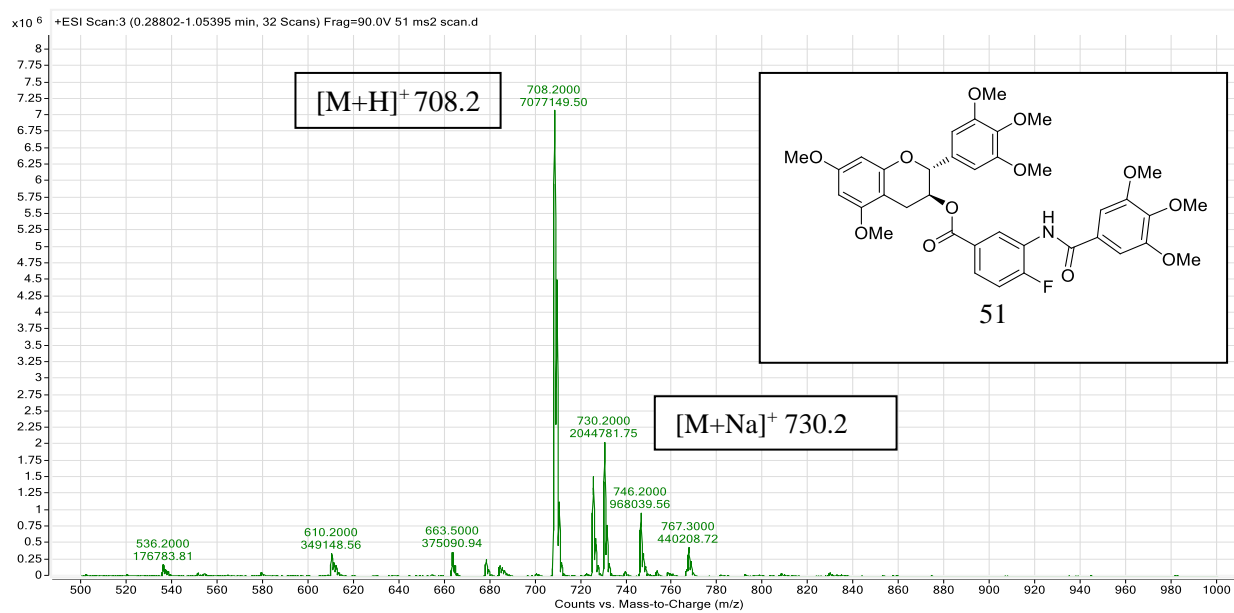
| Compound | Fragmentor | Collision Energy (eV) |
|----------|------------|-----------------------|
| 23 | 195 | 35 |
| 51 | 195 | 40 |
| FX3 | 175 | 40 |
| WBC5 | 135 | 30 |

The optimized fragmentor and collision energy for galloylated catechins derivatives detection were listed.

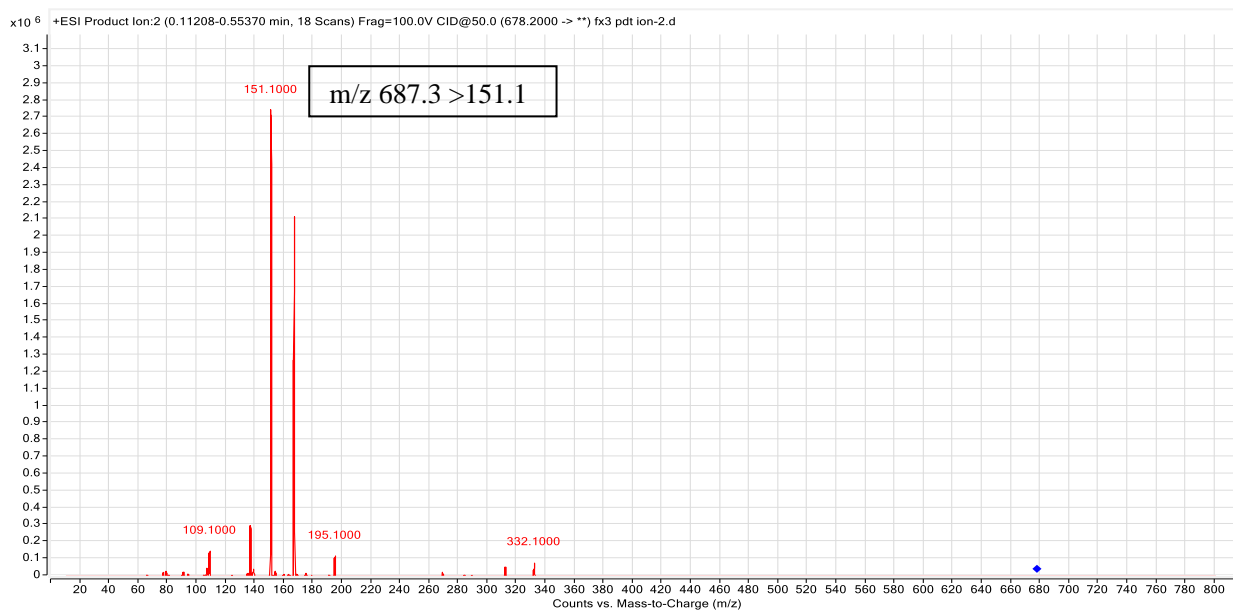
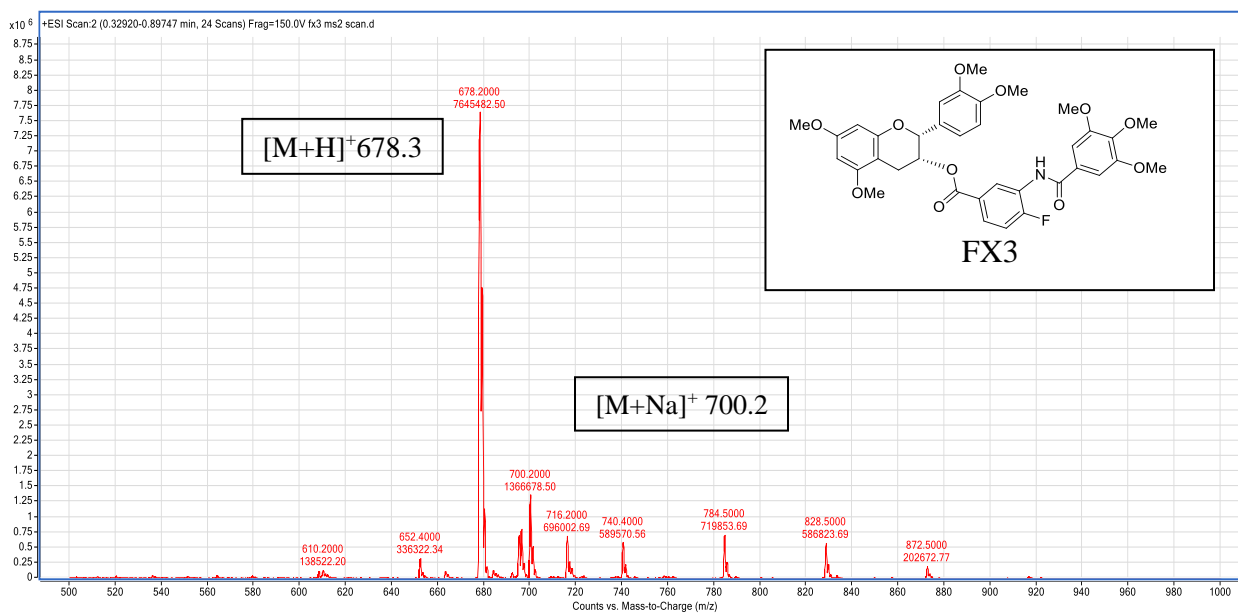
(A)



(B)



(C)



(D)

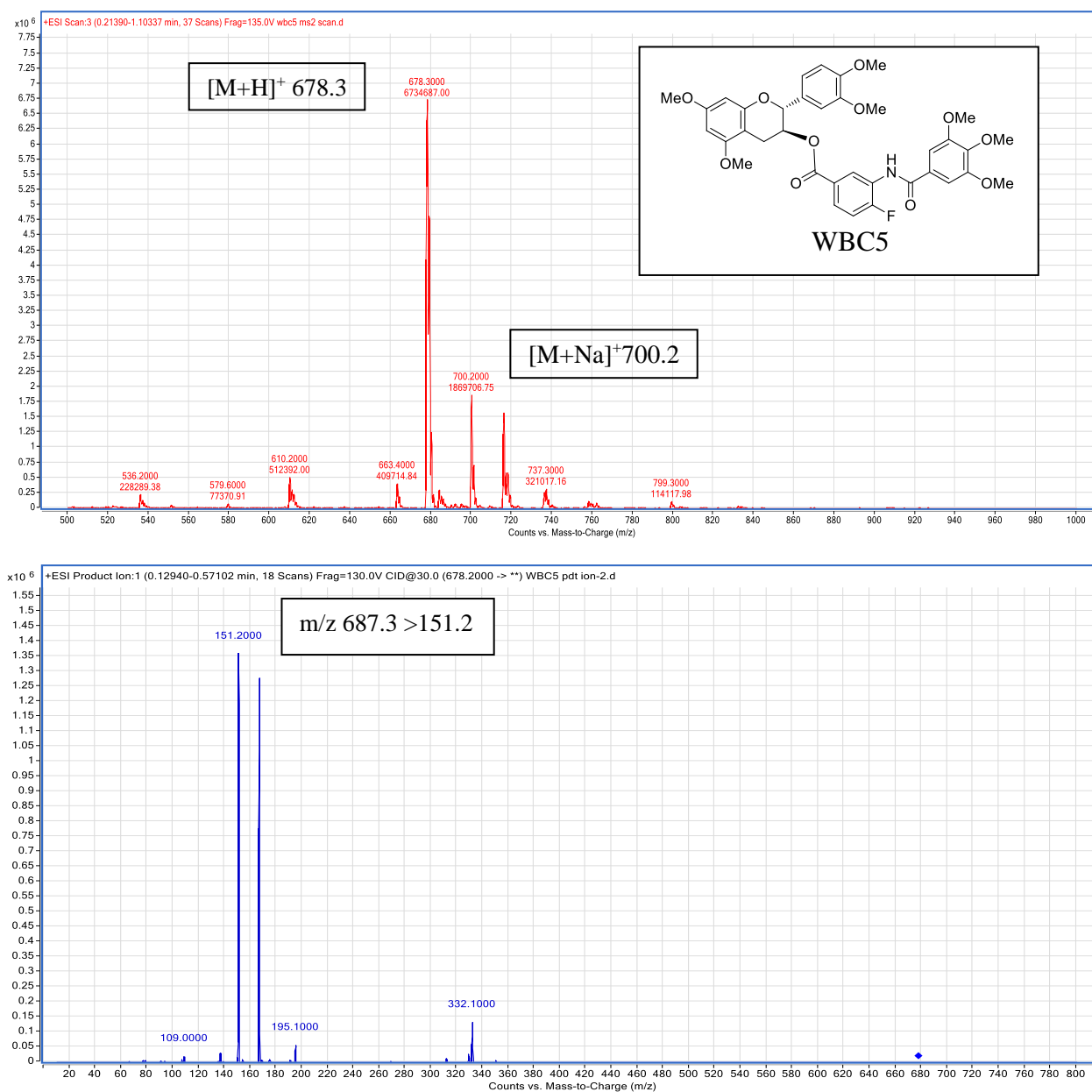
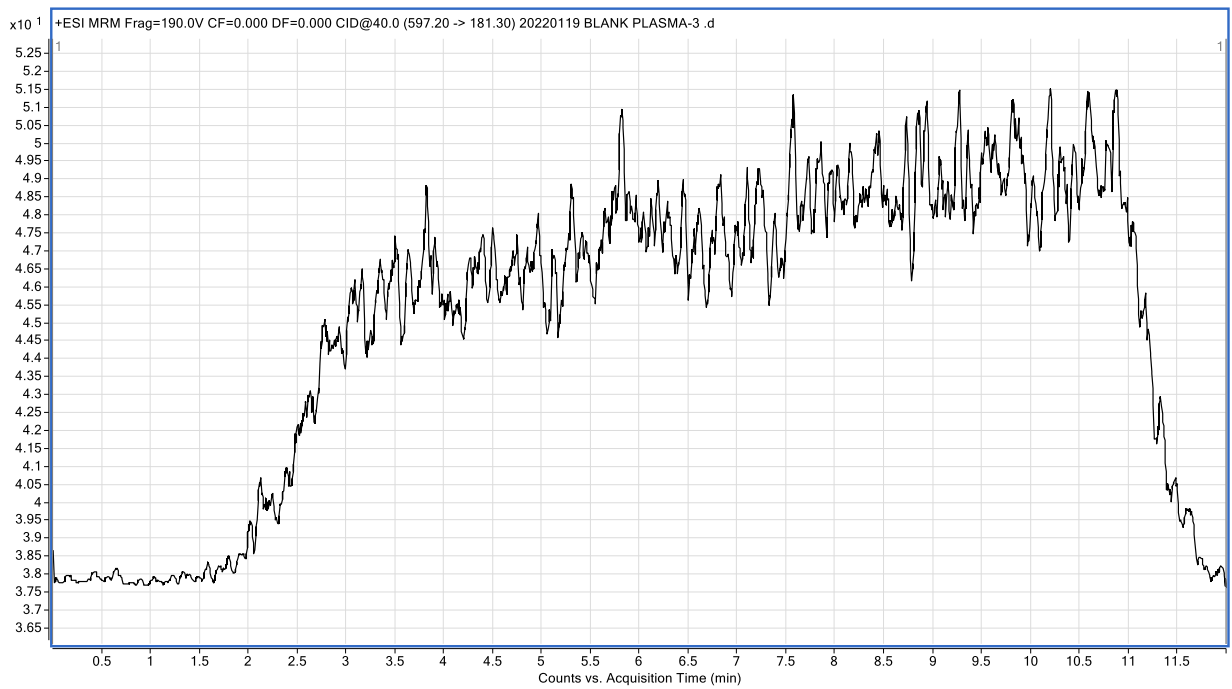
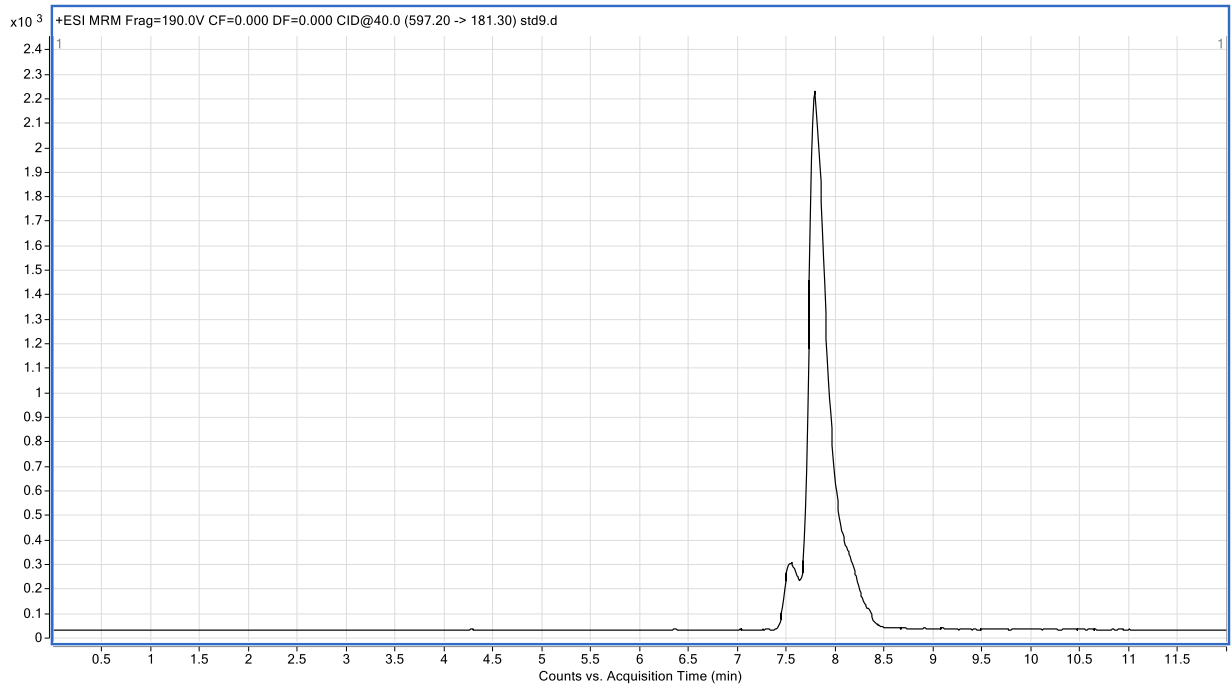


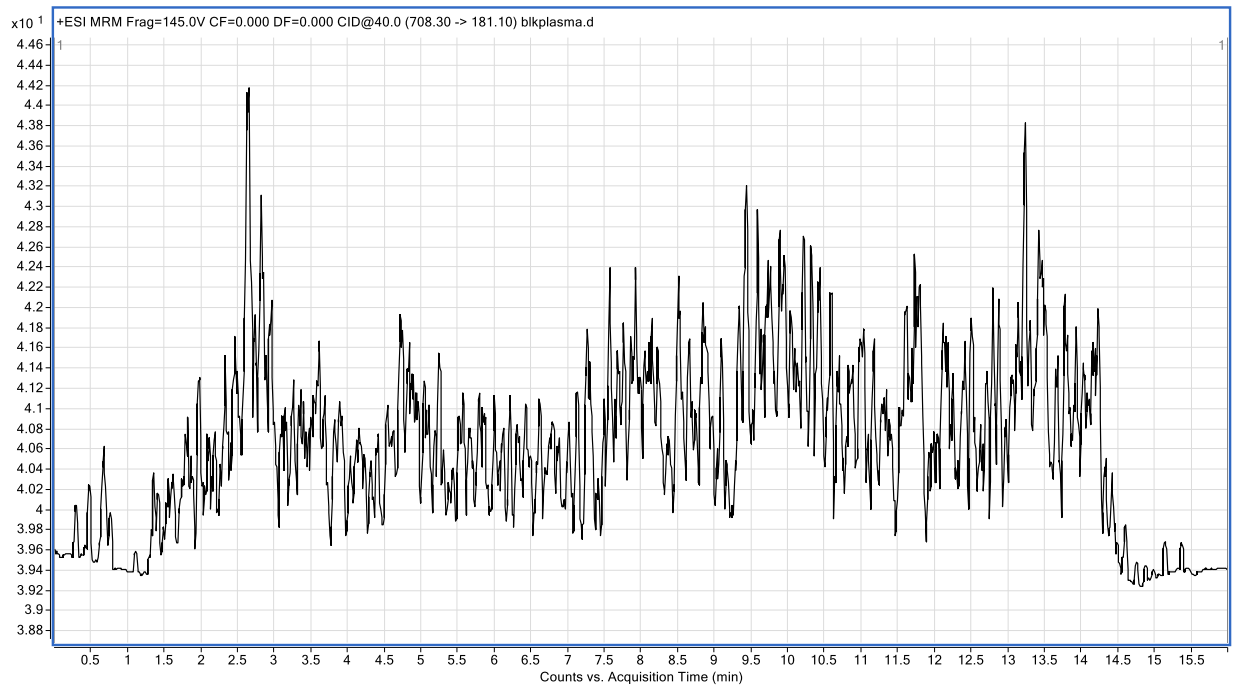
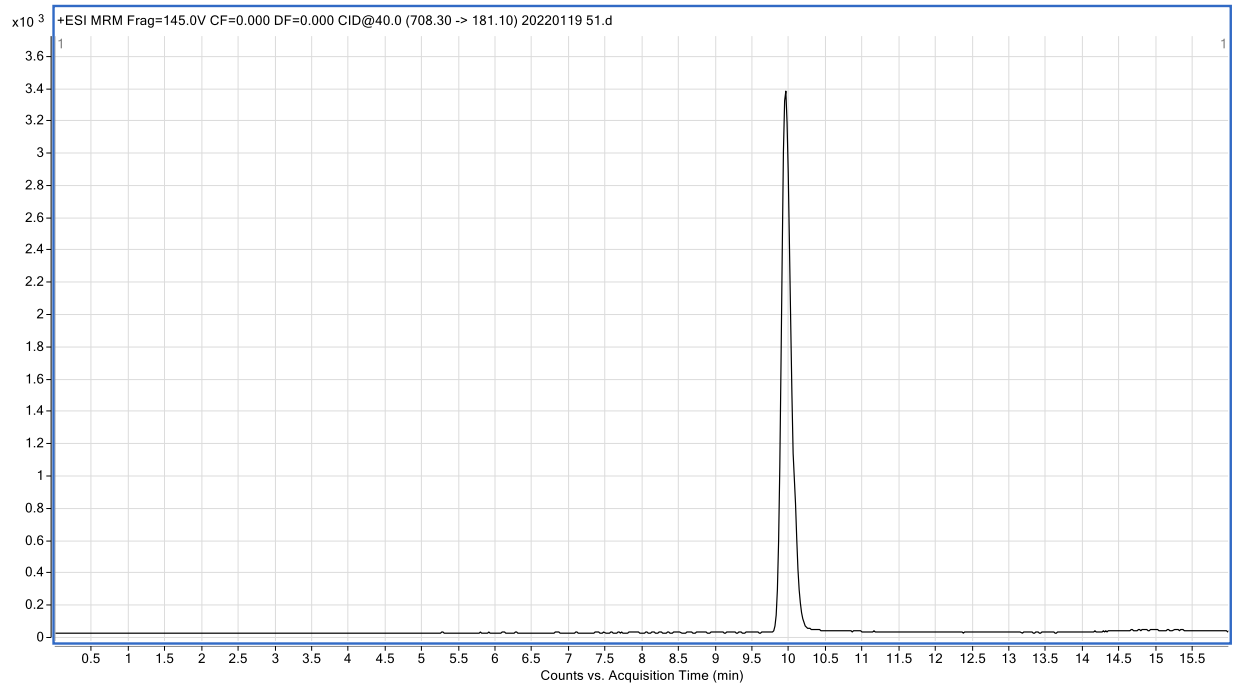
Figure 4. 1 MRM detection of galloylated catechins derivatives

The standard solution of galloylated catechins derivatives was subjected to MS/MS analysis. (A) MS spectrum of 23 was 597.2 m/z and the major fragment was 181.0 m/z. (B) MS spectrum of 51 was 708.2 m/z and the major fragment was 181.0 m/z. (C) MS spectrum of FX3 was 678.2 m/z and the major fragment was 151.1 m/z. (D) MS spectrum of WBC5 was 678.3 m/z and the major fragment was 151.2 m/z.

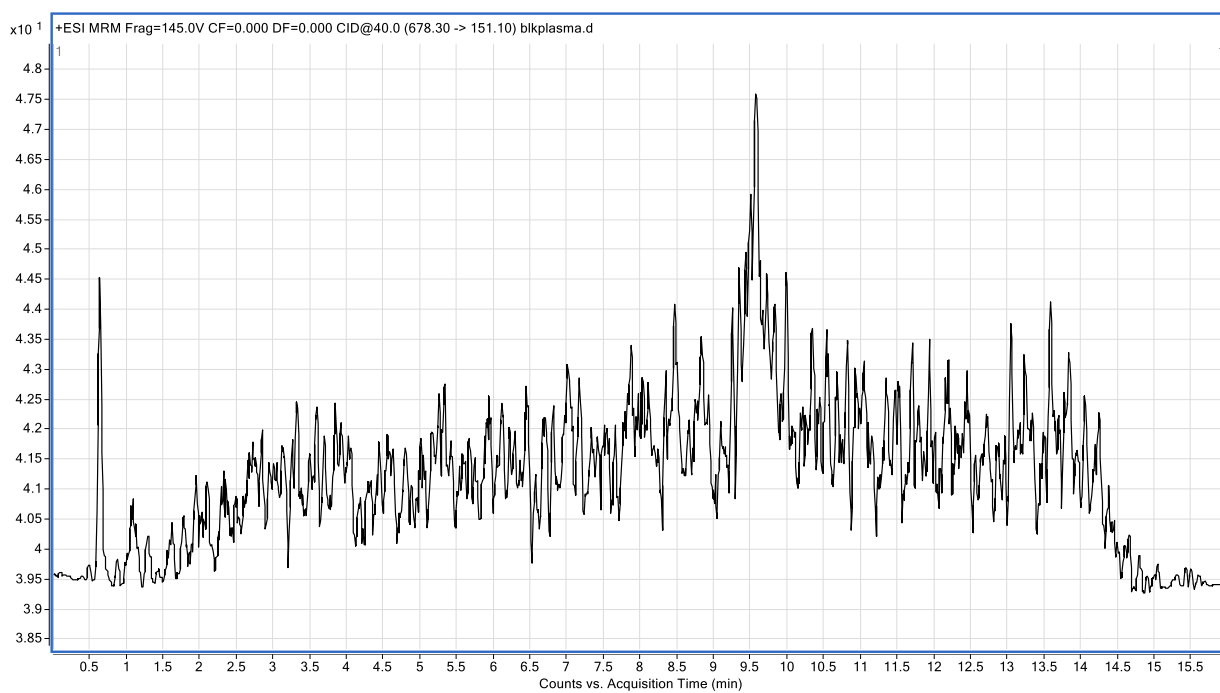
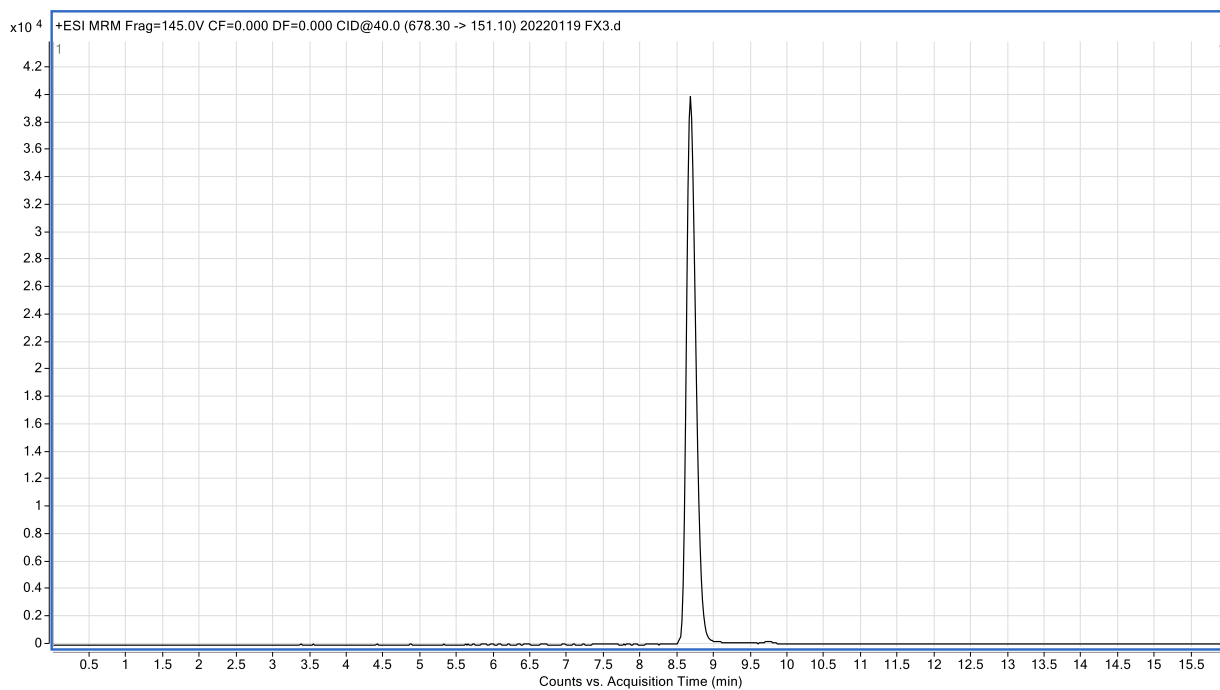
(A)



(B)



(C)



(D)

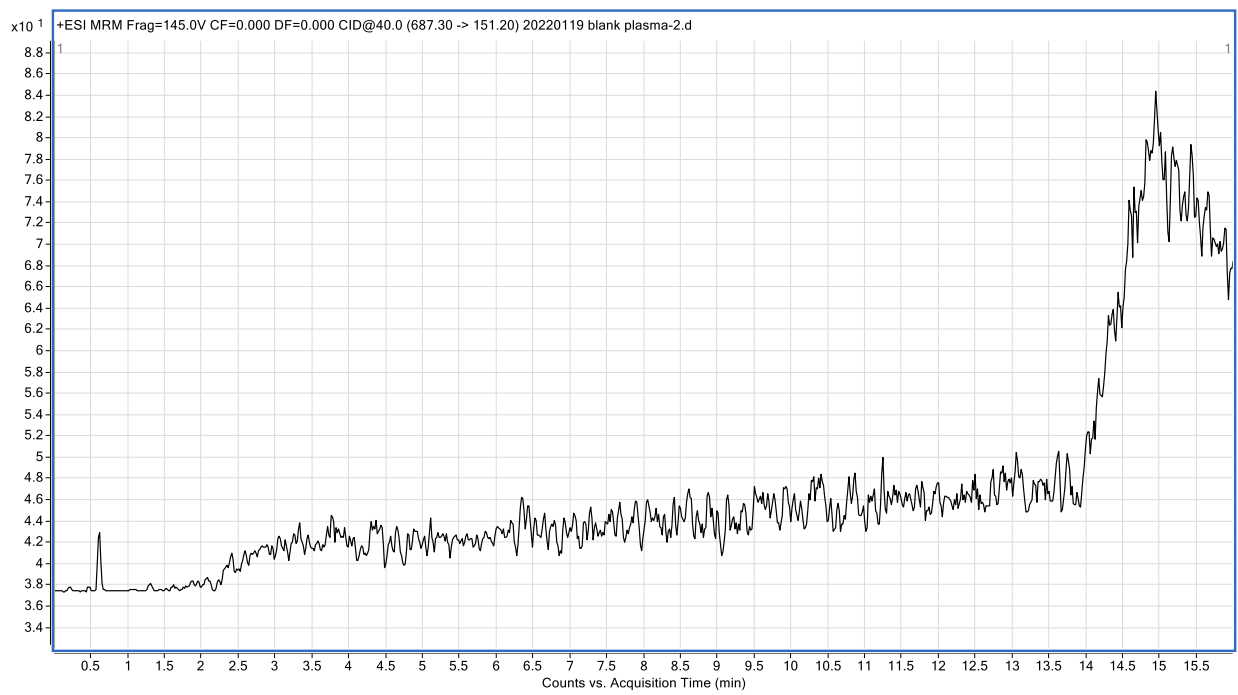
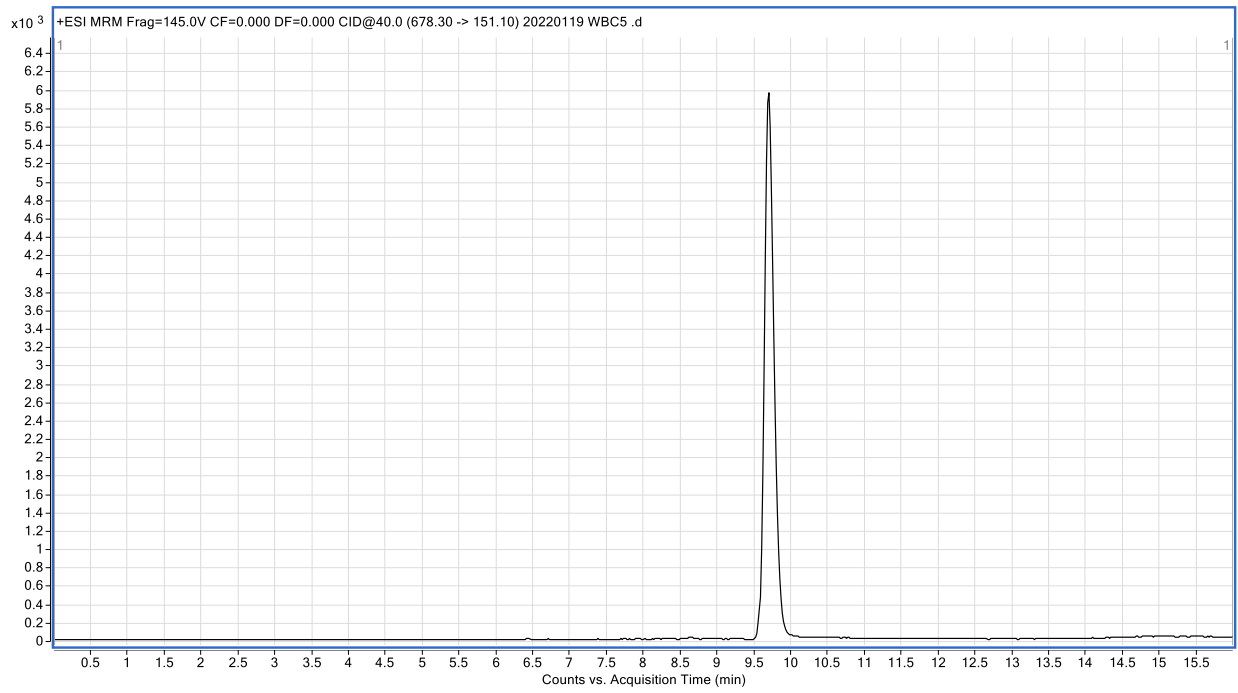


Figure 4. 2 Blank plasma and derivatives in plasma chromatography

Chromatography of derivatives in the presence of plasma and blank mice plasma by monitoring MRM 597.2 > 181.3 m/z (23), 708.3 > 181.0 m/z (51) and 687.3 > 151.1 m/z (FX3 or WBC5) respectively. (A) 23 was eluted at 7.9 minutes. The blank plasma was monitored by MRM 597.2 > 181.3 m/z for endogenous interference detection. (B) 51 was eluted at 9.8 minutes. The blank plasma was monitored by MRM 708.3 > 181.1 m/z for endogenous interference detection. (C) FX3 was eluted at 8.7 minutes. The blank plasma was monitored by MRM 687.3 > 151.1 m/z for endogenous interference detection. (D)WBC5 was eluted at 9.7 minutes. The blank plasma was monitored by MRM 687.3 >151.1 m/z for endogenous interference detection.

Table 4. 2 Standard curve of 23, 51, FX3 and WBC5

| Compound | Elution time (min) | Standard curve | R ² | Detection range (ng/mL) | Limit of quantification (ng/mL) (LOQ) | Noise to Signal ratio (N/S) |
|----------|--------------------|------------------|----------------|-------------------------|---------------------------------------|-----------------------------|
| 23 | 7.9 | y=5.5945x-0.2805 | 0.9940 | | 2.75 | 13.4 |
| 51 | 9.8 | y=1.6779x+0.0231 | 0.9991 | 5.5-5500 | 5.50 | 14.4 |
| FX3 | 8.7 | y=2.7088x-0.0421 | 0.9997 | | 1.37 | 11.1 |
| WBC5 | 9.7 | y=1.7788x+0.0437 | 0.9999 | | 5.50 | 9.70 |

Standard curve was constructed to determine the linear relationship between the concentration of galloylated catechins derivatives in plasma (x) and peak area ratio of galloylated catechins derivatives by internal standard (y). The concentration of derivatives in plasma was serially diluted from 5500 to 5.5 ng/mL.

4.2.2 Formulation selection of galloylated catechins derivatives for animal study

Galloylated catechins derivatives were hydrophobic because the phenolic hydroxyl groups were all replaced by methoxy groups for improving P-gp modulating activity. This might result in absorption and solubility problems when they were used in animal study. Different formulations were used to dissolve FX3 to determine the ideal combination of solvent and co-solvent for maintaining a high level of FX3 in plasma. FX3 was dissolved in six formulations and administrated by i.v. to BALB/c mice. Blood was collected at two time points at 30- and 60-minutes post administration. Plasma level of FX3 was determined by UPLC-MS/MS. The detection method was described in Chapter 2. The six formulations in the study were formulation A (Ethanol: Cremophor EL: PBS=1:1:8), formulation B (Ethanol: Tween80: PBS=1:1:8), formulation C (Ethanol: Tween20: PBS=1:1:8), formulation D (NMP: Cremophor EL: PBS=1:1:8), formulation E (NMP: Tween 80: PBS= 1:1:8) and formulation F (NMP: Tween 20: PBS=1:1:8).

Pharmacokinetic results (**Figure 4. 3** and **Table 4. 3**) showed that FX3 in formulation D gave the highest plasma level among the six formulations. At 30 minutes post administration, the plasma level of FX3 in formulation D was 1.5- to 2.5- fold higher than that in the other five formulations. At 60 minutes post administration, the plasma level of FX3 in formulation D was 2.3- to 5.4- fold higher than that in the other five formulations. In the subsequent *in vivo* experiments, formulation D was used for dissolving 23, 51, FX3 and WBC5.

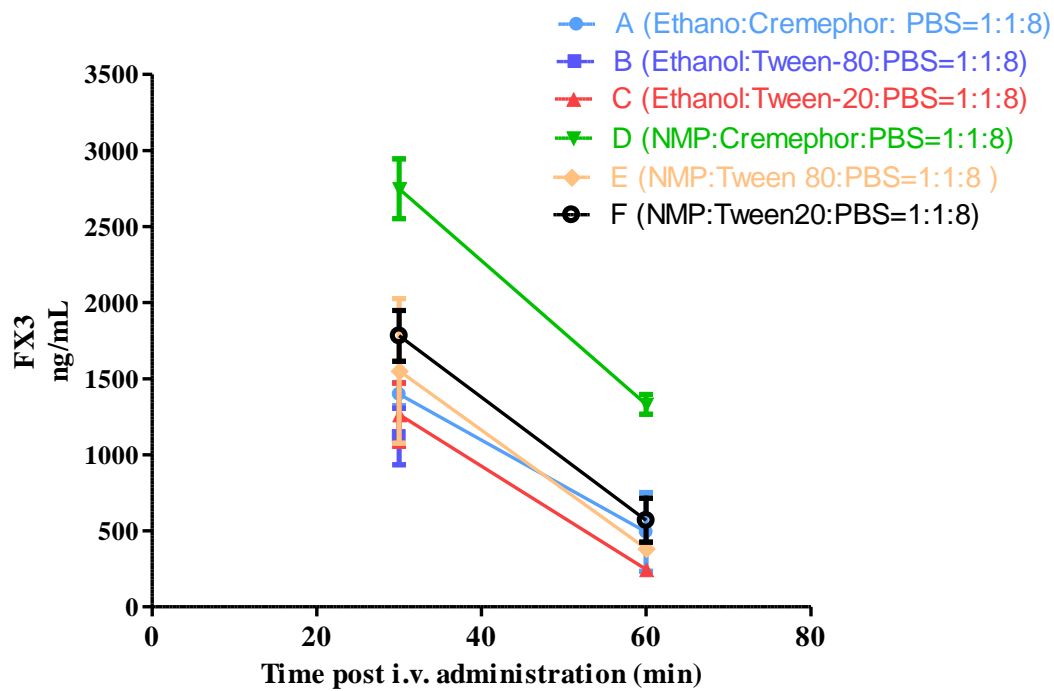


Figure 4. 3 Plasma level of FX3 in different formulations

FX3 was prepared in six different formulations (A to F) at 1 mg/mL and i.v. administrated to BALB/c mice at 10 mg/kg. At 30- and 60- minutes post administration, the blood was collected. The plasma level of FX3 was detected using UPLC-MS/MS as described previously. Each time point represented as mean \pm sem. (n=2)

Table 4. 3 Plasma level of FX3 in different formulations

| Formulation | Concentration of FX3 in plasma (ng/mL) | |
|-------------|--|----------------------------|
| | 30 min post administration | 60 min post administration |
| A | 1398.9 ± 54.2 | 492.9 ± 182.6 |
| B | 1120.5 ± 131.0 | N.D |
| C | 1264.2 ± 147.0 | 247.0 ± 29.8 |
| D | 2748.4 ± 139.0 | 1331.2 ± 46.4 |
| E | 1551.1 ± 336.2 | 382.8 ± 20.4 |
| F | 1781.9 ± 117.7 | 569.8 ± 102.2 |

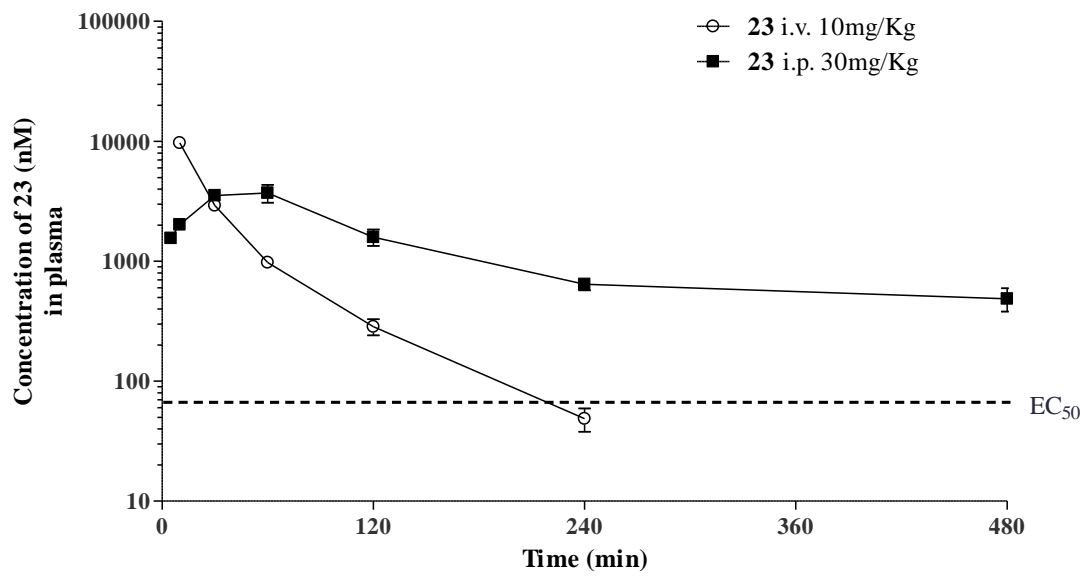
FX3 was prepared in six different formulations (A-F) at the same concentration (1 mg/mL). FX3 was i.v. injected to mice at 10 mg/kg. Blood was collected at 30- and 60- min post administration. The concentration of FX3 in plasma was measured by UPLC-MS/MS. The pharmacokinetic profiles were presented in **Figure 4. 3** and the concentration of FX3 was listed here. There were two mice in each time point. N.D meant not done. (n=2)

4.2.3 Plasma level of galloylated catechins derivatives

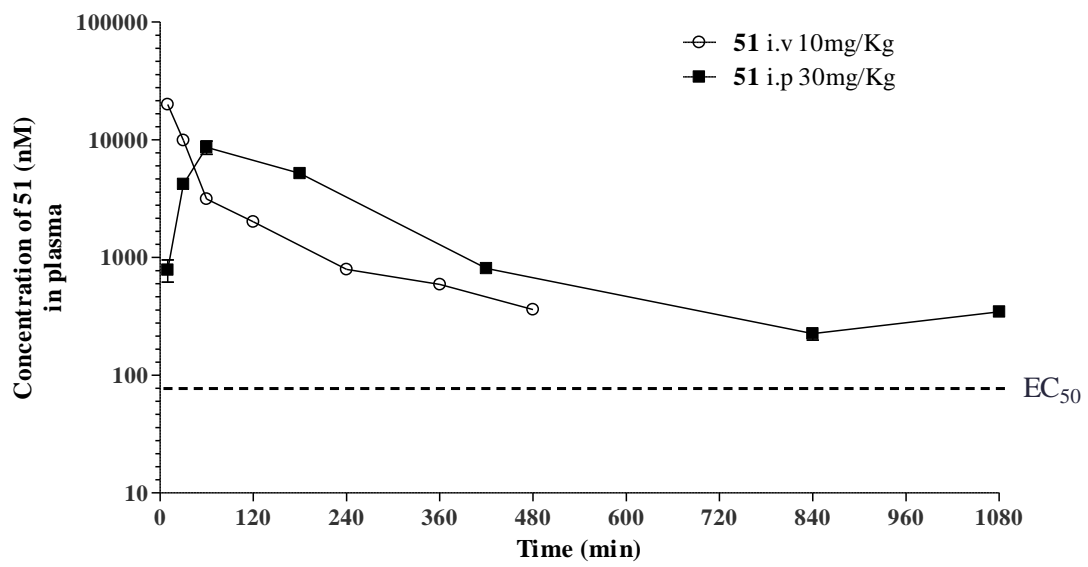
Pharmacokinetic study of 23, 51, FX3 and WBC5 (either i.v. at 10 mg/kg or i.p. at 30 mg/kg) was performed to investigate how long the plasma level of the derivatives could be maintained above their corresponding EC₅₀ levels (**Figure 4. 4**). Blood was collected at different time points after administration up to 18 hours. The PK parameters of the galloylated catechins derivatives were summarized in **Table 4. 4**.

After i.p. administration at 30 mg/kg, the plasma level of the three derivatives (51, FX3 and WBC5) could exceed their corresponding *in vitro* EC₅₀ for about 18 hours. In contrast, the i.v. administration route resulted in a faster clearance. The plasma level of 23, FX3 and WBC5 dropped below their corresponding *in vitro* EC₅₀ after 180, 360 and 240 minutes respectively. The plasma concentration of 51 (10 mg/kg, i.v.) could exceed its *in vitro* EC₅₀ for about 480 minutes. I.p. administration of the four derivatives yielded a high bioavailability with dose-normalized AUC_{i.p./AUC_{i.v.}} ranging from 66% to 81%. The high bioavailability of i.p. administration indicated good absorption and stability to metabolism.

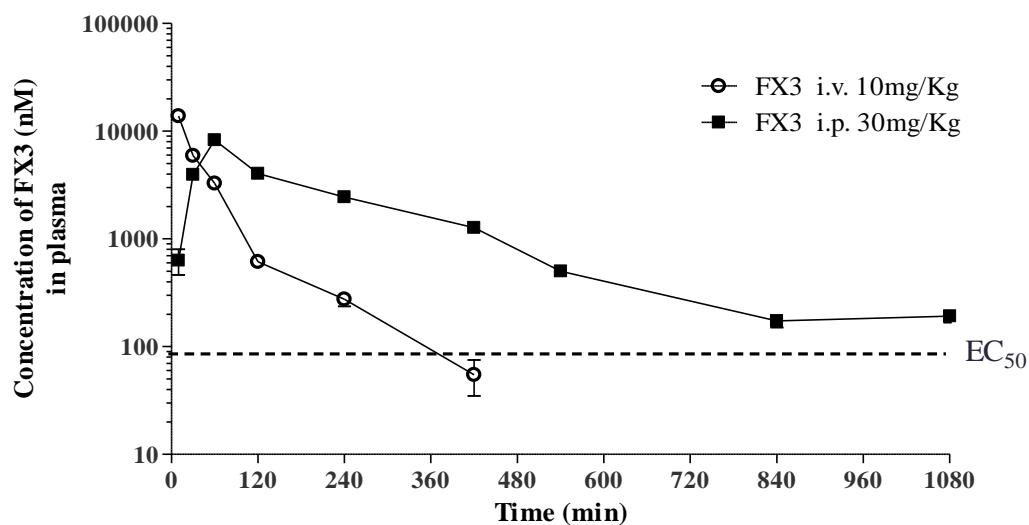
(A)



(B)



(C)



(D)

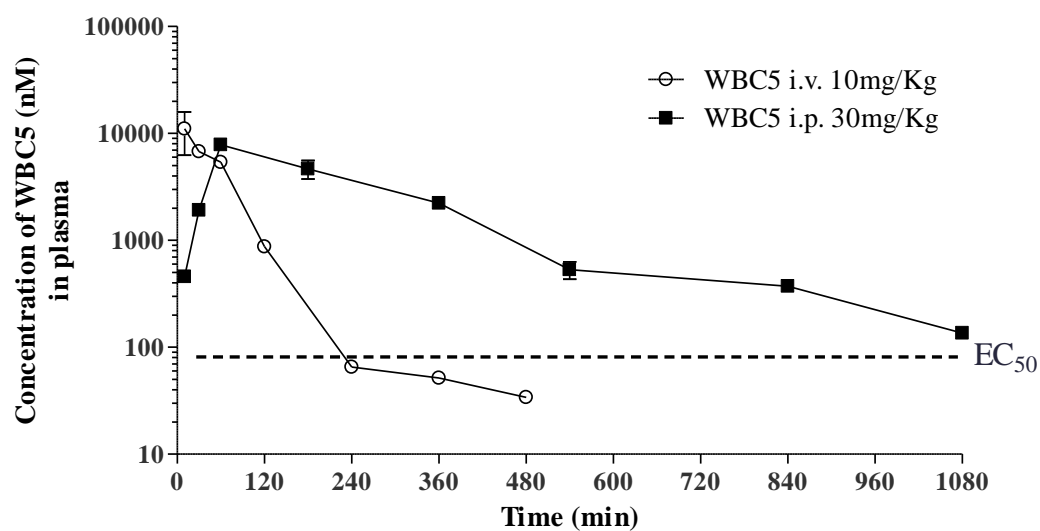


Figure 4. 4 Pharmacokinetics profiles of galloylated catechins derivatives in BALB/c mice

The derivatives of 23, 51, FX3 and WBC5 were administrated to BALB/c mice at indicated dosage and route of administration. At different time points, mice were sacrificed and blood was collected. Plasma level of the derivatives was detected using UPLC-MS/MS. Each time point represented as mean \pm sem. (n=3)

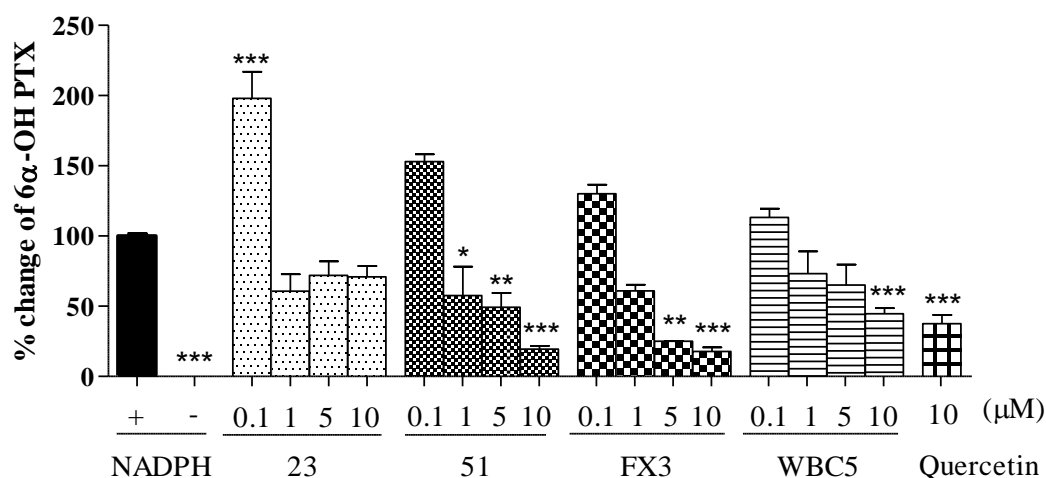
Table 4. 4 Pharmacokinetics parameters of galloylated catechins derivatives in BALB/c mice

| Compounds | | 23 | | 51 | | FX3 | | WBC5 | |
|----------------------------|------------|---------|--------|---------|---------|---------|---------|---------|---------|
| Administration Route | | i.v. | i.p. | i.v. | i.p. | i.v. | i.p. | i.v. | i.p. |
| Dosage (mg/kg) | | 10 | 30 | 10 | 30 | 10 | 30 | 10 | 30 |
| AUC ng-min/mL | 0-t | 191132 | 360577 | 779549 | 1471569 | 434224 | 1065748 | 531963 | 1270490 |
| | 0-infinity | 192484 | 457783 | 813290 | 1542337 | 437163 | 1103273 | 533621 | 1295737 |
| Cmax (ng/mL) | | / | 2210.4 | / | 6120.7 | / | 5609.3 | / | 5257.8 |
| Tmax (min) | | / | 60 | / | 60 | / | 60 | / | 60 |
| Half-life (min) | | 32.3 | 157.6 | 91.5 | 229.9 | 54.713 | 199.7 | 51.011 | 187.3 |
| Half-life D/A (min) | | / | 31.3 | / | 103.5 | / | 101.8 | / | 42.8 |
| AUC _(0-t) /dose | | 19113.2 | 12019 | 77954.9 | 49052.3 | 43422.4 | 35524.9 | 53196.3 | 42349.7 |
| Bio-availability (%) | | 62.9 | | 62.9 | | 81.8 | | 79.6 | |

4.2.4 Effect of galloylated catechin derivatives on PTX metabolism with human liver microsomes

Human cytochrome P450s CYP3A4 and CYP2C8 metabolized PTX into 6 α -OH-PTX and 3*p*-OH-PTX, which were the main PTX metabolites, respectively (Monsarrat et al. 1990). Many P-gp modulators can inhibit these P450s and delay PTX metabolism and clearance, causing undesirable toxicity. The effect of four derivatives on PTX metabolism was investigated (**Figure 4. 5**). Galloylated catechin derivatives stimulated the production of 6 α -OH-PTX by 1.13- to 1.98- fold when the concentration of these four derivatives was 0.1 μ M, which corresponded to the EC₅₀ levels of the modulation (**Figure 4. 5. A**). Inhibition of the production of 6 α -OH PTX was observed with treatment of derivatives at over 1 μ M and the inhibition performed in a dose-dependent manner (**Figure 4. 5. A**). On the other hand, these derivatives stimulated the metabolism from PTX to 3*p*-OH PTX (**Figure 4. 5. B**). The results suggested that these derivatives stimulated the metabolism of PTX via CYP3A4 but inhibited the metabolism of PTX via CYP2C8 in dose dependent manner.

(A)



(B)

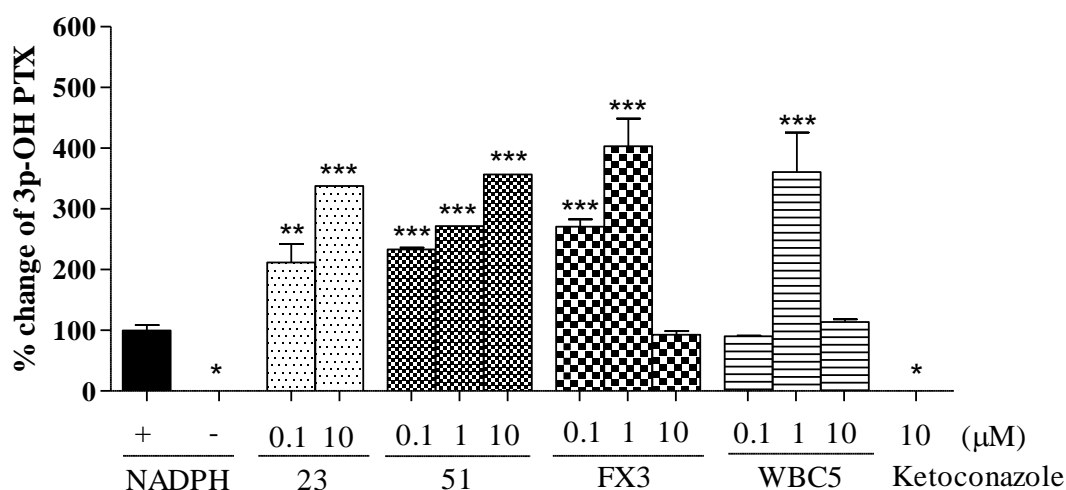


Figure 4. 5 Effect of galloylated catechin derivatives on the metabolism of PTX with the human liver microsomes

Human liver microsomes was incubated with PTX and NADPH in the presence of galloylated catechin derivatives or positive controls (quercetin or ketoconazole). Human liver microsomes and PTX without incubation of NADPH was the negative control. Production of PTX metabolites 6α-OH PTX (A) or 3p-OH PTX (B) was measured by UPLC-MS/MS. Percentage change of metabolites was normalized to the amount of metabolites treated by PTX alone (+ NADPH). The results were analyzed by Prism 5.0 by one-way ANOVA. *, $p < 0.05$; **, $p < 0.01$; ***, $p < 0.001$

4.2.5 Pharmacokinetics study of PTX with or without 51, FX3 or WBC5

To measure the drug-drug interaction between PTX and the galloylated catechin derivatives, PTX was i.v. administrated at 12 mg/kg with or without FX3, WBC5 or 51 (administrated i.p. at 30 mg/kg) (**Figure 4. 6**). The plasma level of PTX was determined at up to 420 minutes post administration. $AUC_{0-420min}$ of PTX alone in plasma was 400972 ± 21277 ng/mL-min. With co-administration of FX3, WBC5 or 51, $AUC_{0-420min}$ of PTX in plasma was 478526 ± 61912 , 585661 ± 18423 and 632407 ± 12900 ng/mL-min respectively. It was found that co-administration of 51, FX3 or WBC5 could slightly increase the AUC_{PTX} by 1.2 ($p = 0.337$) to 1.6 ($p = 0.002$) -fold in plasma (**Table 4. 5**). The PTX plasma level with the combination treatment of 23 and PTX were not conducted. Because 23 did not show the same level of P-gp modulating potency and plasma stability as the other three derivatives, according to previous results. The results suggested that FX3 had no significant ($p > 0.1$) enhancement effect on the pharmacokinetics profile of PTX whereas WBC5 and 51 enhanced the PTX level in plasma ($p < 0.05$).

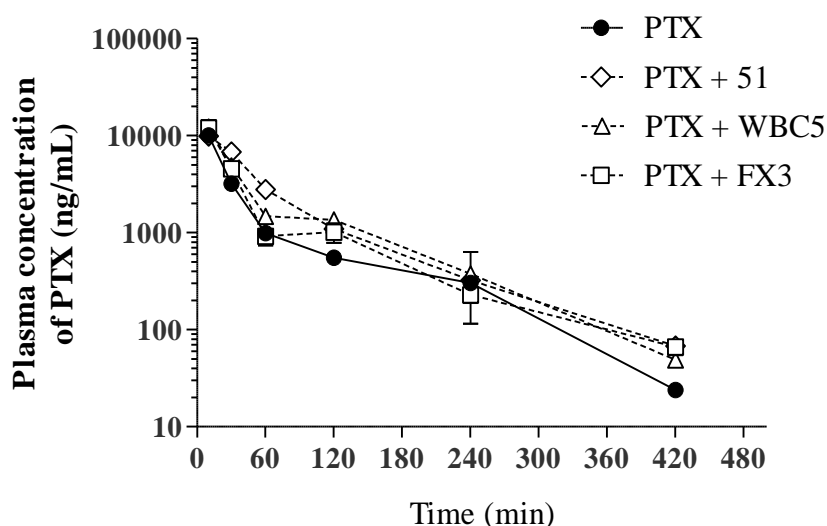


Figure 4. 6 Effect of galloylated catechin derivatives on the pharmacokinetics profile of PTX in BALB/c mice

Galloylated catechin derivatives were i.p. administrated at 30 mg/kg one hour before i.v. injection of PTX at 12 mg/kg. The PTX plasma level was measured at up to 420 minutes post administration by UPLC-MS/MS. There were 3 mice for each time point.

Table 4. 5 Effect of galloylated catechin derivatives on AUC of PTX in plasma

| PTX (12mg/kg i.v.) | Galloylated catechins (30 mg/kg i.p.) | AUC of PTX (ng-min/mL) | <i>p</i> value (Compared with PTX alone group) |
|-----------------------|---|---------------------------|--|
| + | - | 400,972 ± 21,277 | - |
| + | FX3 | 478,526 ± 61,912 | 0.337 (N.S) |
| + | WBC5 | 585,661 ± 18,423 | 0.003 (**) |
| + | 51 | 632,407 ± 12,900 | 0.002 (**) |

Non-compartmental analysis of PTX in BALB/c mice and AUC was calculated by PK solutions 2.0 (Summit Research Service, Ashland, U.S.A). Plasma level at each time point in co-treatment group was compared with that in control group respectively by two tailed unpaired t-test. *, $p < 0.05$; **, $p < 0.01$

4.3 Summary

Optimization for the detection of 23, 51, FX3, WBC5 and PTX using UPLC-MS/MS was performed, aiming to improve selectivity and linearity of the detection method. It was found that linearity of the four modulators between (5.5- 5500 ng/mL) was good. These derivatives (23, 51, FX3 and WBC5) were hydrophobic. The solubility problem was solved by formulation optimization. Solvents such as ethanol and NMP and co-solvents such as Tween 20, Tween 80 and Cremophor EL were used in different combinations. FX3 in formulation of 10% NMP, 10% Cremophor EL and 80% PBS displayed the highest plasma level at 30- and 60- min post administration among the six different formulations. This formulation was applied in the subsequent *in vivo* experiments.

In pharmacokinetics study, the plasma level of the four derivatives rapidly decreased to a level lower than their *in vitro* EC₅₀ in 6 hours by i.v. injection in BALB/c mice. I.p. injection at 30 mg/kg of these derivatives can maintain a plasma level over its EC₅₀ for more than 18 hours, which provided sufficient exposure *in vivo*. Therefore i.p. injection was used in subsequent *in vivo* efficacy studies

One obstacle of P-gp modulator development was the systematic toxicity induced by the drug-drug interaction between modulator and anti-cancer drug. Therefore, PTX metabolism and PTX pharmacokinetics profiles were studied.

Two main metabolites of PTX were 3*p*-OH PTX and 6*α*-OH PTX. The four derivatives (23, 51, FX3 and WBC5) had no effect on the production of 3*p*-OH PTX. In contrast, derivatives inhibited the production of 6*α*-OH PTX in a dose-dependent manner. Inhibition of PTX metabolism was observed when the concentration of four derivatives were used over 1 μM. When 23, 51, FX3 and WBC5 were used at 0.1 μM,

which was their EC₅₀, there were no inhibitory effect on PTX metabolism. The results suggested that these derivatives could be used at an effective concentration without affecting PTX metabolism.

In PTX pharmacokinetics profile, the AUC_{PTX} of co-treatment of PTX with 51, FX3 and WBC5 was increased by 1.2- to 1.6- fold respectively. The increase of PTX level in plasma mainly occurred for 90-180 minutes post derivatives administration. In that period, the plasma level of derivatives (51, FX3 and WBC5) was over 5 μM which inhibited 6α-OH PTX production. It could explain the enhancement of AUC_{PTX} in plasma level with combination treatment. At 180 minutes post derivatives administration, there was no difference of PTX plasma level between PTX alone and combination treatment. Among the three derivatives, FX3 had no drug-drug interaction with PTX ($p = 0.337$). Therefore, FX3 would be used in the efficacy study.

Chapter 5: The efficacy study of galloylated catechin derivatives in reversing MDR xenograft model *in vivo*

5.1 Introduction

Murine models were developed for human cancer study for decades. These models were used to study the mechanism of cancer development such as malignant transformation, invasion, metastasis as well as discovery or improvement of anti-cancer therapy.

5.1.1 Nude mice and LCC6MDR xenograft model

Nude mice had *Foxn1* mutation that led to abnormal hair growth and defective development of the thymic epithelium. Nude mice were widely used for s.c transplant of rapidly growing tumor cell lines since they were hairless, thus enabling the easy monitoring of tumor development.

MDA435/LCC6 was the estrogen receptor-negative breast cancer cell line. It was invasive and metastatic when implanted into nude mice. Take-rate of MDA435/LCC6 in nude mice was 100% when administrated at mammary fatpad (m.f.p) and 40% when administrated s.c. Distant metastasis to lymph nodes and lungs in m.f.p recipients could reach 100% (Price et al. 1990). The animal model of LCC6MDR s.c xenograft in nude mice had been established as a drug resistance model in our group previously (Yan et al. 2015). PTX 12 mg/kg i.v. could suppress the tumor growth of LCC6 but had no suppression effect on LCC6MDR.

5.1.2 Application of P-gp modulator in solid tumor

A phase II clinical trial on using tariquidar, a selective third generation P-gp

modulator, was conducted on unresponsive advanced breast carcinoma patients. The study was discontinued because of limited clinical efficacy to restore sensitivity to anthracycline or taxane chemotherapy. The results of the clinical trial still showed that tariquidar was beneficial to a small subset of patients with MDR (Pusztai et al. 2005). The other two phase III clinical trials for lung carcinoma were also discontinued because of high rate of adverse events and undesirable response rate observed in the tariquidar arm from unpublished results of QLT Inc (Pusztai et al. 2005). Such failure of the third-generation modulators led to the development of new P-gp modulators.

5.1.3 Leukemia

Leukemia was a broad term for cancers of the blood cells. The type of leukemia depended on the type of blood cells that became cancerous. Different types of leukemia included lymphoblastic or lymphocytic leukemias and myeloid or myelogenous leukemias.

5.1.4 B6D2F1 mice and murine leukemia animal model of P388ADR

Murine leukemia models used in the initial drug discovery programs were provided by the Division of Cancer Treatment and Diagnosis (DCTD) of the National Cancer Institute (NCI). P388 mouse lymphoma was chemically induced in a DBA/2 mouse by painting the skin with methylcholanthrene. The lymphoma cells could be propagated in DBA/2 mice after i.p. injection. For i.p., s.c, i.v. or intracerebral (i.c.) inoculation of P388 cells, the median days of survival and the tumor doubling times were 10.3, 13.0, 8.0, and 8.0 days and 0.44, 0.52, 0.68, and 0.63 days respectively (Teicher 2011). This model was used for large-scale drug screening projects. P388 cells could also be propagated in either B6D2F1 or CD2F1 mice (Newman et al. 2000). B6D2F1 was the offspring between C57BL female and DBA/2 male. CD2F1

was the offspring of BALB/c female and DBA/2 male (Law et al. 1949).

5.1.5 CML model *in vivo*

CML was a myeloproliferative disorder caused by a reciprocal translocation between chromosomes 9 and 22, also known as the Philadelphia (Ph⁺) chromosome, leading to the formation of BCR-ABL fusion protein. The development of CML could be divided into the following phases, chronic phase (CP), accelerated phase (AP) and blast phase (BC). Although treatment of CML patients with imatinib had a very high response rate of over 95%, a significant proportion of patients developed primary resistance to such therapy (Druker et al. 2006). The primary resistance resulted from resistant clonal selection by protective microenvironment, increased efflux of drug, or changes in the BCR-ABL signaling mechanisms that rendered TKI ineffective (Gorre et al. 2002, Shah et al. 2002, La Rosee and Deininger 2010).

Animal model of CML can be established by transplantation of bone marrow cells that were transduced with a retrovirus encoding BCR-ABL (Voncken et al. 1992, Castellanos et al. 1997). In addition, xenograft of human BCR-ABL⁺ K562 cells may also be used. K562 cells were injected into immunocompromised animals after sublethal irradiation to remove endogenous bone marrow cells (Lozzio et al. 1976, Sirard et al. 1996). This model was used to mimic the blast phase of CML, whose symptom was similar as AML.

SCID and NOD/SCID mice provided a more preferential condition for leukemia cells than nude mice (Dazzi et al. 1998, Wang et al. 1998, Shultz et al. 2007). Because they had mutation at Prkdc gene therefore they were more immunocompromised than nude mice.

5.1.6 Application of P-gp modulator in leukemia treatment

Phase III clinical trials of P-gp modulators (quinine, cyclosporin-A (CsA), PSC833

and zosuquidar) for AML (**Table 5. 1**) were conducted previously. Quinine and CsA but not PSC833 and zosuquidar yielded beneficial effects to P-gp positive AML patients (Solary et al. 1996, Wattel et al. 1999, List et al. 2001, Liu Yin et al. 2001). Although PSC833 and zosuquidar were more potent, specific P-gp modulators than the first-generation modulators. The failure of the clinical trials resulted from (1) the dosage of chemotherapy was reduced to compromise the toxicity, (2) other non-P-gp mechanism of drug resistance overwhelmed the benefit of P-gp modulator (3) insufficient exposure of P-gp modulators to resistant cells due to non-ideal pharmacokinetics (Solary et al. 1996, Wattel et al. 1999, Sonneveld and List 2001, Baer et al. 2002, Greenberg et al. 2004).

In the previous chapter, the four derivatives, 23, 51, FX3 and WBC5, demonstrated potent P-gp modulation function in different cell models including leukemia cell lines and yielded pharmacologically active serum concentrations for 18 hours. Combination treatment of FX3 and PTX had no significant drug-drug interaction *in vivo*. In this Chapter, the efficacy experiment of reversing MDR by FX3 would be carried out in three different resistant tumor models *in vivo* including xenografted solid tumor of LCC6MDR in nude mice, ascite tumor of P388ADR in BDF1 mice and disseminated leukemia of K562/P-gp in NOD-SCID mice.

Table 5. 1 Phase III trials investigating P-gp modulator in AML

| Study group | Modulator (dose) | Diagnosis | No. of patients | Chemotherapy | Outcome; P < .05 | Reference |
|-------------------|----------------------|----------------------------------|-----------------|---------------|---|---------------------------|
| GOELAMS-MAQ2 | Quinine (30 mg/kg/d) | AL | 315 | ID Ara-C+ M | Lower resistance; increased neutropenic deaths | (Solary et al. 1996) |
| GFM and GOELAMS | Quinine (30 mg/kg/d) | RAEB+t, MDS-AML | 131 | ID Ara-C+ M | Increased CR and OS in P-gp ⁺ patients | (Wattel et al. 1999) |
| MRC | CsA (2.5-5 mg/kg) | AML (RoR) | 235 | Ara-C+ DE | Negative | (Liu Yin et al. 2001) |
| SWOG 9126 | CsA (16 mg/kg/d) | RAEB-t, AML (RoR, 2nd AML) | 231 | HiD Ara-C + D | Lower resistance; increased RFS and OS | (List et al. 2001) |
| ECOG 2995 | PSC833 (10 mg/kg/d) | AML (RoR) | 127 | MEC | No increase in CR | (Greenberg et al. 2004) |
| CALGB 9720 | PSC833(10 mg/kg/d) | AML, Age>60 years | 120 | D-E-Ara-C | Premature closure (toxicity) | (Baer et al. 2002) |
| HOVON, MRC (C302) | PSC833(10 mg/kg/d) | AML, Age>60 years | 428 | D+ Ara-C | Negative (RFS) | (Sonneveld and List 2001) |
| Novartis C301 | PSC833 | AML (RoR) | 256 | MEC | Negative (CR) | (Sonneveld and List 2001) |
| ECOG 3999 | zosuquitar (550mg/d) | advanced MDS or AML, age>60 year | 449 | D+ Ara-C | Negative (CR) | (Cripe et al. 2010) |

CsA, cyclosporin-A; AL, acute leukemia; RAEB+/-t, refractory anemia with excess blasts in/no transformation; RoR, relapsed or refractory; ID, intermediate-dose; Ara-C, cytarabine; HiD, high-dose; M, mitoxantrone; E, etoposide; D, daunorubicin and IDA, idarubicin. RFS, relapse-free survival; OS, overall survival and CR, complete remission rate.

5.2 Results

5.2.1 *In vivo* toxicity studies in BALB/c mice

Toxicity study of 51, FX3 and WBC5 was performed in BALB/c mice. FX3 (30 or 60 mg/kg, i.p.), WBC5 (30 or 60 mg/kg, i.p.) or 51 (30 mg/kg, i.p.) with or without PTX (12 mg/kg, i.v.) were administered to BALB/c mice for 12 times. Potential toxicity symptoms were monitored including the loss of bodyweight by 15% for 3 consecutive days, loss of appetite, slowness in activity and treatment-related mortality. The above parameters were monitored during the treatment period (day 0 to day 22), plus 7 more days post treatment (**Figure 5. 1**).

It was found that repeated administration of FX3 (30 mg/kg) or WBC5 (30 mg/kg) alone did not induce any mortality or toxicity symptoms. Repeated co-administration of PTX with FX3 (either 30 or 60 mg/kg), WBC5 (60 mg/kg) or 51 (30 mg/kg) induced slight bodyweight loss but the drop was not more than 15% for more than 3 consecutive days and no other toxicity symptoms was observed. Bodyweight regained after the treatment was completed. The results suggested that co-administration of PTX with FX3, WBC5 or 51 was well tolerated to BALB/c mice. These derivatives would be administered at the dosage of 30 or 60 mg/kg in the subsequent efficacy study.

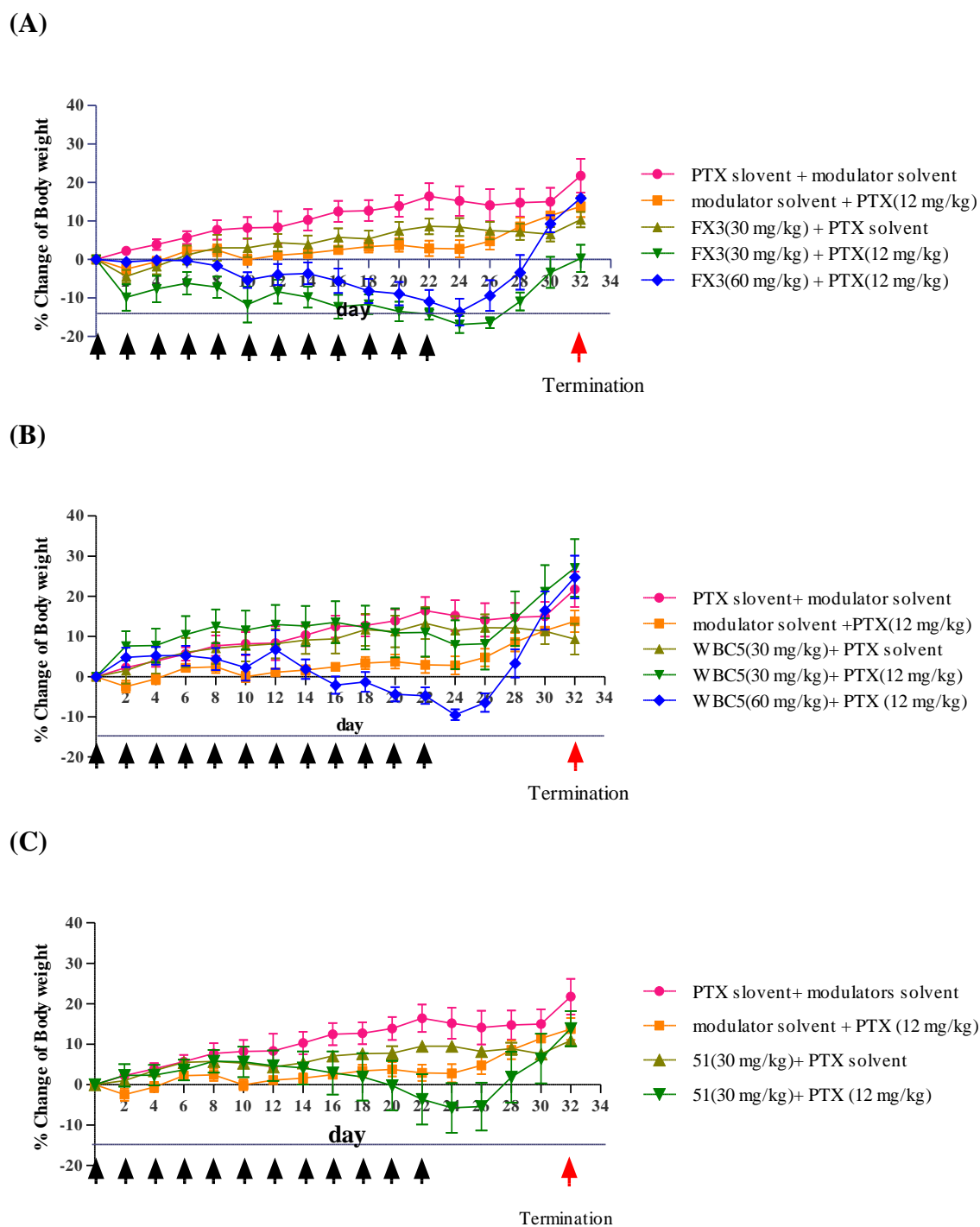


Figure 5. 1 Toxicity assessment of galloylated derivatives with or without PTX

Changes in bodyweight of BALB/c mice in different groups of FX3 (A), WBC5 (B) and 51 (C) were measured every two days (n=5). All derivatives and PTX were prepared in the same solvent as solvent control. The loss of bodyweight and appetite or treatment-related mortality were monitored and recorded as toxicity. Arrowheads indicated the day of administration. Animal were sacrificed on day 32.

5.2.2 *In vivo* efficacy studies of reversing PTX resistance of LCC6MDR xenograft in BALB/c nude mice using derivatives and EGCG.

To determine the efficacy of the derivatives and EGCG in reversing P-gp-mediated PTX resistance in LCC6MDR xenograft model, LCC6MDR solid tumor model was established as described in Methodology. Mice with LCC6MDR tumor were treated with (1) solvent control (10% NMP, 10% Cremophor EL and 80% PBS, i.p. and 5% Ethanol, 5% Cremophor EL, 90% PBS, i.v.), (2) PTX (12 mg/kg, i.v.), (3-6) combination treatment of the derivative (23, 51, FX3 or WBC5) (30 mg/kg, i.p.) with PTX (12 mg/kg, i.v.) or (7) combination treatment of EGCG (30 mg/kg, i.p.) with PTX (12 mg/kg, i.v.). Treatment was given every 2 days for 12 times (**Figure 5. 2. A**). There was no significant difference in tumor growth between the co-treatment groups and PTX alone groups. Among the five combination treatment groups (23, 51, FX3, WBC5, EGCG + PTX), co-treatment of EGCG and PTX displayed the least tumor inhibitory effect whereas co-treatment of FX3 and PTX displayed the best tumor inhibitory effect, but the difference was statistically insignificant (**Figure 5. 2. A**). To optimize the MDR modulating activity by FX3, the administration strategy would be improved in the next round efficacy experiment.

5.2.3 *In vivo* efficacy studies of reversing PTX resistance of LCC6MDR xenograft using FX3.

To improve the efficacy of FX3 in reversing P-gp-mediated PTX resistance in the LCC6MDR xenograft model, the dosage of FX3 was doubled and the administrations were increased from 12 to 14 times. Mice with LCC6MDR tumor were treated with (1) solvent control, (2) PTX (12 mg/kg, i.v.) or (3-4) FX3 (30 mg/kg, i.p., b.i.q.2.d or 60mg/kg, i.p., q.2.d) with PTX (12 mg/kg, i.v.) (**Figure 5. 2. B**).

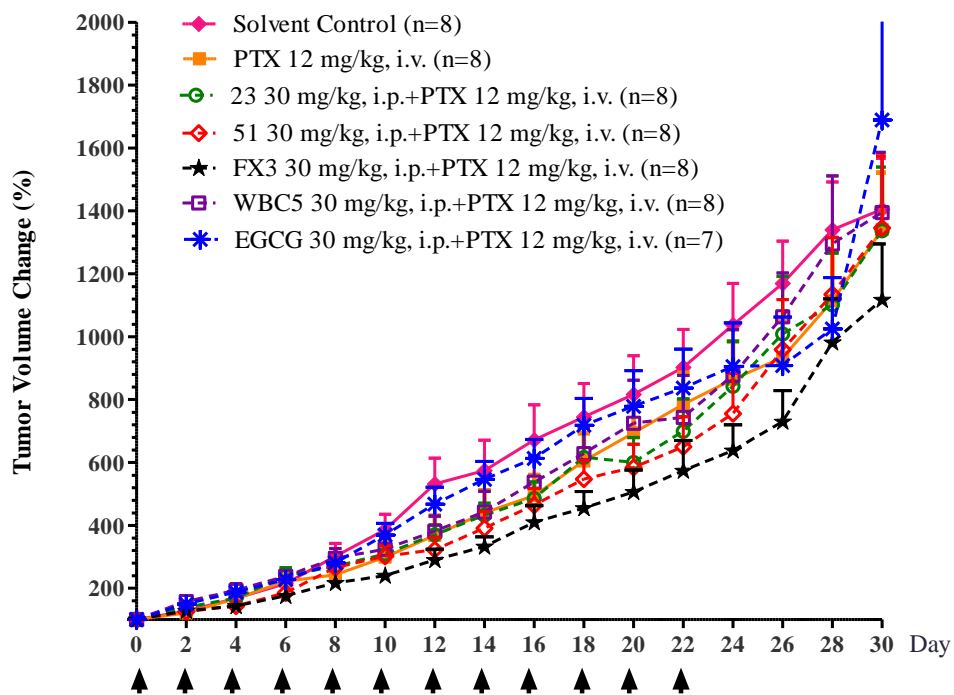
The tumor volume of solvent control group was $823.4 \pm 56.7 \text{ mm}^3$. There was no

significant difference compared with the PTX group ($756.2 \pm 87.9 \text{ mm}^3$) with a *p*-value of 0.25. The results suggested that the LCC6MDR tumor model was PTX resistant and PTX treatment alone could not inhibit tumor growth. Co-treatment of PTX with FX3 (30 mg/kg b.i.q.2.d or 60 mg/kg q.2.d) resulted in a mean tumor volume of 483.2 ± 38.2 and $548.8 \pm 45.0 \text{ mm}^3$ on day 30, respectively. The tumor volume of cotreatment was 27.4- 36.1 % smaller than that of PTX alone group ($756.2 \pm 87.9 \text{ mm}^3$) (*p* = 0.001) (**Figure 5. 2. B**). The tumor weight of co-treatment groups of PTX with FX3 30 mg/kg (b.i.q.2.d) and FX3 60 mg/kg (q.2.d) was 0.33 ± 0.02 and 0.37 ± 0.02 g respectively at the end of experiment which was significantly lighter than PTX alone (0.50 ± 0.03 g) (*p* = 0.0024). Tumor doubling time of co-treatment group of PTX with FX3 30 mg/kg (b.i.q.2.d) was 14.96 days, which was longer than PTX alone group (10.34 days) (*p* < 0.01) (**Figure 5. 2. C**). This suggested that FX3 could sensitize the resistant LCC6MDR cells and inhibit tumor growth with PTX treatment.

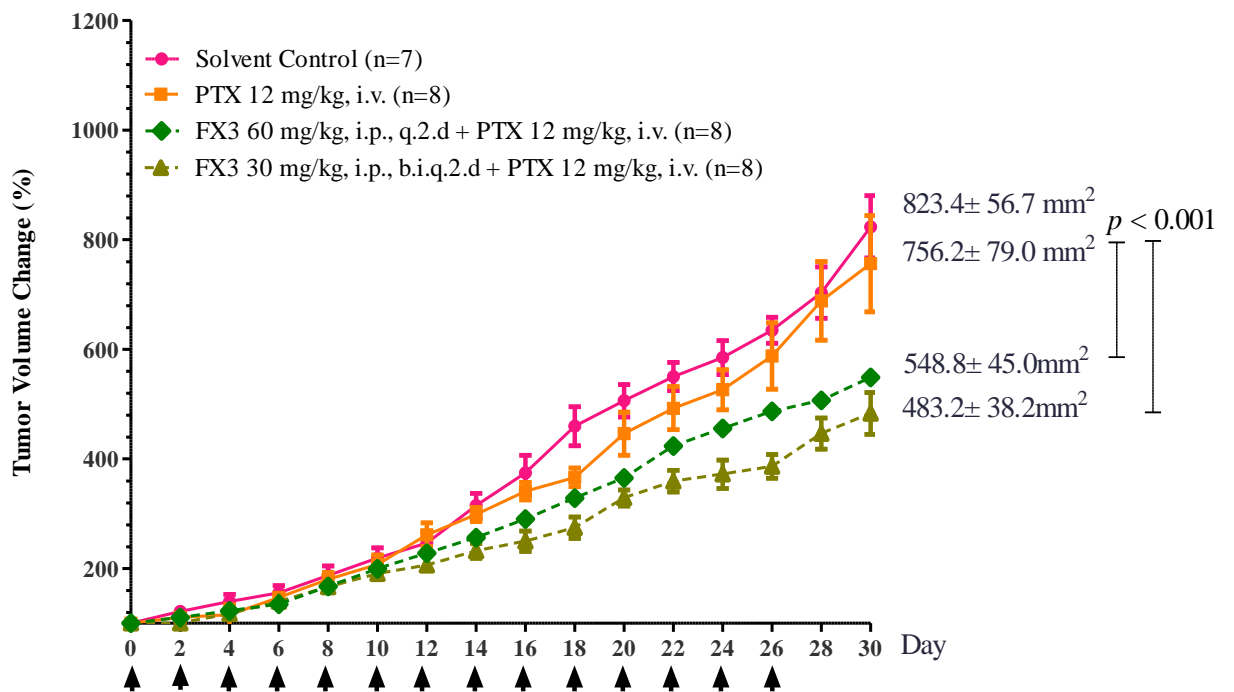
Combination treatment of FX3 30 mg/kg (b.i.q.2.d) or 60 mg/kg q.2.d with PTX for 14 times was safe to use. There was no animal death in any treatment groups. Combination treatments resulted in bodyweight loss but was no more than 15%. In addition, the bodyweight regained 4 days after the end of administration (**Figure 5. 2. D**).

In general, FX3 (30 mg/kg, b.i.q.2.d) administrated twice a day performed better than the single administration with double dosage of FX3 (60 mg/kg q.2.d) in inhibiting tumor growth with a lower bodyweight loss.




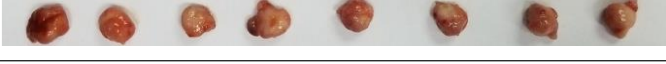
(A)



(B)



(C)

| Exercised LCC6MDR tumor | Treatments | Tumor Volume | Tumor Weight (g) | Doubling Time (day) |
|---|------------------------------|-------------------|------------------|---------------------|
|  | Solvent control | 823.3 ± 56.74 | 0.62 ± 0.06 | 10.34 ± 0.38 |
|  | PTX | 756.2 ± 87.95 | 0.50 ± 0.03 | 11.09 ± 0.60 |
|  | FX3 30mg/kg (b.i.q.2.d)+ PTX | 483.2 ± 38.20 | 0.33 ± 0.02 | 14.96 ± 1.16 |
|  | FX3 60mg/kg (q.2.d)+ PTX | 548.4 ± 45.00 | 0.37 ± 0.02 | 12.41 ± 0.82 |

(D)

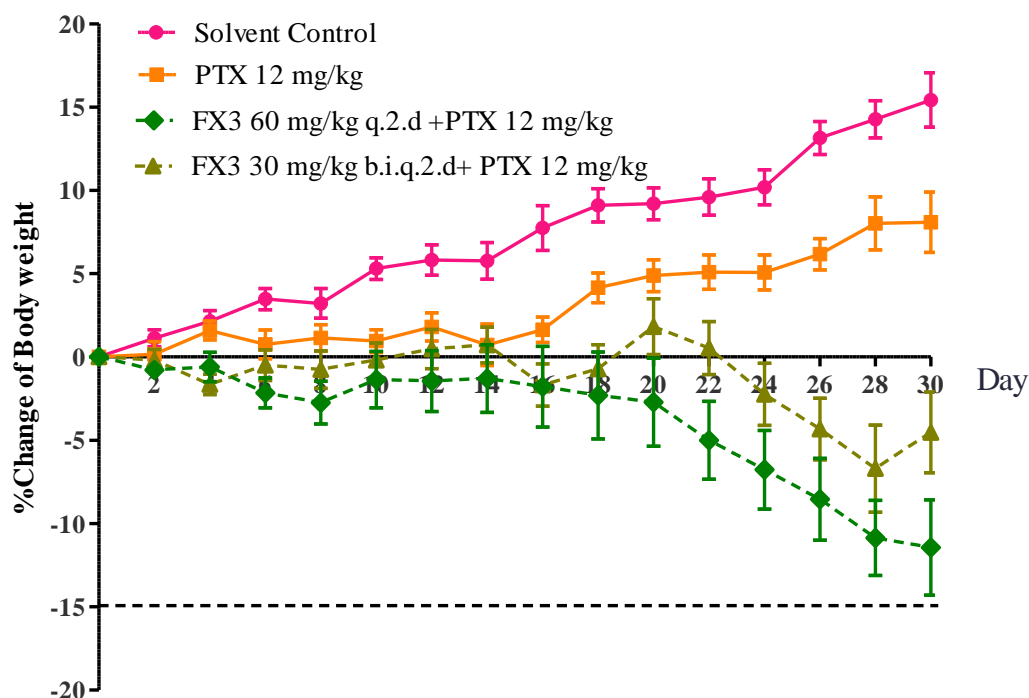


Figure 5. 2 *In vivo* efficacy of derivatives on modulating P-gp mediated PTX resistance on LCC6MDR

BALB/c nude mice were subcutaneously inoculated with LCC6MDR tumor slices. Tumor volume was measured by calipers every two days. (A) The inoculated mice were given seven different administration strategies. (B) The inoculated mice were treated with four different strategies. Tumors were removed and weighed on the day the mice were sacrificed. (C) Tumor volume, tumor weight and doubling time were shown as mean \pm sem. (D) Changes in bodyweight during the treatment period were monitored. The statistical significance of tumor volume was calculated by two-way ANOVA, and the statistical significance of tumor weight and doubling time was analyzed by unpaired two-tailed t-test using Prism 5.0. *, $p < 0.05$; **, $p < 0.01$.

5.2.4 FX3 accumulation in LCC6MDR tumor

To determine whether FX3 could penetrate in tumor, the intra-tumor level of the FX3 was measured. It was found that FX3 can reach tumor and it decreased in a time-dependent manner (**Figure 5. 3**). Tumor level of FX3 can be maintained above its *in vitro* EC₅₀ (93.8 nM) level by more than 9 hours, suggesting that FX3 had a good penetrating ability into tumor and can be maintained inside the tumor.

5.2.5 PTX accumulation in LCC6MDR tumor with or without FX3

This section investigated whether PTX could penetrate into tumor and whether FX3 could increase the PTX accumulation in tumor. BALB/c nude mice carrying LCC6MDR xenograft were administered with PTX ± FX3. FX3 was administrated 60 minutes before PTX.

It was found that PTX could be detected in tumor. At 180 minutes post administration of PTX, the PTX level in the combination treatment group (PTX + FX3) was 2736.3 nM, which was 6.3-fold higher than that of the PTX alone group (456.3 nM) (**Figure 5. 3**). FX3 (30 mg/kg, i.p.) could enhance intratumor level of PTX from 60 to 300 minutes post PTX administration. These results suggested that intratumor level of PTX could be increased by co-treatment with FX3.

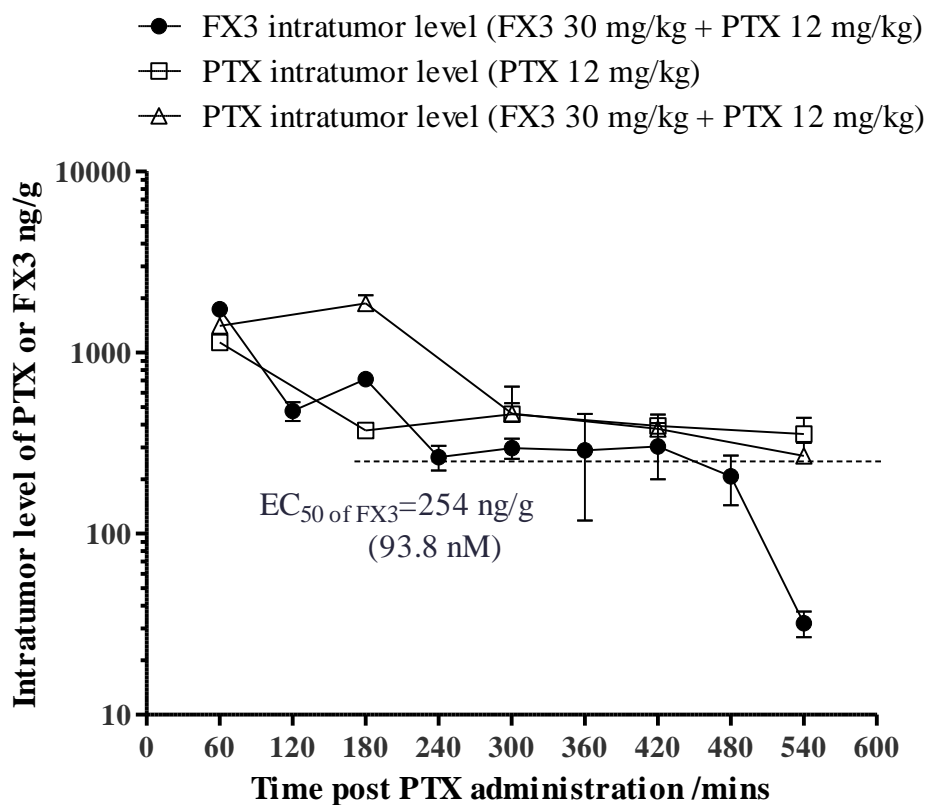


Figure 5. 3 Intra-tumor level of FX3 and PTX in LCC6MDR

BALB/c nude mice bearing LCC6MDR tumor (100-300 mm³) were i.p. administrated with FX3 at 30 mg/kg. After 1 hour, PTX was i.v. injected at 12 mg/kg. The tumors were removed at 60, 180, 300, 420 and 540 minutes post PTX administration. There were 3 mice in each time point. Data were shown in mean ± sem.

5.2.6 *In vivo* efficacy studies using FX3 to reverse DOX resistance in P388ADR xenograft

Another efficacy study was performed to determine whether FX3 could reverse the DOX resistance in P388ADR animal model in B6D2F1 mice. P388ADR cells were injected to mice (i.p.) and ascites were produced. Survival time of the mice was monitored. After inoculation, mice were randomly divided into 4 groups as (1) no treatment, (2) DOX (3 mg/kg, i.p.), (3) FX3 (60 mg/kg, i.p.) with DOX (3 mg/kg, i.p.) or (4) GF120918 (20 mg/kg, i.v.) with DOX (5 mg/kg, i.p.). GF120918 was a well-established dual inhibitor of P-gp and BCRP and was used here as a control.

The mice survival and bodyweight were shown in **Figures 5. 4. A** and **B**. The median survival was summarized in **Table 5. 2**. It was found that the no-treatment group had the shortest median survival of 13.0 days. DOX alone increased the median survival to 16.5 days, representing an increase in lifespan (ILS) percentage of 26.9 % ($p = 0.0028$). Comparing to DOX alone, co-treatment with FX3 could extend the median survival to 21.5 days, representing an ILS of 30.3 % ($p < 0.001$). In contrast, co-treatment with GF120918 did not bring any significant increase in the median survival days (17.0 days), representing an ILS of 3.0 % ($p = 0.26$) (**Table 5. 2**).

During the treatment period, bodyweight of DOX alone group was kept increasing as similar as the no-treatment control. The increase of bodyweight mainly resulted from the ascites production. However, the bodyweight of mice in combination group (FX3+DOX) kept steady during the treatment period. The mice bodyweight in group (GF120918+DOX) dropped significantly (**Figure 5. 4. B**), suggesting potential toxicity of GF120918 in combination with DOX treatment. In short, these results suggested that FX3 was effective and safe in modulating P-gp-mediated DOX resistance to prolong the mice survival in the P388ADR leukemia model.

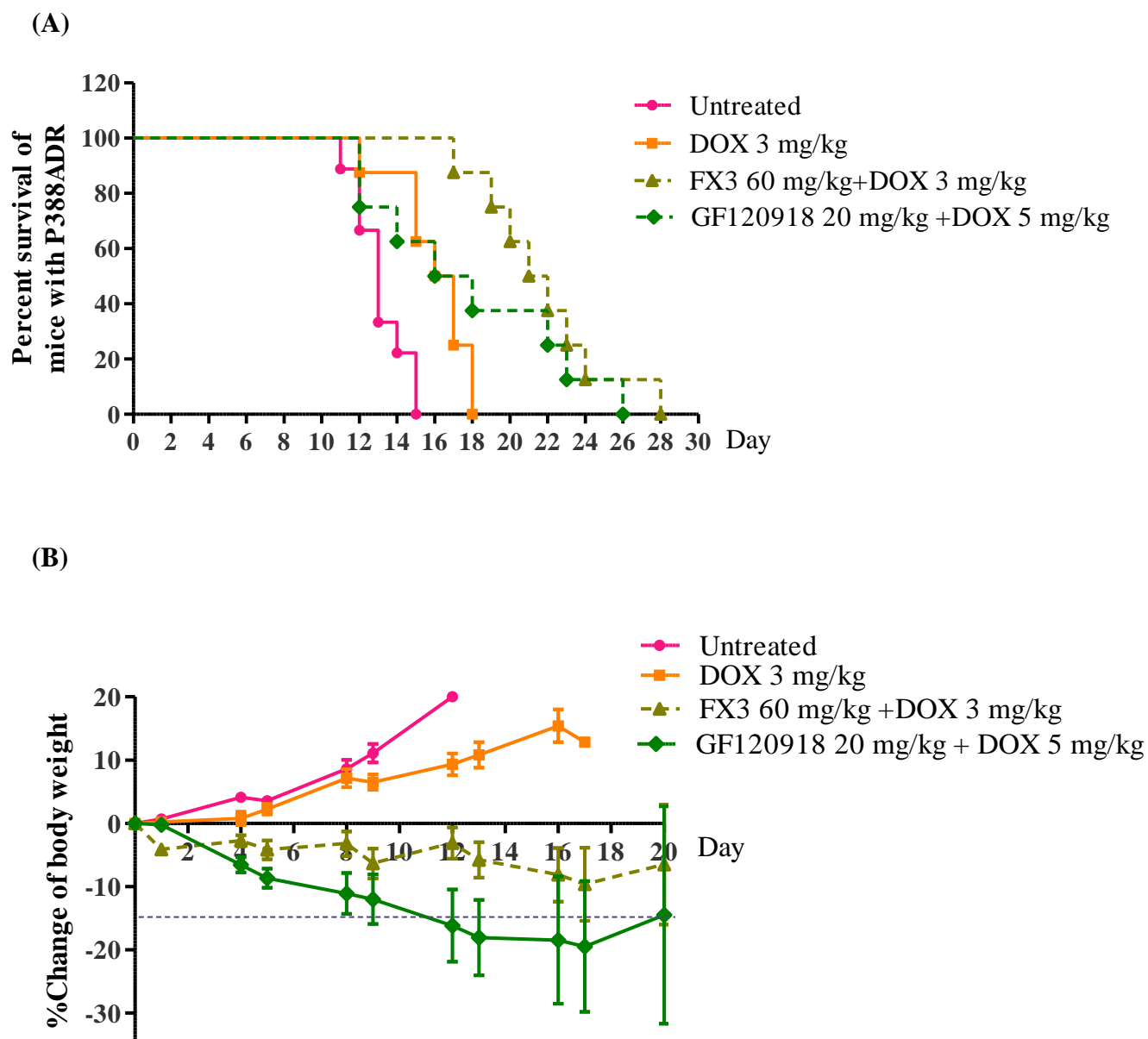


Figure 5. 4 *In vivo* efficacy study of FX3 reversing resistance of DOX in P388ADR

BDF1 mice with i.p.-inoculated P388ADR cells were divided into four treatment groups which are untreated, DOX (3 mg/kg, i.p.), combination of FX3 (60 mg/kg, i.p.) and DOX (3 mg/kg, i.p.) and combination of GF120918 (20 mg/kg, i.v.) and DOX (5 mg/kg, i.p.). The survival (A) and the bodyweight change (B) were monitored. There were 8 mice in each group.

Table 5. 2 Median survival day and ILS% in P388ADR efficacy study *in vivo*.

| Groups | Median day | |
|--------------|------------|----------------------------------|
| Untreated | 13.0 | } ILS% = 26.9; $p= 0.0028$ (**) |
| DOX alone | 16.5 | |
| FX3+DOX | 21.5 | } ILS% = 30.3; $p= 0.0004$ (***) |
| GF120918+DOX | 17.0 | |
| | | } ILS% = 3.0; $p= 0.2669$ (N.S) |

The median survival day was the survival time of 50% of mice in each group. ILS was the percentage of increase of survival time over DOX alone treatment group. The significance was calculated by Log-rank (Mantel-COX) test in prism 5.0. **, $p < 0.01$; ***, $p < 0.001$.

5.2.7 Establishment of leukemia model (K562/P-gp)

In this section, human K562/P-gp leukemia model was established in immunocompromised NOD/SCID mice. To establish the K562/P-gp *in vivo* model, irradiation was needed to abolish the endogenous population of immune cells in NOD/SCID mice. First, the irradiation dosage was optimized (**Figure 5. 5. A**). NOD/SCID mice were irradiated with either 2.5 or 1.5Gy. The NOD/SCID mice died on day 14 post irradiation at 2.5Gy. No animal death was observed for the group irradiated with 1.5Gy after 80 days post irradiation. Changes in the bodyweight of the mice were also monitored (**Figure 5. 5. B**). Although there was no death induced by 1.5Gy irradiation, there were severe bodyweight loss of about -20% on 20 days post irradiation (**Figure 5. 5. B**). A lower dosage of irradiation with less than 1.5Gy should be optimized.

In the next trial, lower irradiation dosages of 1.2 or 0.8 Gy were used with the inoculation of 1×10^7 K562/P-gp cells. The bodyweight and survival time were monitored and shown in **Figures 5. 5. C and D**. The median survival day was 37 and 34.5 for the group irradiated with 1.2 and 0.8 Gy respectively. Bodyweight reduction was no more than 10% during the 20-day monitoring period after irradiation. The irradiation dosage of 1.2 Gy was therefore used in the subsequent studies.

The symptoms of mice after inoculation were monitored and shown in **Figure 5. 5. E**.

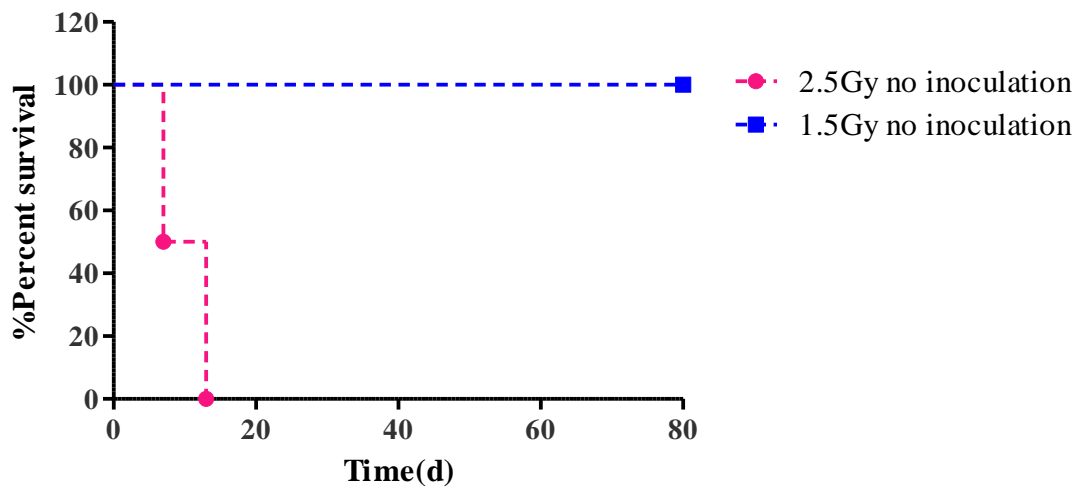
There was severe bodyweight loss after about 30 days post inoculation also including the symptoms of paralysis, slow movement, blindness and swelling of the forehead. Some mice died with heavy burden of tumor. Tumors were found in the brain, peritoneum around kidney and at the back of the neck. Ascites was also found in some mice (**Figure 5. 5. E**).

To confirm that the symptoms were indeed caused by the inoculation of K562/P-g-cells, the tumor, ascites and the fluid from the brain were collected and cultured *in vitro*. These samples were confirmed with P-gp expressing by flow cytometry (**Figure 5. 5 F and G**).

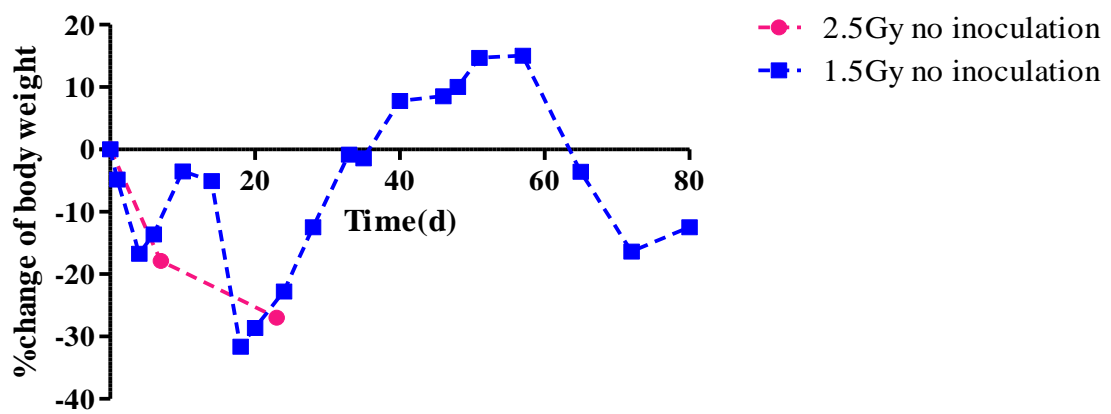
5.2.8 *In vivo* efficacy studies of reversing DOX resistance on K562/P-gp in NOD/SCID mice with or without FX3

To determine the efficacy of FX3 in reversing MDR of K562/P-gp *in vivo*, survival time of NOD/SCID with K562/P-gp was monitored. After inoculation, mice were randomly divided into 3 groups. They were treated with either (1) solvent control (10% NMP, 10% Cremophor EL and 80% saline), (2) DOX (0.9 mg/kg, i.v.) or (3) FX3 (30 mg/kg, i.p.) with DOX (0.9 mg/kg, i.v.). The median survival of the co-treatment group (37.0 days) was longer than the solvent control (29.0 days) and DOX alone (32.0 days) groups (**Figure 5. 6**) (**Table 5. 3**). There were no significant differences between the survival time of the solvent control and DOX alone group ($p = 0.8582$). It indicated that K562/P-gp was DOX resistant and DOX-alone treatment cannot prolong the survival time. Combination treatment significantly prolonged the survival time, comparing to the DOX-alone treatment ($p = 0.0052$). These results suggested that FX3 could sensitize the K562/P-gp cells to DOX and prolong the mice survival *in vivo*.

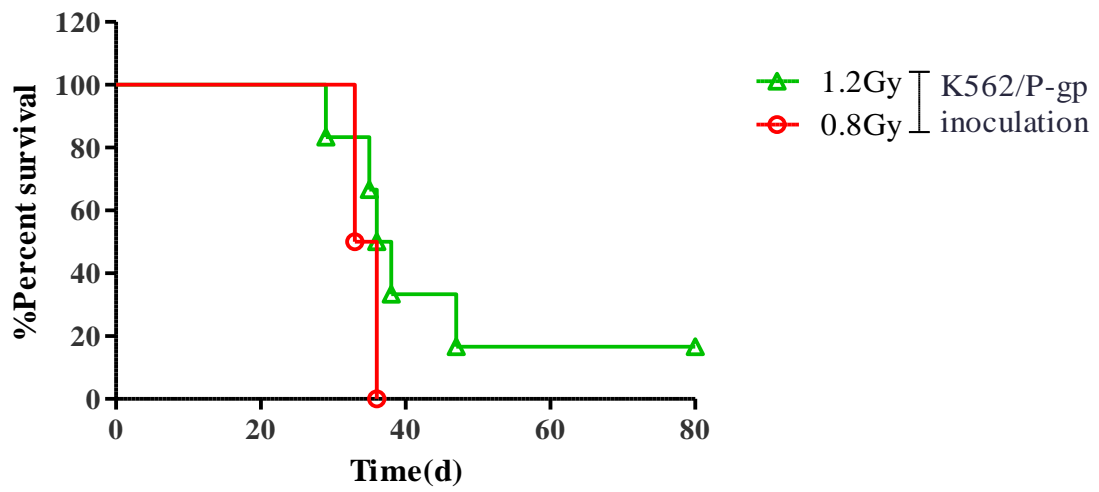
(A)



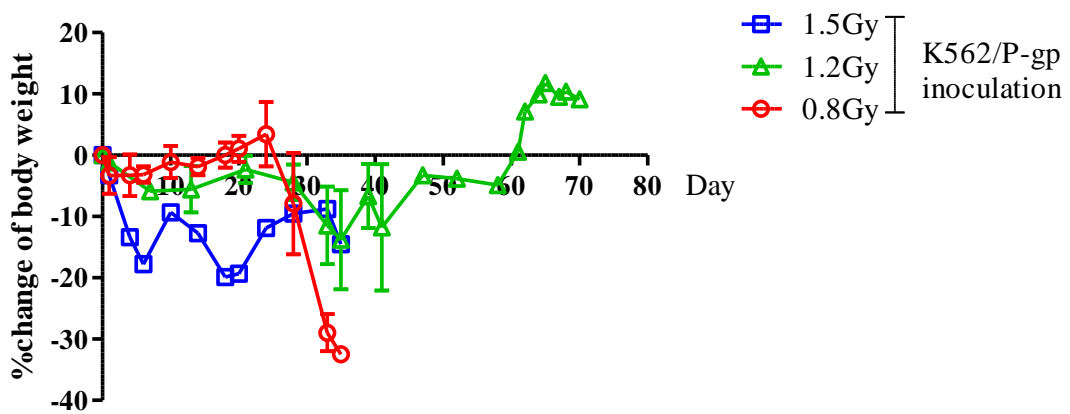
(B)



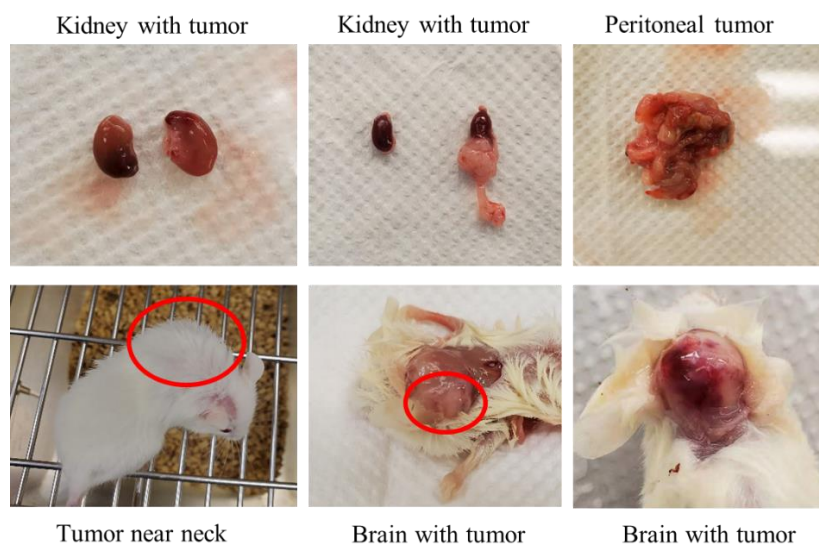
(c)



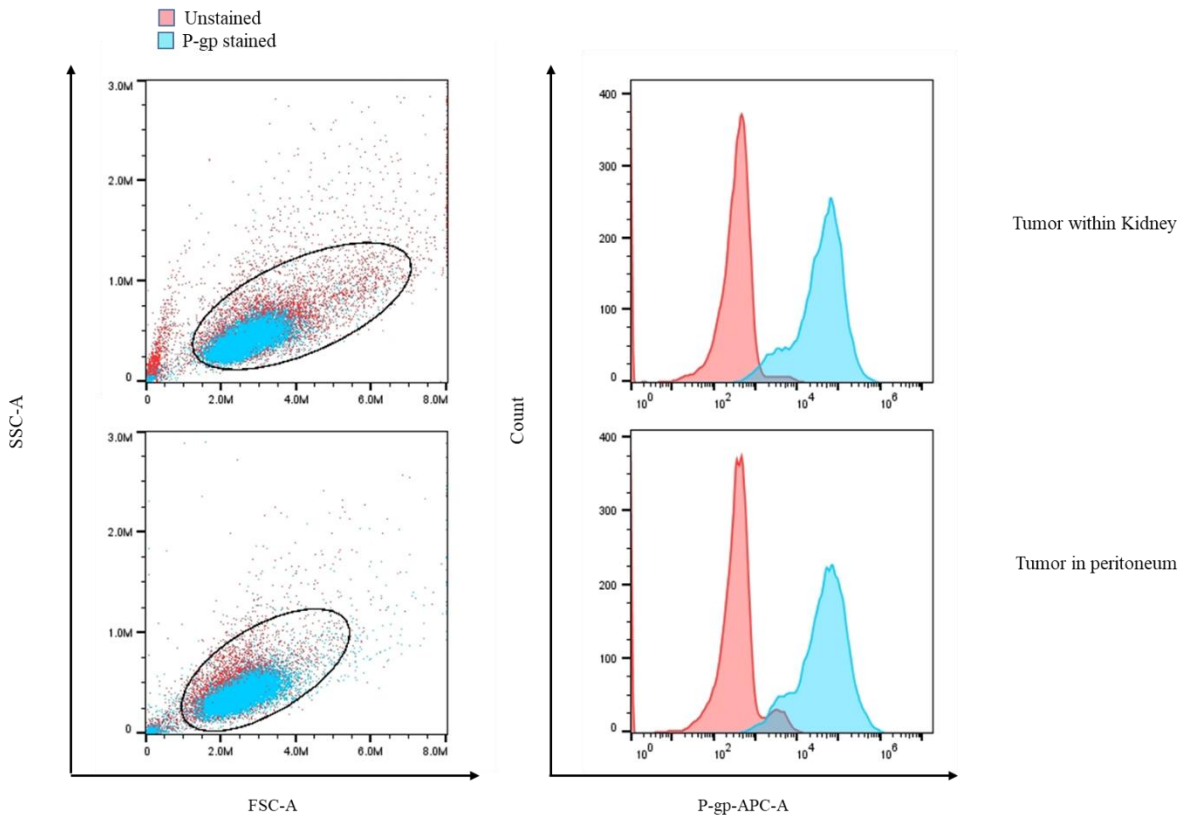
(D)



(E)



(F)



(G)

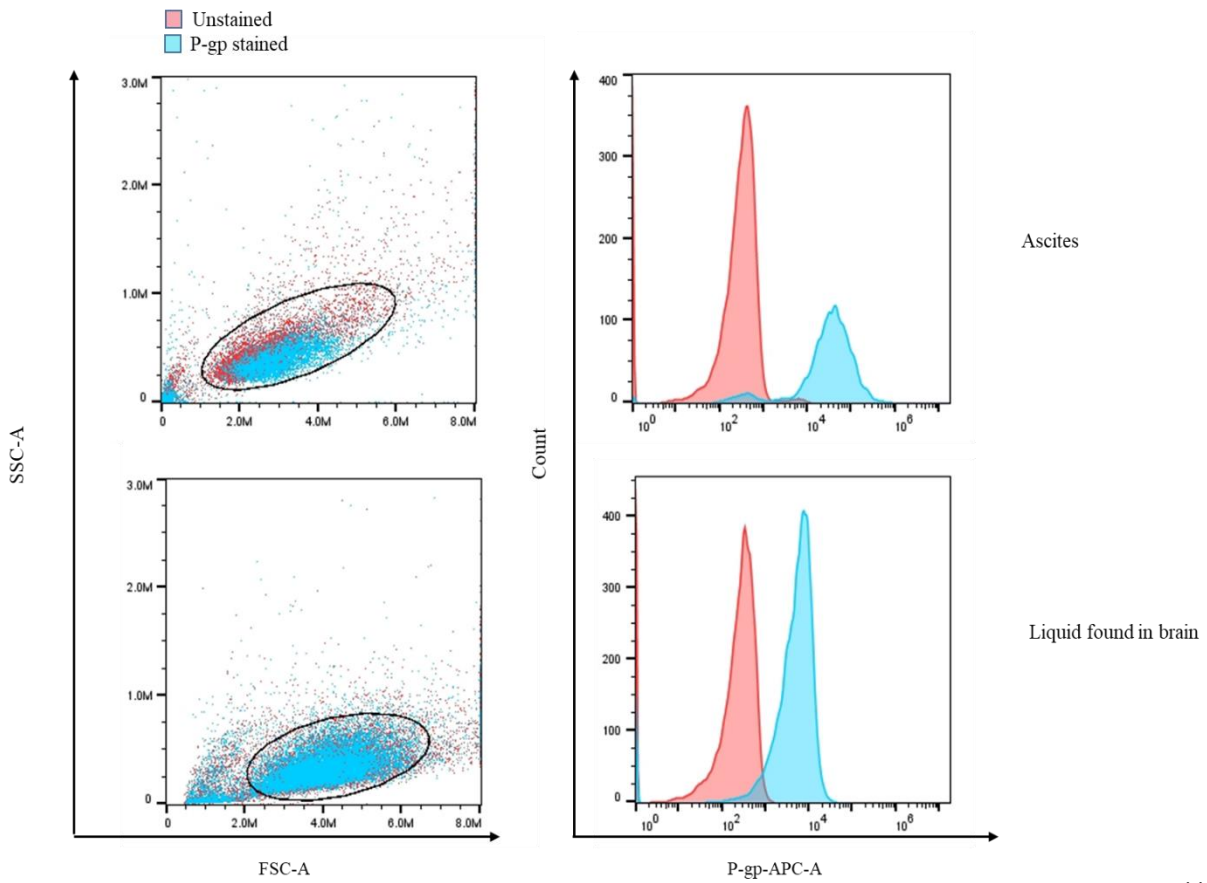


Figure 5. 5 Establishment of K562/P-gp model *in vivo*

NOD/SCID mice were irradiated at 2.5, 1.5, 1.2 or 0.8 Gy with or without 1×10^7 K562/P-gp cells inoculation. The survival (A) and bodyweight (B) of mice without inoculation and the survival (C) and bodyweight (D) of mice with inoculation were monitored. Tumor within the kidney, in peritoneum, on back neck and in brain were found in mice with K562/P-gp cells inoculation (E). Ascites, liquid found in brain (F), tumor within kidney and tumor in peritoneum (G) were collected from mice with inoculation. After isolation, cells were stained with or without antibody of P-gp and checked by flow-cytometry.

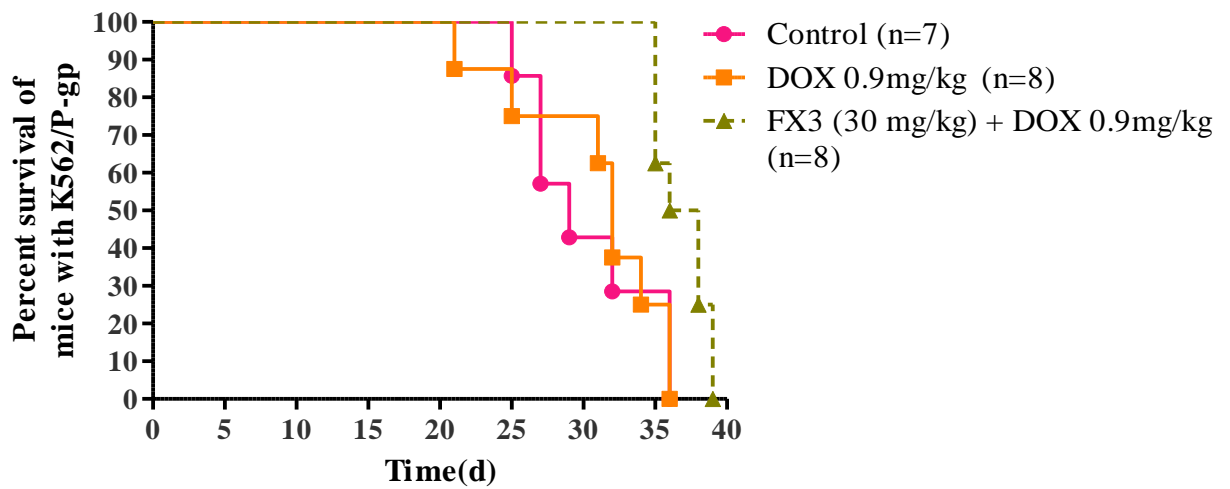


Figure 5. 6 *In vivo* efficacy study of FX3 reversing resistance of DOX on K562/P-gp

NOD/SCID mice with i.v.-inoculated K562/P-gp cells were divided into three groups which were control, DOX (0.9 mg/kg, i.v.) in combination with FX3 (30 mg/kg, i.p.) and DOX (0.9 mg/kg, i.v.). The mice survival was monitored. There were 7-8 mice in each group.

Table 5. 3 Median survival day and ILS% in K562/P-gp efficacy study *in vivo*

| Groups | Median day | |
|-----------|------------|-----------------------------------|
| Control | 29.0 | } ILS% = 10.3; $p = 0.8582$ (N.S) |
| DOX alone | 32.0 | |
| FX3+DOX | 37.0 | } ILS% = 15.6; $p = 0.0052$ (**) |

The median survival day was the survival time of 50% of the mice in each group. ILS was the percentage of increase of survival time over DOX alone treatment group. **, $p < 0.01$. p value was calculated by Log-rank (Mental-COX) test in prism 5.0.

5.3 Summary

In previous Chapters, the four derivatives (23, 51, FX3 and WBC5) displayed potent activity of reversing MDR *in vitro* and the plasma level of four derivatives could be maintained over EC₅₀ for treatment *in vivo*.

Three animal models of LCC6MDR, P388ADR and K562/P-gp were established to assess the P-gp modulation activity of the four derivatives in reversing MDR. Among the four derivatives, FX3 was the most promising one and it was co-treated with PTX or DOX in the three animal models. Combination treatment could significantly inhibit the tumor growth and prolong the survival time by sensitizing the resistance of solid tumor (LCC6MDR) ($p < 0.001$), peritoneal tumor (P388ADR) ($p < 0.001$) and dissemination leukemia (K562P-gp) ($p = 0.0052$) without toxicity.

5.4 Discussion

To verify whether FX3 can sensitize MDR by increasing the intracellular accumulation of PTX, the FX3 and PTX level in tumor was assessed. FX3 could penetrate into tumor and maintain the intratumor level over EC₅₀ for 480 minutes. The intratumor level of PTX was enhanced by co-treatment with FX3 (**Figure 5. 3**). According to the efficacy result of LCC6MDR xenografted model, the potency of single treatment of FX3 (30 mg/kg, b.i.q.2.d) administrated twice was better than double dosage (60 mg/kg, q.2.d). This could be explained by the fact that the enhancement of PTX accumulation in tumor by FX3 only happened during 60 to 300 minutes post PTX administration (**Figure 5. 3**). Another injection of FX3 could prolong the time of effective level of PTX in tumor and improve the tumor inhibitory efficacy.

In P388ADR animal model, the mice bodyweight in control and DOX alone groups kept increasing because of the increase of ascites in peritoneum. The mice bodyweight with FX3 and DOX combination treatment kept steady indicating the suppression of ascites development. The combination treatment of GF120918 and DOX was given only one administration. The frequency of administration was different from other treatments. Because the severe bodyweight decreased in combination treatment (GF120918+DOX) limited the administration frequency.

Although FX3 displayed significant effect on sensitizing resistance, there were disadvantages of using the P388ADR animal model and administration strategy. P388ADR cells, FX3 and DOX were all injected i.p., which artificially increased the exposure of the DOX and FX3 to the tumor cells and magnified the cytotoxicity of DOX. This could explain that DOX alone treatment could inhibit the growth of resistant cells and prolong the survival of mice.

To resurrect the shortcoming of P388ADR animal model, another animal model of K562/P-gp cells was established. K562/P-gp cells were human CML, however, P388ADR were murine lymphoma cells. Therefore, K562/P-gp leukemia model was more clinical relevance to human. In addition, DOX and K562/P-gp cells were i.v. injected and FX3 was i.p. injected. Tumor cells and compounds were injected separately which avoided the direct interaction between cells and drugs. This mimicked the actual situation in treating leukemia.

Despite the combination treatment displayed some effect on prolonging the survival ($p = 0.0052$), this animal model and the treatment protocol could be further improved. First, irradiation was necessary for the establishment of the dissemination leukemia model. The mice had wide individual differences in the responses to irradiation, including the wide range of the bodyweight change. One possible way to solve this problem was to use NSG mice which can be used to establish the dissemination

leukemia model without irradiation. Second, the bodyweight loss after irradiation limited the dosage and frequency of DOX to be used. In the presence of 1 μ M of FX3, K562/P-gp cells (IC_{50} of DOX = 219.3 nM) were more DOX resistant than P388ADR cells (IC_{50} of DOX = 57.3 nM) *in vitro*. The dosage of DOX used in the K562/P-gp efficacy study was lower than that in P388ADR *in vivo*. The insufficient dosage of DOX might explain why the survival time was not prolonged by as much as expected.

Chapter 6 Conclusions and perspectives

6.1 Conclusions

Chemotherapy was the most common treatment for cancer. The success rate of chemotherapy varied with patients. ABC transporter-induced drug efflux was one of the most common reasons for chemotherapy failure. ABC transporters had broad substrate specificity. DOX, PTX and VCR were common antineoplastics and they were substrates of ABC transporter. P-gp was the first identified ABC transporter. Overexpression of P-gp increased the likelihood of developing chemotherapy failure (Choi and Yu 2014). P-gp modulators may overcome MDR. There were three generations of P-gp modulators, but they were limited by problems of low potency and toxic side effects (Padowski and Pollack 2010). The fourth generation of P-gp modulators was developed from natural compounds such as gallate catechins that displayed P-gp modulation activity (Jodoin et al. 2002, Sugihara et al. 2011). One of the hypotheses of this project was that the chemical modification of galloylated catechins could enhance the P-gp modulation activity of derivatives both *in vitro* and *in vivo*. A library of galloylated catechins derivatives was synthesized previously (Wong et al. 2015, Wong et al. 2021), with four of them, namely 23, 51, FX3 and WBC5 being studied here.

The four derivatives were tested for their activity in reversing the resistance to a broad spectrum of chemotherapy drugs including PTX, DOX and VCR in LCC6MDR, P388ADR and K562/P-gp cell lines. These three cell lines with P-gp overexpressing were resistant cell lines. The IC₅₀ of PTX, DOX and VCR in resistant cell lines could be reduced to a level comparable to that of sensitive cells by using 1 μM of the four derivatives. In contrast, EGCG at 1 μM could not decrease the IC₅₀ of DOX or PTX in

resistant cell lines of LCC6MDR, P388ADR and K562/P-gp. In DOX accumulation assay, the four derivatives could enhance the DOX accumulation in a dose-dependent manner. The four derivatives at 1 μ M could increase the DOX accumulation in resistant cells to that of the sensitive cells, whereas 1 μ M EGCG could not. This indicated that the chemical modification on galloylated catechins successfully enhanced the P-gp modulation activity.

P-gp, BCRP and MRP-1 were well-known ABC transporters that could induce MDR. Many P-gp modulators also inhibited other ABC transporters. For instance, PSC833 and biricodar were not specific to P-gp and can affect MRP-1 as well (Fischer et al. 1998, Rowinsky et al. 1998). However, the inhibition of non-target transporters may lead to great adverse effects of anticancer drugs, including neutropenia and other myelotoxic effects. For example, the ABC transporter, BCRP, was a functional regulator of hematopoietic stem cells (Bunting 2002) and its inhibition may contribute to the side effects. In this study, FX3 displayed the most potent and specific P-gp modulation activity among the four derivatives.

This project also investigated the interaction between the galloylated catechins derivatives and P-gp in terms of their regulation of P-gp expression, P-gp ATPase activity and their efflux in both resistant and sensitive cell lines.

It had been reported that EGCG suppressed the expression of both P-gp at mRNA and protein levels both *in vivo* and *in vitro* (Tang et al. 2017). In this study, protein level was found to be unaffected by any of the four derivatives at 2 μ M, which was higher than its effective dosage. EGCG might bind to the carboxyl-terminal nucleotide binding domain (NBD2) of P-gp (Qian et al. 2005). It was consistent with the inhibition of ATPase activity by EGCG in this study. In addition, FX3 could stimulate ATPase activity, suggesting that it did not bind to NBD which would otherwise inhibit the ATPase activity, which was different from EGCG. In addition, there were no

differences in FX3 accumulation between wild sensitive type and P-gp overexpressing cell lines, suggesting that FX3 was not a P-gp substrate or it cannot be transported. P-gp modulation was significantly improved after chemical modification on galloylated catechins. It was possible that FX3 might bind to TMD without being translocated or to an allosteric site of P-gp, which was different from EGCG.

A study based on rats reported that the bioavailability of EGCG after oral administration was 0.1%. Low bioavailability of EGCG appeared to be linked to its poor membrane permeability and transporter-mediated intestinal efflux (Almatroodi et al. 2020). The solubility of galloylated catechins derivatives decreased after modification. They were dissolved in the formulation (10% NMP, 10% Cremophor EL and 80% PBS) for *in vivo* study. The bioavailability of the four derivatives with i.p. injection ranged from 62.9 to 81.81%. FX3 had the highest bioavailability among the four derivatives with bioavailability of 81.81%. The three derivatives (51, FX3 and WBC5) could maintain a plasma level over EC_{50} over 1080 minutes post administration. The pharmacokinetics study of the four derivatives indicated that the derivatives were stable and potential for application *in vivo*.

The drug-drug interaction between antineoplastic and P-gp modulator could induce systemic toxic side effects, which was a big concern of P-gp modulator development (Padowski and Pollack 2010). In this study, there were no significant differences between AUC_{PTX} and $AUC_{PTX+FX3}$ in plasma. This could be an advantage of FX3.

Three animal models (P388ADR, LCC6MDR and K562/P-gp) were established. P388ADR cells were murine lymphomas with P-gp expressing. BDF1 mice inoculated with P388ADR cells had been used for large-scale drug discovery screening projects. Ascites was observed in the animals due to the amplification of P388ADR cells in peritoneum. The development of ascites could lead to death. The survival time of untreated animals ranged from 10-15 days. Compared with the DOX

alone treatment group, the combination treatment can prolong the median survival time by 30.3 %. This indicated that FX3 could reverse MDR of DOX on P388ADR cells *in vivo*.

LCC6MDR cells were human breast cancer cells overexpressing of P-gp. The tumor growth of LCC6MDR with combination treatment of FX3 and PTX was significantly inhibited when it was compared with that of the PTX alone treatment group. FX3 could be accumulated in the LCC6MDR xenograft for over 10 hours. The intra-tumor level of FX3 could be maintained over its EC₅₀ for 8 hours. In addition, FX3 could enhance the intra-tumor level of PTX from 1 to 5 hours post PTX administration. There was 6.3-fold enhancement of intratumor PTX at 3 hours post PTX administration. The results showed FX3 could reverse PTX resistance in LCC6MDR xenograft study by enhancing PTX intratumor level *in vivo*.

Leukemia model (dissemination type) was also established by i.v. injection of K562/P-gp cells in sublethally-irradiated NOD/SCID mice. Compared with DOX alone group, the combination treatment significantly prolonged the median survival time by 15.6% ($p < 0.01$).

These results suggested that combination treatments of FX3 with different anticancer drugs, including PTX or DOX, could reverse MDR induced by P-gp in ascite tumor, solid tumor and dissemination leukemia models.

It was reported that P-gp expression in acute leukemia cells was correlated with clinical drug resistance. In previous clinical trials, 9 of 17 patients with AML and 4 of 11 patients with ALL had P-gp-positive results at the initial presentation, and most P-gp positive patients did not respond to chemotherapy (Kuwazuru et al. 1990). Some phase III clinical trials of P-gp modulators in AML failed because of the toxicity and adverse side effect found in the combination treatment of modulator and antineoplastic (**Table 5. 1**). FX3 showed high bioavailability, stability in plasma and

no significant drug-drug interaction, making it a promising P-gp modulator for further clinical development.

6.2 Perspectives and further study

In the present study, 23, 51, FX3 and WBC5 were derived from EGCG and other galloylated catechins. The phenolic hydroxyl groups on benzene rings were all methylated. Although the P-gp modulation activity was significantly improved, the antioxidative activity of EGCG were decreased. Because the phenolic hydroxyl groups played main functions of antioxidation. It proposed that the functions of EGCG including preventing cancer, cardiovascular and neurodegenerative might be decreased.

The derivatives could reverse MDR in leukemia model. The K562/P-gp dissemination leukemia model was established in NOD/SCID mice here. It was hypothesized that FX3, with good plasma stability, might be a good candidate to reverse MDR in K562/P-gp cells in peripheral blood. However, K562/P-gp cells could not be found in peripheral blood and therefore the high plasma stability of FX3 would not be beneficial as expected. Tumors could be found in spine, brain and peritoneum but not in peripheral blood and bone marrow. It indicated that inoculation of K562/P-gp cells by i.v. did not induce the hematopoietic dysfunction but only induced the cancerous cell metastasis to organs. There were two possible reasons. One possible explanation was that the cells were transfected with P-gp and they might be different from K562 cells used by others (Zheng et al. 2017) and these transfected cells did not prefer grow in peripheral blood. Another reason was that the irradiator was from an X-ray resource. Gamma-ray irradiator was commonly used by others and the sublethal dosage of 2 to 3Gy was used instead (Zhang et al. 2012).

This project mainly focused on demonstrating the efficacy of galloylated catechins derivatives *in vitro* and *in vivo* in reversing P-gp induced MDR. The study could be further improved in the following three directions.

First, the binding pocket of the four derivatives on P-gp and mechanism of P-gp modulation could be further studied. According to those results, the P-gp modulation activity of the compounds could be further improved. In addition, FX3 could stimulate ATPase activity and it cannot be transported by P-gp. This raised an interesting question whether FX3 competitively modulated P-gp by binding at TMD or no-competitively modulated P-gp by binding at the allosteric site between NBD and TMD. Second, the derivatives could be further modified to improve their P-gp modulation activity. Third, FX3 and WBC5 were isomers. Their potency was similar *in vitro*, but different *in vivo*. FX3 showed a higher potency in reversing MDR on LCC6MDR xenografted model than WBC5. It would be interesting to find the reason why these two isomers behaved differently. However, the efficacy of WBC5 needed to be confirmed by the *in vivo* efficacy study with the optimization of administration first.

References

Ai, Z., S. Liu, F. Qu, H. Zhang, Y. Chen and D. Ni (2019). "Effect of Stereochemical Configuration on the Transport and Metabolism of Catechins from Green Tea across Caco-2 Monolayers." Molecules **24**(6).

Akashi, M., A. Tanaka and H. Takikawa (2006). "Effect of cyclosporin A on the biliary excretion of cholephilic compounds in rats." Hepatol Res **34**(3): 193-198.

Almatroodi, S. A., A. Almatroudi, A. A. Khan, F. A. Alhumaydhi, M. A. Alsahli and A. H. Rahmani (2020). "Potential Therapeutic Targets of Epigallocatechin Gallate (EGCG), the Most Abundant Catechin in Green Tea, and Its Role in the Therapy of Various Types of Cancer." Molecules **25**(14).

Ambudkar, S. V., C. Kimchi-Sarfaty, Z. E. Sauna and M. M. Gottesman (2003). "P-glycoprotein: from genomics to mechanism." Oncogene **22**(47): 7468-7485.

Baer, M. R., S. L. George, R. K. Dodge, K. L. O'Loughlin, H. Minderman, M. A. Caligiuri, J. Anastasi, B. L. Powell, J. E. Kolitz, C. A. Schiffer, C. D. Bloomfield and R. A. Larson (2002). "Phase 3 study of the multidrug resistance modulator PSC-833 in previously untreated patients 60 years of age and older with acute myeloid leukemia: Cancer and Leukemia Group B Study 9720." Blood **100**(4): 1224-1232.

Bin, J. W., I. L. Wong, X. Hu, Z. X. Yu, L. F. Xing, T. Jiang, L. M. Chow and W. S. Biao (2013). "Structure-activity relationship study of permethyl ningalin B analogues as P-glycoprotein chemosensitizers." J Med Chem **56**(22): 9057-9070.

Borst, P., R. Evers, M. Kool and J. Wijnholds (2000). "A family of drug transporters: the multidrug resistance-associated proteins." J Natl Cancer Inst **92**(16): 1295-1302.

Brangi, M., T. Litman, M. Ciotti, K. Nishiyama, G. Kohlhagen, C. Takimoto, R. Robey, Y. Pommier, T. Fojo and S. E. Bates (1999). "Camptothecin resistance: role of the ATP-binding cassette (ABC), mitoxantrone-resistance half-transporter (MXR), and potential for glucuronidation in MXR-expressing cells." Cancer Res **59**(23): 5938-5946.

Brinkley, B. R., P. T. Beall, L. J. Wible, M. L. Mace, D. S. Turner and R. M. Cailleau

(1980). "Variations in cell form and cytoskeleton in human breast carcinoma cells in vitro." Cancer Res **40**(9): 3118-3129.

Brooks, T. A., H. Minderman, K. L. O'Loughlin, P. Pera, I. Ojima, M. R. Baer and R. J. Bernacki (2003). "Taxane-based reversal agents modulate drug resistance mediated by P-glycoprotein, multidrug resistance protein, and breast cancer resistance protein." Mol Cancer Ther **2**(11): 1195-1205.

Bunting, K. D. (2002). "ABC transporters as phenotypic markers and functional regulators of stem cells." Stem Cells **20**(1): 11-20.

Cabrera, C., R. Artacho and R. Gimenez (2006). "Beneficial effects of green tea--a review." J Am Coll Nutr **25**(2): 79-99.

Castellanos, A., B. Pintado, E. Weruaga, R. Arevalo, A. Lopez, A. Orfao and I. Sanchez-Garcia (1997). "A BCR-ABL(p190) fusion gene made by homologous recombination causes B-cell acute lymphoblastic leukemias in chimeric mice with independence of the endogenous bcr product." Blood **90**(6): 2168-2174.

Chen, C. J., J. E. Chin, K. Ueda, D. P. Clark, I. Pastan, M. M. Gottesman and I. B. Roninson (1986). "Internal duplication and homology with bacterial transport proteins in the *mdr1* (P-glycoprotein) gene from multidrug-resistant human cells." Cell **47**(3): 381-389.

Chen, D., V. Milacic, M. S. Chen, S. B. Wan, W. H. Lam, C. Huo, K. R. Landis-Piwowar, Q. C. Cui, A. Wali, T. H. Chan and Q. P. Dou (2008). "Tea polyphenols, their biological effects and potential molecular targets." Histol Histopathol **23**(4): 487-496.

Chen, H., C. N. Landen, Y. Li, R. D. Alvarez and T. O. Tollefsbol (2013). "Epigallocatechin gallate and sulforaphane combination treatment induce apoptosis in paclitaxel-resistant ovarian cancer cells through hTERT and Bcl-2 down-regulation." Exp Cell Res **319**(5): 697-706.

Chen, S. H., C. C. Kuo, C. F. Li, C. H. Cheung, T. C. Tsou, H. C. Chiang, Y. N. Yang, S. L. Chang, L. C. Lin, H. Y. Pan, K. Y. Chang and J. Y. Chang (2015). "O(6) -methylguanine DNA methyltransferase repairs platinum-DNA adducts following cisplatin treatment and predicts prognoses of nasopharyngeal carcinoma." Int J Cancer

137(6): 1291-1305.

Choi, Y. H. and A. M. Yu (2014). "ABC transporters in multidrug resistance and pharmacokinetics, and strategies for drug development." Curr Pharm Des **20(5):** 793-807.

Chowdhury, A., J. Sarkar, T. Chakraborti, P. K. Pramanik and S. Chakraborti (2016). "Protective role of epigallocatechin-3-gallate in health and disease: A perspective." Biomed Pharmacother **78:** 50-59.

Cole, S. P., G. Bhardwaj, J. H. Gerlach, J. E. Mackie, C. E. Grant, K. C. Almquist, A. J. Stewart, E. U. Kurz, A. M. Duncan and R. G. Deeley (1992). "Overexpression of a transporter gene in a multidrug-resistant human lung cancer cell line." Science **258(5088):** 1650-1654.

Cripe, L. D., H. Uno, E. M. Paietta, M. R. Litzow, R. P. Ketterling, J. M. Bennett, J. M. Rowe, H. M. Lazarus, S. Luger and M. S. Tallman (2010). "Zosuquidar, a novel modulator of P-glycoprotein, does not improve the outcome of older patients with newly diagnosed acute myeloid leukemia: a randomized, placebo-controlled trial of the Eastern Cooperative Oncology Group 3999." Blood **116(20):** 4077-4085.

Dasari, S. and P. B. Tchounwou (2014). "Cisplatin in cancer therapy: molecular mechanisms of action." Eur J Pharmacol **740:** 364-378.

Dazzi, F., D. Capelli, R. Hasserjian, F. Cotter, M. Corbo, A. Poletti, W. Chinswangwatanakul, J. M. Goldman and M. Y. Gordon (1998). "The kinetics and extent of engraftment of chronic myelogenous leukemia cells in non-obese diabetic/severe combined immunodeficiency mice reflect the phase of the donor's disease: an in vivo model of chronic myelogenous leukemia biology." Blood **92(4):** 1390-1396.

Druker, B. J., F. Guilhot, S. G. O'Brien, I. Gathmann, H. Kantarjian, N. Gattermann, M. W. Deininger, R. T. Silver, J. M. Goldman, R. M. Stone, F. Cervantes, A. Hochhaus, B. L. Powell, J. L. Gabilove, P. Rousselot, J. Reiffers, J. J. Cornelissen, T. Hughes, H. Agis, T. Fischer, G. Verhoef, J. Shepherd, G. Saglio, A. Gratwohl, J. L. Nielsen, J. P. Radich, B. Simonsson, K. Taylor, M. Baccarani, C. So, L. Letvak, R. A. Larson and I. Investigators (2006). "Five-year follow-up of patients receiving imatinib

for chronic myeloid leukemia." N Engl J Med **355**(23): 2408-2417.

Eng, Q. Y., P. V. Thanikachalam and S. Ramamurthy (2018). "Molecular understanding of Epigallocatechin gallate (EGCG) in cardiovascular and metabolic diseases." J Ethnopharmacol **210**: 296-310.

Esmaeili, M. A. (2016). "Combination of siRNA-directed gene silencing with epigallocatechin-3-gallate (EGCG) reverses drug resistance in human breast cancer cells." J Chem Biol **9**(1): 41-52.

Feng, D. D., H. Zhang, P. Zhang, Y. S. Zheng, X. J. Zhang, B. W. Han, X. Q. Luo, L. Xu, H. Zhou, L. H. Qu and Y. Q. Chen (2011). "Down-regulated miR-331-5p and miR-27a are associated with chemotherapy resistance and relapse in leukaemia." J Cell Mol Med **15**(10): 2164-2175.

Ferte, J., J. M. Kuhnel, G. Chapuis, Y. Rolland, G. Lewin and M. A. Schwaller (1999). "Flavonoid-related modulators of multidrug resistance: synthesis, pharmacological activity, and structure-activity relationships." J Med Chem **42**(3): 478-489.

Fischer, V., A. Rodriguez-Gascon, F. Heitz, R. Tynes, C. Hauck, D. Cohen and A. E. Vickers (1998). "The multidrug resistance modulator valspodar (PSC 833) is metabolized by human cytochrome P450 3A. Implications for drug-drug interactions and pharmacological activity of the main metabolite." Drug Metab Dispos **26**(8): 802-811.

Fox, E. and S. E. Bates (2007). "Tariquidar (XR9576): a P-glycoprotein drug efflux pump inhibitor." Expert Rev Anticancer Ther **7**(4): 447-459.

Fujiki, H., T. Watanabe, E. Sueoka, A. Rawangkan and M. Suganuma (2018). "Cancer Prevention with Green Tea and Its Principal Constituent, EGCG: from Early Investigations to Current Focus on Human Cancer Stem Cells." Mol Cells **41**(2): 73-82.

Gardner, E. R., N. F. Smith, W. D. Figg and A. Sparreboom (2009). "Influence of the dual ABCB1 and ABCG2 inhibitor tariquidar on the disposition of oral imatinib in mice." J Exp Clin Cancer Res **28**: 99.

Gorre, M. E., K. Ellwood-Yen, G. Chiosis, N. Rosen and C. L. Sawyers (2002).

"BCR-ABL point mutants isolated from patients with imatinib mesylate-resistant chronic myeloid leukemia remain sensitive to inhibitors of the BCR-ABL chaperone heat shock protein 90." Blood **100**(8): 3041-3044.

Greenberg, P. L., S. J. Lee, R. Advani, M. S. Tallman, B. I. Sikic, L. Letendre, K. Dugan, B. Lum, D. L. Chin, G. Dewald, E. Paietta, J. M. Bennett and J. M. Rowe (2004). "Mitoxantrone, etoposide, and cytarabine with or without valspodar in patients with relapsed or refractory acute myeloid leukemia and high-risk myelodysplastic syndrome: a phase III trial (E2995)." J Clin Oncol **22**(6): 1078-1086.

Hait, W. N., S. Choudhury, S. Srimatkandada and J. R. Murren (1993). "Sensitivity of K562 human chronic myelogenous leukemia blast cells transfected with a human multidrug resistance cDNA to cytotoxic drugs and differentiating agents." J Clin Invest **91**(5): 2207-2215.

Han, L. W., C. Gao and Q. Mao (2018). "An update on expression and function of P-gp/ABCB1 and BCRP/ABCG2 in the placenta and fetus." Expert Opin Drug Metab Toxicol **14**(8): 817-829.

Hayes, J. D. and D. J. Pulford (1995). "The glutathione S-transferase supergene family: regulation of GST and the contribution of the isoenzymes to cancer chemoprotection and drug resistance." Crit Rev Biochem Mol Biol **30**(6): 445-600.

Hung, L. W., I. X. Wang, K. Nikaido, P. Q. Liu, G. F. Ames and S. H. Kim (1998). "Crystal structure of the ATP-binding subunit of an ABC transporter." Nature **396**(6712): 703-707.

Hyafil, F., C. Vergely, P. Du Vignaud and T. Grand-Perret (1993). "In vitro and in vivo reversal of multidrug resistance by GF120918, an acridonecarboxamide derivative." Cancer Res **53**(19): 4595-4602.

Jin, X., B. Zhou, L. Xue and W. San (2015). "Soluplus((R)) micelles as a potential drug delivery system for reversal of resistant tumor." Biomed Pharmacother **69**: 388-395.

Jodoin, J., M. Demeule and R. Beliveau (2002). "Inhibition of the multidrug resistance P-glycoprotein activity by green tea polyphenols." Biochim Biophys Acta **1542**(1-3): 149-159.

- Jones, P. M. and A. M. George (2014). "A reciprocating twin-channel model for ABC transporters." Q Rev Biophys **47**(3): 189-220.
- Juliano, R. L. and V. Ling (1976). "A surface glycoprotein modulating drug permeability in Chinese hamster ovary cell mutants." Biochim Biophys Acta **455**(1): 152-162.
- Khan, N. and H. Mukhtar (2008). "Multitargeted therapy of cancer by green tea polyphenols." Cancer Lett **269**(2): 269-280.
- Kim, Y. and J. Chen (2018). "Molecular structure of human P-glycoprotein in the ATP-bound, outward-facing conformation." Science **359**(6378): 915-919.
- Krishnamurthy, P. and J. D. Schuetz (2005). "The ABC transporter Abcg2/Bcrp: role in hypoxia mediated survival." Biometals **18**(4): 349-358.
- Kundranda, M. N. and J. Niu (2015). "Albumin-bound paclitaxel in solid tumors: clinical development and future directions." Drug Des Devel Ther **9**: 3767-3777.
- Kurahashi, N., S. Sasazuki, M. Iwasaki, M. Inoue, S. Tsugane and J. S. Group (2008). "Green tea consumption and prostate cancer risk in Japanese men: a prospective study." Am J Epidemiol **167**(1): 71-77.
- Kuwazuru, Y., A. Yoshimura, S. Hanada, A. Utsunomiya, T. Makino, K. Ishibashi, M. Kodama, M. Iwahashi, T. Arima and S. Akiyama (1990). "Expression of the multidrug transporter, P-glycoprotein, in acute leukemia cells and correlation to clinical drug resistance." Cancer **66**(5): 868-873.
- La Rosee, P. and M. W. Deininger (2010). "Resistance to imatinib: mutations and beyond." Semin Hematol **47**(4): 335-343.
- Law, L. W., T. B. Dunn and et al. (1949). "Observations on the effect of a folic-acid antagonist on transplantable lymphoid leukemias in mice." J Natl Cancer Inst **10**(1): 179-192.
- Lee, M. J., P. Maliakal, L. Chen, X. Meng, F. Y. Bondoc, S. Prabhu, G. Lambert, S. Mohr and C. S. Yang (2002). "Pharmacokinetics of tea catechins after ingestion of green tea and (-)-epigallocatechin-3-gallate by humans: formation of different

metabolites and individual variability." Cancer Epidemiol Biomarkers Prev **11**(10 Pt 1): 1025-1032.

Leonessa, F., D. Green, T. Licht, A. Wright, K. Wingate-Legette, J. Lippman, M. M. Gottesman and R. Clarke (1996). "MDA435/LCC6 and MDA435/LCC6MDR1: ascites models of human breast cancer." Br J Cancer **73**(2): 154-161.

Lin, L. C., M. N. Wang, T. Y. Tseng, J. S. Sung and T. H. Tsai (2007). "Pharmacokinetics of (-)-epigallocatechin-3-gallate in conscious and freely moving rats and its brain regional distribution." J Agric Food Chem **55**(4): 1517-1524.

List, A. F., K. J. Kopecky, C. L. Willman, D. R. Head, D. L. Persons, M. L. Slovak, R. Dorr, C. Karanes, H. E. Hynes, J. H. Doroshow, M. Shurafa and F. R. Appelbaum (2001). "Benefit of cyclosporine modulation of drug resistance in patients with poor-risk acute myeloid leukemia: a Southwest Oncology Group study." Blood **98**(12): 3212-3220.

Litman, T., M. Brangi, E. Hudson, P. Fetsch, A. Abati, D. D. Ross, K. Miyake, J. H. Resau and S. E. Bates (2000). "The multidrug-resistant phenotype associated with overexpression of the new ABC half-transporter, MXR (ABCG2)." J Cell Sci **113** (Pt 11): 2011-2021.

Liu, X. and G. Pan (2019). Drug Transporters in Drug Disposition, Effects and Toxicity, Springer.

Liu Yin, J. A., K. Wheatley, J. K. Rees, A. K. Burnett and U. M. A. L. W. Party (2001). "Comparison of 'sequential' versus 'standard' chemotherapy as re-induction treatment, with or without cyclosporine, in refractory/relapsed acute myeloid leukaemia (AML): results of the UK Medical Research Council AML-R trial." Br J Haematol **113**(3): 713-726.

Loo, T. W., M. C. Bartlett and D. M. Clarke (2003). "Simultaneous binding of two different drugs in the binding pocket of the human multidrug resistance P-glycoprotein." J Biol Chem **278**(41): 39706-39710.

Lozzio, B. B., C. B. Lozzi and E. Machado (1976). "Human myelogenous (Ph+) leukemia cell line: transplantation into athymic mice." J Natl Cancer Inst **56**(3): 627-629.

Lozzio, C. B. and B. B. Lozzio (1975). "Human chronic myelogenous leukemia cell-line with positive Philadelphia chromosome." Blood **45**(3): 321-334.

Lu, J. F., D. Pokharel and M. Bebawy (2015). "MRP1 and its role in anticancer drug resistance." Drug Metab Rev **47**(4): 406-419.

Lund, M., T. S. Petersen and K. P. J. D. Dalhoff (2017). "Clinical implications of P-glycoprotein modulation in drug–drug interactions." **77**(8): 859-883.

Maekawa, T., E. Ashihara and S. Kimura (2007). "The Bcr-Abl tyrosine kinase inhibitor imatinib and promising new agents against Philadelphia chromosome-positive leukemias." Int J Clin Oncol **12**(5): 327-340.

McKay, D. L. and J. B. Blumberg (2002). "The role of tea in human health: an update." J Am Coll Nutr **21**(1): 1-13.

Meenakshi Sundaram, D. N., X. Jiang, J. M. Brandwein, J. Valencia-Serna, K. C. Remant and H. Uludag (2019). "Current outlook on drug resistance in chronic myeloid leukemia (CML) and potential therapeutic options." Drug Discov Today **24**(7): 1355-1369.

Mei, Y., F. Qian, D. Wei and J. Liu (2004). "Reversal of cancer multidrug resistance by green tea polyphenols." J Pharm Pharmacol **56**(10): 1307-1314.

Michael, M. and M. M. Doherty (2005). "Tumoral drug metabolism: overview and its implications for cancer therapy." J Clin Oncol **23**(1): 205-229.

Monsarrat, B., E. Mariel, S. Cros, M. Gares, D. Guenard, F. Gueritte-Voegelein and M. Wright (1990). "Taxol metabolism. Isolation and identification of three major metabolites of taxol in rat bile." Drug Metab Dispos **18**(6): 895-901.

Mora Lagares, L., N. Minovski and M. Novic (2019). "Multiclass Classifier for P-Glycoprotein Substrates, Inhibitors, and Non-Active Compounds." Molecules **24**(10).

Newman, M. J., J. C. Rodarte, K. D. Benbatoul, S. J. Romano, C. Zhang, S. Krane, E. J. Moran, R. T. Uyeda, R. Dixon, E. S. Guns and L. D. Mayer (2000). "Discovery and characterization of OC144-093, a novel inhibitor of P-glycoprotein-mediated multidrug resistance." Cancer Res **60**(11): 2964-2972.

Noguchi, K., K. Katayama and Y. Sugimoto (2014). "Human ABC transporter ABCG2/BCRP expression in chemoresistance: basic and clinical perspectives for molecular cancer therapeutics." Pharmgenomics Pers Med **7**: 53-64.

Ota, S., G. Ishii, K. Goto, K. Kubota, Y. H. Kim, M. Kojika, Y. Murata, M. Yamazaki, Y. Nishiwaki, K. Eguchi and A. Ochiai (2009). "Immunohistochemical expression of BCRP and ERCC1 in biopsy specimen predicts survival in advanced non-small-cell lung cancer treated with cisplatin-based chemotherapy." Lung Cancer **64**(1): 98-104.

Padowski, J. M. and G. M. Pollack (2010). "Pharmacokinetic and pharmacodynamic implications of P-glycoprotein modulation." Methods Mol Biol **596**: 359-384.

Palmeira, A., E. Sousa, M. H. Vasconcelos and M. M. Pinto (2012). "Three decades of P-gp inhibitors: skimming through several generations and scaffolds." Curr Med Chem **19**(13): 1946-2025.

Patil, Y., T. Sadhukha, L. Ma and J. Panyam (2009). "Nanoparticle-mediated simultaneous and targeted delivery of paclitaxel and tariquidar overcomes tumor drug resistance." J Control Release **136**(1): 21-29.

Prentis, R. A., Y. Lis and S. R. Walker (1988). "Pharmaceutical innovation by the seven UK-owned pharmaceutical companies (1964-1985)." Br J Clin Pharmacol **25**(3): 387-396.

Price, J. E., A. Polyzos, R. D. Zhang and L. M. Daniels (1990). "Tumorigenicity and metastasis of human breast carcinoma cell lines in nude mice." Cancer Res **50**(3): 717-721.

Pusztai, L., P. Wagner, N. Ibrahim, E. Rivera, R. Theriault, D. Booser, F. W. Symmans, F. Wong, G. Blumenschein, D. R. Fleming, R. Rouzier, G. Boniface and G. N. Hortobagyi (2005). "Phase II study of tariquidar, a selective P-glycoprotein inhibitor, in patients with chemotherapy-resistant, advanced breast carcinoma." Cancer **104**(4): 682-691.

Qian, F., D. Wei, Q. Zhang and S. Yang (2005). "Modulation of P-glycoprotein function and reversal of multidrug resistance by (-)-epigallocatechin gallate in human cancer cells." Biomed Pharmacother **59**(3): 64-69.

Rees, D. C., E. Johnson and O. Lewinson (2009). "ABC transporters: the power to change." Nat Rev Mol Cell Biol **10**(3): 218-227.

Rice-Evans, C. A., N. J. Miller and G. Paganga (1996). "Structure-antioxidant activity relationships of flavonoids and phenolic acids." Free Radic Biol Med **20**(7): 933-956.

Riordan, J. R., K. Deuchars, N. Kartner, N. Alon, J. Trent and V. Ling (1985). "Amplification of P-glycoprotein genes in multidrug-resistant mammalian cell lines." Nature **316**(6031): 817-819.

Rowinsky, E. K., L. Smith, Y. M. Wang, P. Chaturvedi, M. Villalona, E. Campbell, C. Aylesworth, S. G. Eckhardt, L. Hammond, M. Kraynak, R. Drengler, J. Stephenson, Jr., M. W. Harding and D. D. Von Hoff (1998). "Phase I and pharmacokinetic study of paclitaxel in combination with biricodar, a novel agent that reverses multidrug resistance conferred by overexpression of both MDR1 and MRP." J Clin Oncol **16**(9): 2964-2976.

Rumpold, H., A. M. Wolf, K. Gruenewald, G. Gastl, E. Gunsilius and D. Wolf (2005). "RNAi-mediated knockdown of P-glycoprotein using a transposon-based vector system durably restores imatinib sensitivity in imatinib-resistant CML cell lines." Exp Hematol **33**(7): 767-775.

Sampath, D., J. Cortes, Z. Estrov, M. Du, Z. Shi, M. Andreeff, V. Gandhi and W. Plunkett (2006). "Pharmacodynamics of cytarabine alone and in combination with 7-hydroxystaurosporine (UCN-01) in AML blasts in vitro and during a clinical trial." Blood **107**(6): 2517-2524.

Sargent, J. M., C. J. Williamson, M. Maliepaard, A. W. Elgie, R. J. Scheper and C. G. Taylor (2001). "Breast cancer resistance protein expression and resistance to daunorubicin in blast cells from patients with acute myeloid leukaemia." Br J Haematol **115**(2): 257-262.

Shaffer, B. C., J. P. Gillet, C. Patel, M. R. Baer, S. E. Bates and M. M. Gottesman (2012). "Drug resistance: still a daunting challenge to the successful treatment of AML." Drug Resist Updat **15**(1-2): 62-69.

Shah, N. P., J. M. Nicoll, B. Nagar, M. E. Gorre, R. L. Paquette, J. Kuriyan and C. L. Sawyers (2002). "Multiple BCR-ABL kinase domain mutations confer polyclonal

resistance to the tyrosine kinase inhibitor imatinib (STI571) in chronic phase and blast crisis chronic myeloid leukemia." Cancer Cell **2**(2): 117-125.

Shultz, L. D., F. Ishikawa and D. L. Greiner (2007). "Humanized mice in translational biomedical research." Nat Rev Immunol **7**(2): 118-130.

Sirard, C., T. Lapidot, J. Vormoor, J. D. Cashman, M. Doedens, B. Murdoch, N. Jamal, H. Messner, L. Addey, M. Minden, P. Laraya, A. Keating, A. Eaves, P. M. Lansdorp, C. J. Eaves and J. E. Dick (1996). "Normal and leukemic SCID-repopulating cells (SRC) coexist in the bone marrow and peripheral blood from CML patients in chronic phase, whereas leukemic SRC are detected in blast crisis." Blood **87**(4): 1539-1548.

Solary, E., B. Witz, D. Caillot, P. Moreau, B. Desablens, J. Y. Cahn, A. Sadoun, B. Pignon, C. Berthou, F. Maloisel, D. Guyotat, P. Casassus, N. Ifrah, Y. Lamy, B. Audhuy, P. Colombat and J. L. Harousseau (1996). "Combination of quinine as a potential reversing agent with mitoxantrone and cytarabine for the treatment of acute leukemias: a randomized multicenter study." Blood **88**(4): 1198-1205.

Sonneveld, P. and A. F. List (2001). "Chemotherapy resistance in acute myeloid leukaemia." Best Pract Res Clin Haematol **14**(1): 211-233.

Srivalli, K. M. R. and P. J. B. J. o. P. S. Lakshmi (2012). "Overview of P-glycoprotein inhibitors: a rational outlook." **48**: 353-367.

Steevens, J., L. J. Schouten, B. A. Verhage, R. A. Goldbohm and P. A. van den Brandt (2007). "Tea and coffee drinking and ovarian cancer risk: results from the Netherlands Cohort Study and a meta-analysis." Br J Cancer **97**(9): 1291-1294.

Sugihara, N., Y. Tsutsui, T. Tagashira, T. Choshi, S. Hibino, J. Kamishikiryou and K. J. J. o. F. F. Furuno (2011). "The ability of gallate and pyrogallol moieties of catechins to inhibit P-glycoprotein function." J Funct Foods **3**: 298-304.

Syed, D. N., N. Khan, F. Afaq and H. Mukhtar (2007). "Chemoprevention of prostate cancer through dietary agents: progress and promise." Cancer Epidemiol Biomarkers Prev **16**(11): 2193-2203.

Tamaki, A., C. Ierano, G. Szakacs, R. W. Robey and S. E. Bates (2011). "The

controversial role of ABC transporters in clinical oncology." Essays Biochem **50**(1): 209-232.

Tang, H., L. Zeng, J. Wang, X. Zhang, Q. Ruan, J. Wang, S. Cui and D. Yang (2017). "Reversal of 5-fluorouracil resistance by EGCG is mediated by inactivation of TFAP2A/VEGF signaling pathway and down-regulation of MDR-1 and P-gp expression in gastric cancer." Oncotarget **8**(47): 82842-82853.

Tang, R., A. M. Faussat, J. Y. Perrot, Z. Marjanovic, S. Cohen, T. Storme, H. Morjani, O. Legrand and J. P. Marie (2008). "Zosuquidar restores drug sensitivity in P-glycoprotein expressing acute myeloid leukemia (AML)." BMC Cancer **8**: 51.

Teicher, B. A. (2011). Tumor models in cancer research. New York, Humana Press.

Tejada-Berges, T., C. O. Granai, M. Gordinier and W. Gajewski (2002). "Caelyx/Doxil for the treatment of metastatic ovarian and breast cancer." Expert Rev Anticancer Ther **2**(2): 143-150.

Trock, B. J., F. Leonessa and R. Clarke (1997). "Multidrug resistance in breast cancer: a meta-analysis of MDR1/gp170 expression and its possible functional significance." J Natl Cancer Inst **89**(13): 917-931.

Urbatsch, I. L., B. Sankaran, J. Weber and A. E. Senior (1995). "P-glycoprotein is stably inhibited by vanadate-induced trapping of nucleotide at a single catalytic site." J Biol Chem **270**(33): 19383-19390.

Visani, G., D. Milligan, F. Leoni, J. Chang, S. Kelsey, R. Marcus, R. Powles, S. Schey, A. Covelli, A. Isidori, M. Litchman, P. P. Piccaluga, H. Mayer, M. Malagola and C. Pfister (2001). "Combined action of PSC 833 (Valspodar), a novel MDR reversing agent, with mitoxantrone, etoposide and cytarabine in poor-prognosis acute myeloid leukemia." Leukemia **15**(5): 764-771.

Voncken, J. W., C. Morris, P. Pattengale, G. Dennert, C. Kikly, J. Groffen and N. Heisterkamp (1992). "Clonal development and karyotype evolution during leukemogenesis of BCR/ABL transgenic mice." Blood **79**(4): 1029-1036.

Wang, J. C., T. Lapidot, J. D. Cashman, M. Doedens, L. Addy, D. R. Sutherland, R. Nayar, P. Laraya, M. Minden, A. Keating, A. C. Eaves, C. J. Eaves and J. E. Dick

(1998). "High level engraftment of NOD/SCID mice by primitive normal and leukemic hematopoietic cells from patients with chronic myeloid leukemia in chronic phase." Blood **91**(7): 2406-2414.

Wang, P., S. M. Henning, D. Heber and J. V. Vadgama (2015). "Sensitization to docetaxel in prostate cancer cells by green tea and quercetin." J Nutr Biochem **26**(4): 408-415.

Wattel, E., E. Solary, B. Hecquet, D. Caillot, N. Ifrah, A. Brion, N. Milpied, M. Janvier, A. Guerci, H. Rochant, C. Cordonnier, F. Dreyfus, A. Veil, L. Hoang-Ngoc, A. M. Stoppa, N. Gratecos, A. Sadoun, H. Tilly, P. Brice, B. Lioure, B. Desablens, B. Pignon, J. P. Abgrall, M. Leparrier, P. Fenaux and et al. (1999). "Quinine improves results of intensive chemotherapy (IC) in myelodysplastic syndromes (MDS) expressing P-glycoprotein (PGP). Updated results of a randomized study. Groupe Francais des Myelodysplasies (GFM) and Groupe GOELAMS." Adv Exp Med Biol **457**: 35-46.

Wilkins, S. (2015). "Structure and mechanism of ABC transporters." F1000Prime Rep **7**: 14.

Wong, I. L., B. C. Wang, J. Yuan, L. X. Duan, Z. Liu, T. Liu, X. M. Li, X. Hu, X. Y. Zhang, T. Jiang, S. B. Wan and L. M. Chow (2015). "Potent and Nontoxic Chemosensitizer of P-Glycoprotein-Mediated Multidrug Resistance in Cancer: Synthesis and Evaluation of Methylated Epigallocatechin, Gallocatechin, and Dihydromyricetin Derivatives." J Med Chem **58**(11): 4529-4549.

Wong, I. L. K., X. K. Wang, Z. Liu, W. Sun, F. X. Li, B. C. Wang, P. Li, S. B. Wan and L. M. C. Chow (2021). "Synthesis and evaluation of stereoisomers of methylated catechin and epigallocatechin derivatives on modulating P-glycoprotein-mediated multidrug resistance in cancers." Eur J Med Chem **226**: 113795.

Yan, C. S., I. L. Wong, K. F. Chan, J. W. Kan, T. C. Chong, M. C. Law, Y. Zhao, S. W. Chan, T. H. Chan and L. M. Chow (2015). "A New Class of Safe, Potent, and Specific P-gp Modulator: Flavonoid Dimer FD18 Reverses P-gp-Mediated Multidrug Resistance in Human Breast Xenograft in Vivo." Mol Pharm **12**(10): 3507-3517.

Zhang, J., W. H. Yang, X. D. Yang, Z. X. Shi, X. L. Wang, W. J. Yu and Z. Hao

(2012). "[Establishment and identification of CML model via injection of K562 cells into the murine caudal vein]." Zhongguo Shi Yan Xue Ye Xue Za Zhi **20**(3): 773-776.

Zhang, P. Y., I. L. Wong, C. S. Yan, X. Y. Zhang, T. Jiang, L. M. Chow and S. B. Wan (2010). "Design and syntheses of permethyl ningalin B analogues: potent multidrug resistance (MDR) reversal agents of cancer cells." J Med Chem **53**(14): 5108-5120.

Zhang, Q., D. Wei and J. Liu (2004). "In vivo reversal of doxorubicin resistance by (-)-epigallocatechin gallate in a solid human carcinoma xenograft." Cancer Lett **208**(2): 179-186.

Zhang, Y., S. X. Wang, J. W. Ma, H. Y. Li, J. C. Ye, S. M. Xie, B. Du and X. Y. Zhong (2015). "EGCG inhibits properties of glioma stem-like cells and synergizes with temozolomide through downregulation of P-glycoprotein inhibition." J Neurooncol **121**(1): 41-52.

Zhang, Y., X. Wang, L. Han, Y. Zhou and S. Sun (2015). "Green tea polyphenol EGCG reverse cisplatin resistance of A549/DDP cell line through candidate genes demethylation." Biomed Pharmacother **69**: 285-290.

Zheng, X., X. Fan, B. Fu, M. Zheng, A. Zhang, K. Zhong, J. Yan, R. Sun, Z. Tian and H. Wei (2017). "EpCAM Inhibition Sensitizes Chemoresistant Leukemia to Immune Surveillance." Cancer Res **77**(2): 482-493.

Zhu, A., X. Wang and Z. Guo (2001). "Study of tea polyphenol as a reversal agent for carcinoma cell lines' multidrug resistance (study of TP as a MDR reversal agent)." Nucl Med Biol **28**(6): 735-740.

Zhu, C. Y., Y. P. Lv, D. F. Yan and F. L. Gao (2013). "Knockdown of MDR1 increases the sensitivity to adriamycin in drug resistant gastric cancer cells." Asian Pac J Cancer Prev **14**(11): 6757-6760.

Zhu, H., H. Wu, X. Liu, B. R. Evans, D. J. Medina, C. G. Liu and J. M. Yang (2008). "Role of MicroRNA miR-27a and miR-451 in the regulation of MDR1/P-glycoprotein expression in human cancer cells." Biochem Pharmacol **76**(5): 582-588.